THE REGULATION OF IL-33 AND ARGINASE-1 BY ONCOSTATIN M IN MOUSE LUNG SYSTEMS

THE REGULATION OF IL-33 AND ARGINASE-1 BY ONCOSTATIN M IN MOUSE LUNG SYSTEMS

By: Anisha Dubey, BSc. Honours (McMaster University)

A Thesis Submitted to the School of Graduate Studies in Partial Fulfillment of the Requirements for the Degree Master of Science in Medical Sciences

McMaster University

MASTERS OF SCIENCE (2017) McMaster University, Hamilton Ontario

(Medical Sciences: Infection and Immunology)

TITLE: The Regulation of IL-33 and Arginase-1 by Oncostatin M in Mouse Lung Systems

AUTHOR: Anisha Dubey, B.Sc. Hons. (McMaster University)

SUPERVISOR: Dr. Carl Richards, BSc., MSc., Ph.D.

NUMBER OF PAGES: xvi, 145

ABSTRACT

Excessive tissue fibrosis in various lung diseases contributes to decline in lung function and subsequent morbidity and mortality. Mechanisms involve complex networks of molecules such as cytokines that are not clearly worked out in conditions such as Idiopathic pulmonary fibrosis (IPF). Furthermore, pulmonary virus infection has been linked to exacerbations of IPF. Previous studies have demonstrated that transient pulmonary over-expression of Oncostatin M (OSM) leads to increased extracellular matrix (ECM) accumulation, Th2-skewed cytokines and Arg1+ M2-like macrophage accumulation in mouse models. OSM can also robustly induce interleukin-33 (IL-33), an IL1 family cytokine or alarmin, both *in vivo* and *in vitro* mouse lung systems. Since others have shown that soluble IL-33 exacerbates bleomycin-induced lung fibrosis in mouse models and is associated with Th2-type lung diseases, IL-33 may mediate OSM effects on ECM and Arg1+ macrophage-like cell accumulation. The main hypothesis in this thesis is that OSM can induce IL-33 expression and Arg1+ cells, that OSM can potentiate IL-33 release from virally-infected epithelial cells, and that OSM can prime lungs to subsequent influenza infection and exacerbate pathology.

Results demonstrated that OSM induced robust up-regulation of pulmonary IL-33 and Arg1 mRNA and protein expression *in vivo*, in comparison to another gp130 cytokine, IL-6. However, IL-6 was required for OSM-induced arginase-1 expression *in vivo*, but not IL-33 expression *in vivo*. OSM-induced Arg1 expression was also dependent upon IL-33 presence as demonstrated in IL-33$^{-/-}$ animals. This finding implicates a role for both IL-33 and IL-6 in mediating OSM-induced Arg1+ macrophage-like cell accumulation within the

lung.

Additionally, results showed that a respiratory Influenza A virus infection *in vivo* alone induced a time-dependent increase in OSM and IL-33 (Day 4), however reduced IL-33 by 7-days post-infection. Influenza infection in AdOSM-primed mice and led to decreased IL-33 expression and eosinophilic infiltration within the lung 5-days post-influenza infection. Collectively, these results demonstrate that OSM can drive Th2-associated pathology correlated to increased IL-33 and Arg1 expression. Contrary to expectations, influenza A virus infection led to a reduction in OSM-induced Th2-phenotype *in vivo*. Further exploration into the OSM-IL-33 pathway will provide insight into innate immune mechanisms of lung inflammation, virus infection and control of ECM accumulation.

ACKNOWLEDGEMENTS

With completion of this thesis, I would like to extend my greatest acknowledgment to my supervisor, Dr. Carl Richards. His encouragement, mentorship, unwavering support and enthusiasm throughout these past two years have provided me with an optimal learning environment and equipped me with the motivation and perseverance for future success. I'd also like to thank Carl for supporting my aspirations and always encouraging me to achieve my goals. To my committee members, Dr. Matthew Miller and Kjetil Ask, I would like to thank you for expert advice regarding my project, for always challenging me to think critically and for all of your encouragement along the way.

To the many friends I have made at the McMaster Immunology Research Centre during these past two years, including but not limited to Ehab Ayaub, Jewel Imani, Tina Nham, Karun Tandon and Chandak Upagupta, thank you for all the laughs, the support and all the memories that we have made together. From late nights in the laboratory, to monthly birthday celebrations and the tasty adventures exploring Hamilton restaurants and bars. Wishing you all the best in your future endeavors and I hope that we will all cross paths again soon.

Last, but definitely not least, I would like to thank my parents, siblings and Ronish for their unconditional support and love during both the good times and more stressful moments as a graduate student. You guys have been there for me and pushed me to succeed, even when I would doubt myself. I would not be able to succeed without your constant support and encouragement throughout these past two years. Thank you.

TABLE OF CONTENTS

LIST OF FIGURES

LIST OF ABBREVIATIONS

Arg-1 - Arginase-1

ANOVA - Analysis of Variance

BALF - Bronchoalveolar Lavage Fluid

BSA - Bovine Serum Albumin

BMDM – Bone-marrow Derived Macrophage

CD - Cluster of Differentiation

cDNA - Complementary DNA

cRPMI - Complete RPMI

DC - Dendritic Cell

DMEM – Dulbecco's Modified Eagle's Medium

DNA - Deoxyribonucleaic Acid

dsRNA - Double stranded RNA

DTT – Diothioretiol

ECM - Extracellular Matrix

ELISA - Enzyme-Link Immunosorbent Assay

ERK - Extracellular signal-regulated kinase

FBS – Fetal Bovine Serum

G-CSF - Granulocyte- Colony stimulating Factor

GM-CSF - Granulocyte Macrophage- Colony stimulating Factor

Gp130 - Glycoprotein 130

Gp130R - Gp130 Receptor

HRV – Human Rhinovirus

HDM - House dust mite

H&E – Haemotoxylin and Eosin

iNOS - induced Nitric Oxide Synthase

ICAM - Intracellular Adhesion Molecule

IFN - Interferon

IgE - Immunoglobulin E

IgG - Immunoglobulin G

IL-1β – Interleukin-1- Beta

IL-4 – Interleukin-4

IL-5 – Interleukin-5

IL-6 – Interleukin-6

IL-10 – Interleukin-10

IL-13 – Interleukin-13

IFNγ – Interferon-gamma

Influenza A/PuertoRico8/1934 (H1N1) – PR8

IP-10/CXCL10 – Interferon-gamma Inducible Protein-10

JAK - Janus Kinase-

LIF - Leukemia Inhibitory Factor

LIFR - LIF Receptor

LPS - Lipopolysaccharide

M-CSF - Macrophage -Colony Stimulating Factor

mAB - Monoclonal Antibody

MAPK - Mitogen-Activated Protein Kinase

MCP - Monocyte chemotactic Factor

MIG/CXCL9 – Monokine-Induced by Interferon-gamma

MMP - Matrix Metalloproteinase

mRNA - Messenger Ribonucleic Acid

MyD88 - Myeloid differentiation primary response gene (88)

NK - Natural Killer

NKT - Natural Killer T cells

NO - Nitric Oxide

OSM - Oncostatin M

OSMR/OSMRβ - Oncostatin M Receptor (beta)

OVA - Ovalbumin

PAMP - Pathogen Associated Molecular Patterns

PBS - Phosphate Buffered Saline

PDAR - Pre-developed Assay reagents

PI3K - Phosphatidylinosinsitol-3 Kinase

PMSF - phenylmethylsulfonyl fluoride

qRT-PCR - Quantitative Reverse Transcription- Polymerase Chain Reaction

RANTES - Regulated on activation, normal T cell expressed and secreted

RIPA - Radioimmunopreciptation Assay

RPMI - Roswell Park Memorial Institute

RSV - Respiratory Syncytial Virus

SD/SEM - Standard Deviation/ Standard Error of the Mean

SDS-PAGE - Sodium dodecyl Sulfate-Polyacrylamide Gel Electrophoresis

ssRNA - Single stranded RNA

STAT1 - Signal Transducer and Activator of Transcription 1

STAT3 – Signal Transducer and Activator of Transcription 3

STAT6 – Signal Transducer and Activator of Transcription 6

TARC- Thymus and activation regulated chemokine

TBS - Tris Buffered Saline

Th - T-helper cell

TIMP1 - Tissue inhibitors of metalloproteinase

TLR - Toll-Like Receptor

TGF-β - Transforming growth factor - Beta

TNF-α - Tumor Necrosis Factor

TSLP - Thymic stromal lymphopoietin

UNG - Uracil-N-glycosylase

CHAPTER 1

- INTRODUCTION -

1.0 Idiopathic Pulmonary Fibrosis

Idiopathic pulmonary fibrosis (IPF) is a chronic progressive lung disease characterized by tissue remodeling and accumulation of extracellular matrix (ECM)-related proteins[1]. It represents approximately 20% of all interstitial lung disease (ILD) cases, and is the most severe idiopathic interstitial pneumonia (IIP), an ILD characterized by heterogeneous patterns of inflammation and fibrosis[2]. IPF is primarily diagnosed in men over 60 years of age who show progressive decline in lung function, 'velcro-type' crackles during inspiration and dyspnea during exertion[1]. IPF patients have a poor prognosis, leading to hospitalization and a 20% 5-year survival rate, accounting for approximately 50.8 deaths/100,000/ year in the United States alone[3]. This condition significantly contributes to economic and societal burden, with treatment costs estimated at 25,000 USD/person-year, exceeding that of breast cancer[4]. Due to the heterogeneity of this disease, current treatment options for late-stage IPF are limited and largely ineffective. Although, fibroblast activation, proliferation and accumulation is believed to significantly contribute to the development of the fibrosis, the cellular and molecular mechanisms leading to pathogenesis remain unclear[5]. Current paradigms suggest that sustained epithelial cell damage or activity of various mediators, including the pro-fibrogenic cytokine Transforming Growth Factor-β (TGF-β) is required for fibrogenesis. However, there may be TGF-β independent pathways also involved. Our laboratory has suggested

Oncostatin M, a cytokine part of the gp130 family, can lead to the development of fibrosis via STAT3 signalling (as discussed below). In addition, a potential role of OSM in exacerbations of chronic inflammatory or fibrotic lung diseases is unknown.

1.1 Acute IPF Exacerbations

Five to ten percent of all IPF patients experience accelerated disease progression and respiratory deterioration, known as acute-exacerbations in IPF (AE-IPF), each year[1,6]. Patients experiencing acute exacerbations present with worsening dyspnea and rapid decline in lung function over a short period of time [6,7]. There is currently no effective treatment for AE-IPF and outcome is extremely poor. AE-IPF associated mortality occurs in over 50% of hospitalized patients and up to 80% in patients after one-year of follow-up[7]. The cause of acute exacerbation remains unknown, however several factors, such as toxic exposure, mechanical stress, or aspiration of gastric contents have been associated with increased risk for event onset and considered potential triggers for chronic lung injury[8–11]. An emerging hypothesis for acute exacerbation is that epithelial cell damage caused by a virus infection initiates a cascade of inflammatory events, release of soluble mediators which activate fibrotic processes and leads to accelerated disease pathology.

1.1.1 Viral-Induced Exacerbations

The three main stages of the viral lifecycle include attachment and entry into the cell, intracellular replication and release from the cell via budding [12]. Cell lysis causes the cell membrane to rupture and release its intracellular contents[12]. Viral-induced

epithelial cell damage provides the basis for a potential link between viral infections and exacerbations of lung disease. A recent study reported elevated levels of pro-inflammatory cytokines, such as IL-6, IL-1β, or IL-12, and neutrophil accumulation in the bronchoalveolar lavage fluid (BAL) of AE-IPF patients, which reflects a classic innate immune response to virus infection. However, the prevalence of virus-induced AE-IPF remains controversial due to conflicting results among patient studies. A study conducted by Wootton *et al*. in 2011 attempted to investigate the potential role of virus infection in mediating AE-IPF by assessing the presence of viral RNA in the bronchoalveolar lavage (BAL) fluid of AE-IPF patients compared to stable-IPF patients. Respiratory virus infection from either rhinovirus, coronavirus or parainfluenza, was evident in 9% of AE-IPF patients, whereas viral RNA was undetected in stable-IPF patients[6]. In another study conducted by Ushiki et al. in 2014, 1 of 7 AE-IPF patients tested positive for respiratory syncytial virus (RSV) B RNA in the BAL fluid. However, due to the limited sample size, researchers were unable to make a strong conclusion about this finding. Virus-induced IPF exacerbations are difficult to study due to suspected viral clearance prior to the appearance of clinical manifestations of IPF. However, we propose that the sustained epithelial cell damage caused by lytic viruses contributes to the pathogenesis of acute exacerbations in fibrotic lung disease.

1.3 Gp130 Cytokines

GP130 cytokines, also referred to as the IL-6 family cytokines, are proteins involved in various inflammatory and immunoregulatory mechanisms. Members of this family

include IL-6, Oncostatin M (OSM), Leukocyte Inhibitory Factor (LIF), IL-11, cardiotrophin-1 (CT-1), ciliary neurotrophic factor (CNTF), IL-31 and IL-27. All of these proteins, except IL-31, elicit their cellular effects by binding to specific receptor complexes that include the signal transducing molecule, glycoprotein 130 (gp130) as a subunit. Due to their shared use of the gp130 transmembrane receptor, these molecules have similar biological activities and cellular functions in certain cells[13]. However, unique responses are also observed due to the presence of the cytokine-specific receptor subunits on a variety of cell-types. The gp130 cytokines play an important role in complex cellular processes such as cell differentiation, proliferation, hematopoiesis or gene regulation[13-16]. Activation of the receptor complexes by these cytokines can initiate multiple signaling cascades, such the MAP Kinase, Janus family of tyrosine kinases (JAK/STAT), or PI3' Kinase pathways. Of the gp130 cytokines, IL-6, OSM and IL-11 have been studied in relation to pulmonary fibrosis. Moodley et al., reported mitogenic activity of IL-11 and demonstrated its inhibitory effect on Fas-ligand induced apoptosis of lung fibroblasts *in vitro*[17]. IL-6 is increased in the bronchoalveolar lavage fluid of IPF patients and has been shown to increase the expression of the anti-apoptic factor, BCL-2, in IPF lung fibroblasts[17-18]. Researchers have also demonstrated that removal of IL-6 during the late inflammatory stage of the bleomycin mouse model of pulmonary fibrosis can prevent the development of disease[19]. IL-6 has also been shown to skew bone-marrow derived macrophages toward a fibrotic or alternatively activated phenotype *in vitro* in combination with IL-4/IL-13 signalling[20]. This report will primarily focus on OSM and its role in fibrotic disease.

1.31 Oncostatin M

Oncostatin M (OSM) is a 252 amino acid polypeptide that was first discovered *in vitro* by Zarling et al., in 1986 due to its anti-proliferative effects on the human melanoma cell line, A375. Initially, OSM was studied in the context of cancer, however its role in cell differentiation, hematopoiesis, metabolism, and immunity was later established. In humans, OSM is most closely related to the gp130 cytokine, LIF, allowing it to signal through both the LIF/gp130 and OSMRβ/gp130 receptor complexes. Released primarily by lymphocytes, macrophages, and neutrophils, OSM has been linked to a diverse range of pathologies, such as arthritis, cancer, bone remodeling, scleroderma, as well as pulmonary inflammation and fibrosis [13], [21]–[23].

In 2008, Mozzaffarien et al., reported increased OSM expression in the bronchoalveolar lavage fluid of IPF and scleroderma patients, suggesting a role for this cytokine in the progression of fibrosis[23]. Over-expression of OSM in the lungs of mice lead to significant infiltration of inflammatory cells, such as macrophages and neutrophils, and correlated to an increase in collagen-deposition. Interestingly, these results were sustained in $Rag2^{-/-}$ mice, indicating a unique function of OSM in regulating inflammation and extracellular matrix deposition independent of T- and B- lymphocytes[23]. Although, TGF-β is the commonly accepted central mediator in fibrogenesis, Wong et al., found that OSM pro-fibrotic effects occurred independently of the canonical TGF-β-SMAD signaling. Over-expression of OSM enhanced ECM accumulation and collagen-1A1 and -3A1 in the TGF-β -resistant Balb/c mouse strain, which mimicked the phenotype observed in the susceptible C57Bl/6 mouse strain[24]. Additionally, Lauber et al., discovered a novel role

for OSM in enhancing pro-fibrotic M2 macrophage accumulation in the lungs of mice treated with Adenovirus encoding OSM[25]. Although these results were studied in the context of lung cancer, M2 macrophages have been extensively implicated in several fibrotic disorders based on their ability to produce fibronectin, TGF-β, and tissue metalloprotease inhibitors[26]–[28]. *In vitro* studies conducted by Nagahama et al., using human lung fibroblasts showed enhanced α-SMA production after OSM stimulation in a dose-dependent manner. Additionally, they demonstrated that OSM augmented collagen-gel contraction and fibronectin chemotaxis in these cells and that the effects were dependent on STAT3 activation[29]. Many researchers have focused on the ability of OSM to potently induce the activation of JAK/STAT pathway, particularly STAT3, which has also been implicated in mediating fibrogenesis.

1.3.2 The JAK/STAT pathway

The JAK/STAT pathway has largely been associated with mediating inflammatory mechanisms and activating transcriptional factors called STAT proteins [reviewed in 30]. There are four types of Janus tyrosine kinases present in mammals: Jak1, Jak2, Jak3, Tyk[30]. Following ligand binding, Jak kinases located on the cytoplasmic domain of the dimerized receptor complexes auto-phosphorylate and act as a docking site for STAT proteins. The Jak kinases then phosphorylate the STAT proteins, allowing them to translocate into the nucleus. Once in the nucleus, they bind to DNA specific promoter regions and modulate gene expression[30]. Of the seven known STAT proteins (STAT1, 2, 3, 4, 5a,b, 6.), gp130 cytokines have been shown to predominantly induce the phosphorylation of STAT3. STAT3 regulation has been extensively studied in several

disease pathologies and may play an important role in IPF pathogenesis[31]. Phosphorylated STAT3 has been shown to be increased in IPF patient lung biopsies and in bleomycin-induced fibrotic mouse lung tissue[32]. A study conducted by Pedroza et al., found that inhibiting STAT3 activation using the pharmacological inhibitor, C-188-9, attenuates bleomycin-induced pulmonary fibrosis and was associated with decreased α-SMA accumulation and collagen deposition[32]. Interestingly, experiments in our laboratory have demonstrated STAT3-depenedent regulation of IL-33, an IL-1 family alarmin implicated in various pulmonary diseases.

1.4 Alarmins

Alarmins are ubiquitously expressed endogenous molecules, also known as danger-associated molecular patterns, which are released upon cellular death or damage and induce innate and adaptive immune responses. defensins, high-motility group box-1 (HMGB-1), calcium binding proteins from the S100 family, Heat Shock proteins, IL-1α, ATP, uric acid and the more recently discovered IL-33, are some of the alarmins implicated in various biological processes. The term ‘alarmin’ was first developed by J. Oppenheim in 2005 to represent a group of structurally diverse host molecules released or secreted from dead or dying cells during trauma or infection[33]. Once released from necrotic cells, these molecules initiate a pro-inflammatory response by binding to their specific receptors on surrounding cells and provoke local damage or systemic inflammation[33]. Interestingly, some of these molecules have dual-functions, acting as both a nuclear factor and pro-inflammatory cytokine. IL-33 has been extensively studied as a mediator in various lung

disorders, such as pulmonary fibrosis or allergic asthmas, and will be further discussed below.

1.5 IL-33

Interleukin-33 (IL-33) was first discovered in 2003 as a nuclear factor expressed in high-endothelial venules, and therefore initially referred to as NF-HEV[34]. In 2005, Schmitz et al., determined that NF-HEV was in fact part of the IL-1 cytokine family and therefore renamed to IL-33 in order to reflect its new classification[35]. Human full-length IL-33 is comprised of 270 amino acids, weighing approximately 31kDa, and contains a nuclear localization sequence and a homeodomain-helix-turn-helix DNA binding region. Consequently, full-length IL-33 can translocate into the nucleus and modulate gene expression. For instance, it has been shown that intranuclear IL-33 acts as a transcriptional repressor to p65-NFkappaB subunit, inhibiting the activation of this pathway and expression of NFkappaB-regulated genes, such as TNF-α or IL-1[36]. Cleavage of full-length IL-33 by caspase 3 and 7, activated by apoptosis, produce biologically inactive forms of mature IL-33 (18kDa) [37], [38] . However, cleavage of extracellular full-length IL-33 by calpain, neutrophil elastase or cathepsin G produce biologically active forms of IL-33, which are 10 times more active than the full-length protein[39]–[41]. It has also been recently reported that IL-33 can be oxidized within the extracellular environment as a additional mechanism of protein function regulation. Specifically, Cohen et al., showed that IL-33 can be found in a reduced active form, as well as an oxidized inactive state. The oxidized form of IL-33 has the addition of two disulphide bonds, leading to a

conformational change which disrupts the ST2 binding site within the molecule[42]. Both forms of IL-33 can be detected in a *Alternaria* mouse model of inflammation using a commercially available enzyme-linked immunosorbent assay (ELISA) or in-house specific ELISA to detect reduced IL-33 protein[42]. IL-33 is constitutively expressed in various epithelial and endothelial cells as well as other immune cells, such as neutrophils and fibroblasts. It signals through the transmembrane ST2 receptor, formally known as the orphan receptor of the IL-1 family (IL-1R1). IL-33 binding to the ST2 receptor induces a conformational change and leads to the dimerization of ST2 with the IL-1R-Accessory Protein (IL-1RAcP)[43]. The ST2 receptor is located on a variety of cells, such as mast cells, eosinophils, Th2, and innate lymphoid type 2 cells, and therefore reflects the multi-faceted nature of IL-33[44]. The gene corresponding to ST2 also encodes an additional isoform, known as soluble ST2 (sST2). Soluble ST2 has been identified as an antagonistic receptor and binds to soluble IL-33 to inhibit its activity[45]. IL-33 expression is regulated similarly to other IL-1 cytokines. Meephansan et al., have shown that stimulation with pro-inflammatory cytokines, such as interferon-γ (IFN-γ) and tumour necrosis factor-α (TNF-α), enhances IL-33 expression in human keratinocytes, while Llop-Guevara et al., demonstrated a similar finding in human alveolar type 2 epithelial cells[46], [47]. Additionally, researchers have shown that IL-33 is also regulated by Th2-type cytokines. For instance, Zhao et al, demonstrated increased IL-33 production from various mouse cells following IL-3/IL-4 stimulation[48]. Kearley et al., also demonstrated enhanced expression of IL-33 in mouse lung epithelial cells upon cigarette smoke exposure, suggesting that IL-33 regulation is also affected by environmental factors[49]. Viral infections have also been

shown to regulate IL-33 expression. In a study conducted by Holtzman et al., mice infected with Sendai virus, a strain of parainfluenza, show highly induced expression of the IL-33 gene and IL-33R gene based on whole genome-wide gene expression array[50]. Recently, Robinson et al., have demonstrated regulation of IL-33 protein in lung tissue following viral and bacterial co-infection. Specifically, they observed significantly decreased IL-33 expression in mice with a influenza A virus infection prior to exposure to Staphylococcus aureus, leading to attenuated host-defense and worsened mortality[51]. Additionally, our laboratory has identified a novel regulator for IL-33 in mouse lung systems- Oncostatin M. OSM stimulation increases IL-33 expression in mouse lung epithelial cells *in vitro* and in mouse lung tissues *in vivo*[52]. Although intracellular regulation of IL-33 has been extensively studied, its release into the extracellular mileu is less understood[53]. Since IL-33 is an alarmin, researchers postulate that IL-33 is primarily released by cellular necrosis or active necropolis rather than a defined secretory pathway[43, p. -1]. Bian et al., demonstrated increased serum levels of soluble IL-33 in patients infected with Influenza B[54]. A study conducted by Goffic et al., showed a significant up-regulation of IL-33 in the tissues and in the bronchoalveolar lavage fluid of mice infected with 1.5×10^5 plaque-forming units (pfu) of Influenza A/WSN/1933 H1N1 virus, which correlated to increases in other pro-inflammatory cytokines (IL-1β, TNF-α, IL-6). They also showed up-regulation of soluble IL-33 in the culture supernatants from mouse epithelial cell lines infected with the same virus at a multiplicity of infection of 5[55]. This data suggests that viral infections may play a significant role in mediating IL-33 release. While many researchers have studied IL-33 in relation to various disease pathologies, this report will

focus on its role in pulmonary conditions.

1.5.1 IL-33 as a Th2-associated Cytokine

Schmitz et al., first identified the function of IL-33 as a Th2-type cytokine in 2005[35]. These researchers found that Th2 polarized cells stimulated with IL-33 increased IL-5 and IL-13 expression *in vitro* and enhanced IL-4, IL-5 and IL-13 mRNA levels *in vivo*[35]. IL-33 has also been strongly associated with Th2 diseases, such as allergy and asthma. In 2012, Chu et al., identified a critical role for IL-33 in mediating allergic sensitization to mites and peanut[56]. Additionally, Llop-Guevara et al., found that IL-33 induced allergic airway responses in mice after house-dust mite exposure[47]. In 2012, Luzina et al., demonstrated that full-length IL-33 overexpression in mouse lung led to increased lymphocyte and neutrophil infiltration, which was independent of ST2 receptor signalling[57]. They also showed that overexpression of mature IL-33 protein in mouse lung induced typical type 2 immune responses, such as increased IL-4, IL-5 and IL-13 as well as pulmonary eosinophilia. More recently, researchers have shown that the IL-33/ST2 pathway is critical for type-2 airway responses, such as eosinophilia, globet cell hyperplasia and bronchial hyperreactivity, in response to a Staphylococcus aureus-derived allergen exposure, which was independent of TLR4-receptor signalling[58]. Within this study, they also demonstrated that mice lacking IL-33-receptor signalling demonstrated decreased IL-13+ innate lymphoid group 2 cells, IL-13+ Th2 cells and IL-5 and IL-13 production following exposure to the bacterial allergen peptide. Innate lymphoid cells (ILCs) have recently gained interest due to their pleotropic functionality and non-lymphoid characteristics. These cells lack antigen specific receptors but can respond to stimulation by various

external mediators and activate an innate immune response[59]. A subset of ILCs 1, 2 and 3 [reviewed in [60]), ILC2s represents a sub-population producing large amounts of Th2-associated cytokines, such as IL-5, IL-13 or IL-9 in response to epithelial-derived cytokine (IL-25, TSLP, IL-33) stimulation and have been implicated in eosinophil homeostasis, lung tissue repair, antiviral response and the maintenance of alternatively activated macrophages[61]–[64]. Barlow *et al*., have demonstrated that IL-33 is more effective than IL-25 in stimulating ILC2s to produce IL-13 and induce airway contraction[65]. Therefore, through activation of Th2 cells or ILC2s, IL-33 plays an important role in Type 2 immunity.

1.5.2 IL-33 and Pulmonary Fibrosis

Luzina et al., reported increased expression of full-length IL-33 in IPF patients and in the bleomycin-induced mouse model of lung fibrosis[66]. In a follow-up study, researchers found that over-expression of full-length IL-33 exacerbated bleomycin-induced lung fibrosis and increased levels of collagen 1A1 and 3A1, suggesting a role for IL-33 in mediating disease pathology[67]. Li *et al.* (2014), obtained similar findings and further demonstrated that IL-33 contributed to the polarization of pro-fibrotic M2 macrophages and activated ILC2s in an ST2-dependent manner[68]. Interestingly, the authours showed that IL-33 exacerbated- lung pathology was attenuated upon depletion of alveolar macrophages and ILC2s. In a recent study conducted in 2015 by Gao et al., researchers found that lentivirus expressing soluble ST2 attenuated bleomycin-induced lung fibrosis, which may be an indirect result of IL-33 inhibition[69]. These findings indicate a role for IL-33 in mediating fibrotic lung disease.

1.6 Arginase-1 and Pulmonary Fibrosis

The current paradigm of macrophage classification describes an association of the "M1" macrophage phenotype with pro-inflammatory secretory products including IL-6, TNF-α, IL-12, IL-1β, and Th1 responses, whereas the "M2" (alternatively activated) macrophage has been linked with Th2 responses and tissue repair[70]. Subsets of M2 cells have also been proposed in the mouse system[71]. Generally, M2 cells show enhanced release of IL-10 or TGF-β and cellular expression of Arginase-1 and mannose receptor (CD206). Arginase-1 expressing M2-like macrophages have previously been implicated in pro-fibrotic pathologies, such as pathological wound healing and tumourigenesis. Specifically, arginase-1 is a critical enzyme in the urea cycle which converts L-arginine to urea and ornithine. It is highly expressed in the liver, however can be expressed within other organs as well. Extrahepatic arginase-1 has been thought to contribute to fibrotic processes, since ornithine is a precursor to polyamines and pro-line, which are molecules involved in cell proliferation and collagen synthesis[72]. Previous publications have supported this concept. For instance, transfection of rat vascular smooth muscle cells with arginase-1 led to elevated levels of polyamines and enhanced cell proliferation[73]. Additionally, researchers have shown increased levels of arginase-1 protein and mRNA levels during bleomycin-induced lung fibrosis in mice. In a model of silicosis, a lung disease characterized by scar tissue and fibrosis, arginase-1 was found to be up-regulated and pre-dominantly located within lung and alveolar macrophages[74]. Although arginase-1 is a marker of alternative macrophages in several animal models, researchers have shown CCL18, a chemokine mediating infiltration of monocytes, to be a marker for M2

macrophages in humans. CCL18 has been shown to be markedly up-regulated in the serum and BALF of IPF patients and alveolar macrophage supernatants, suggesting enhanced M2 macrophage accumulation within the lung[75]. Therefore, it is important to further understand arginase-1 expressing macrophages in the mouse model and investigate their role in mediating pathology.

1.6.1 Arginase-1 and IL-33

IL-33 has also been previously correlated with arginase-1 expression and activity in mouse models both *in vitro* and *in vivo*. Specifically, IL-33 has been shown to directly stimulate bone-marrow derived macrophages *in vitro* to induce robust up-regulation of arginase-1 mRNA, as well as other Th2- associated cytokines, such as IL-5 and IL-13 mRNA[76]. Researchers suggested that IL-33 induction of IL-13 likely drives macrophage polarization in an autocrine fashion through the IL-4Ra/STAT6-signalling pathway[76]. Subsequent to this study, Li *et al.* (2014) showed that IL-33/ST2 signalling was crucial in the development of bleomycin-induced lung fibrosis through IL-13 and IL-33 polarization of bone-marrow derived macrophages and activation of ILC2s, which led to increased production of IL-13[68]. In addition to models of lung inflammation, Tu *et al.* (2016) demonstrated that IL-33 induced robust Arg-1 expression within colonic tissues from a mouse model of Trinitrobenzene sulfonic acid (TNBS)- induced colitis[77]. Although this study was performed in a different organ system, it demonstrates that IL-33, in the presence of inflammation, can promote the production of alternatively activated macrophages. ILC2s have also been reported to constitutively express arginase-1 protein and thus is a key marker to identify these cells within the lung. ILC2s are IL-33-responsive cells which mediate the

production of IL-5 and IL-13 upon activation[78]. For instance, Piehler et al. (2016) demonstrated IL-33-dependent proliferation of IL-33R+/Arg1+ ILC2s following airway fungal infection[79]. Therefore, induction of Arg-1 *in vivo* may suggest increased ILC2 cell accumulation as a result of IL-33 activation.

1.7 Hypothesis and Objectives

The Richards' laboratory has recently discovered that IL-33 and Arg1 is markedly elevated in lung epithelial cells by Oncostatin M overexpression in mice. Interestingly, the IL-33 appears predominately cell (nucleus) associated and is not released in detectable levels by live cells. In other systems, IL-33 is released upon necrosis and exacerbates lung fibrosis in mice. Based on such data from our laboratory and evidence within the literature, we postulated that elevation of OSM primes lung tissue for exacerbated Th2/M2 immunopathology and extracellular matrix deposition upon virus infection *in vivo* through elevation of IL-33 and Arg1+ cell accumulation.

1.7.1 AIM 1: Regulation of IL-33 and arginase-1 by OSM using in vivo and in vitro lung systems

Rationale: Previous *in vivo* experiments in our laboratory have demonstrated consistent induction of IL-33 and arginase-1 expression in mouse lung tissues upon over-expression of OSM. In this aim, we focus on further characterizing this pathway by comparing the effect of OSM to another gp130 cytokine IL-6 on the regulation of IL-33 and arginase-1 expression *in vivo* and studying the mechanism used by OSM to enhance IL-33 and arginase-1. *In vitro* OSM stimulation of a mouse epithelial cell line, C10, has shown robust

induction of IL-33. Reproducibility of these findings across various mouse and human lung cells will provide more insight into an OSM-IL-33 axis and its relevance in human pathology and potentially identify new pathways in inflammatory lung disease.

Experimental Approach: Mice were administered Adenovirus encoding OSM (AdOSM) or IL-6 (AdIL-6) to induce transient over-expression of these cytokines and IL-33 and Arg1 regulation was assessed in the tissues by Western blot and RT-PCR. We also measured cytokine levels in the BAL fluid by ELISA, to verify adenoviral administration and assess release of various soluble mediators. Responses in IL-$6^{-/-}$ mice were also tested.

In vitro, various mouse (LA4) and human lung cell lines (A549, MRC-5, HLF) were stimulated with OSM, alone or in combination with other cytokines such as IL-17a, and assessed for IL-33 modulation by Western blot, RT-qPCR and ELISA.

1.7.2 AIM 2: Examine levels of IL-33 release in response to influenza A virus infection and investigate the ability of OSM to potentiate IL-33 release from influenza-infected cells in vitro

Rationale: Alarmins, such as IL-33, are endogenous molecules released upon cellular necrosis or damage and contribute to innate and adaptive immune responses. Upon entry into the lytic cycle, viruses can cause necrosis or uncontrolled cell death by rupturing the cells membrane following replication. Therefore, we hypothesize that OSM up-regulates intracellular IL-33 expression, and subsequent lytic virus infection causes cellular necrosis and increased release of the IL-33 protein.

Experimental Approach: *In vitro* cell cultures of mouse lung epithelial cells (C10) were infected with PR8 influenza virus strains for different time periods. IL-33 levels was

measured in the supernatants by ELISA to assess its release from virally-infected cells. Next, we focused on determining if OSM potentiated the release of IL-33 by stimulating cell cultures with OSM prior to virus infection and measured soluble IL-33 in culture supernatants by ELISA.

1.7.3 AIM 3: Investigate IL-33 release into the bronchoalveolar lavage fluid following AdOSM administration and subsequent virus infection, as well as assessment of potential exacerbations in pathology.

Rationale: In parallel to aim 2, we assessed the release of IL-33 in the bronchoalveolar lavage fluid of mice following respiratory virus infection *in vivo* and assessed the ability of OSM to exacerbate IL-33 release after exposure to viral infections. In addition, the role of the OSM signalling pathway in IL-33 regulation was assessed using $OSMR^{-/-}$ animals.

Experimental Approach: Wild-type and $OSMR^{-/-}$ mice were infected with different strains of influenza, including influenza A/PeurtoRico/8/1934 and influenza A/FM/1/47 (both H1N1 backbone) and subsequently examined at various time points. IL-33 protein will be measured in the BAL fluid by ELISA to determine release from tissues following infection. Additionally, lung tissues were assessed for IL-33 and Arg1 by Western Blot and ELISA to determine if viral infections regulated IL-33 expression. Mice were endotracheally administered with AdOSM to induce up-regulation of intracellular IL-33 expression in lung tissues. Following adenovirus administration, mice were infected with PR8 for various time points, and assessed for IL-33 and Arg1 expression in the BAL fluid and lung tissue. Examination of lung histopathology and collagen deposition was also assessed by histology.

Overall, this thesis aims to understand the regulation of the alarmin IL-33 by Oncostatin M in the context of an Influenza A virus infection. Specifically, experiments completed will expand knowledge associated with the differential function of OSM and IL-6, as well as the release of IL-33 following a pulmonary viral infection in the presence of excess OSM or absence of OSM receptor signalling.

CHAPTER 2

- MATERIALS AND METHODS -

2.0 Animals

Female wild-type C57Bl/6 mice (age = between 6-8 or 8-10 weeks old) were purchased from Charles River (Ottawa, Canada). IL-$6^{-/-}$ female mice were purchased from Jackson Laboratories (Maine, USA). $OSMR^{-/-}$ female mice were bred (C57Bl/6 background) in the McMaster University Central Animal Facility (Hamilton, Canada). IL-$33^{-/-}$ female mice (C57Bl/6 background) were obtained from a collaborator at MedImmune Corporation (Washington, USA). All mice were housed under specific pathogen-free conditions within the McMaster University Central Animal Facility. All experimental procedures were approved by the McMaster University Animal Research Ethics Board (AUP# 14-08-34).

2.1 Adenovirus and Influenza a Virus Administration

Adenovirus vectors AdDel70 (negative control vector), AdOSM, and AdIL-6 were thawed on ice, and diluted in Phosphate-buffered Saline (PBS) to specific concentrations ($3x10^7$ PFU/mouse, $5x10^7$ PFU/mouse, $1x10^8$ PFU/mouse or $2x10^8$ PFU/mouse, as indicated in figure legends). Each mouse was endotracheally intubated with 50µl of virus solution. Influenza A/Puerto Rico/8/1934 or Influenza A/FM/1/47 aliquots were obtained from Dr. Matthew Miller's laboratory (McMaster Immunology Research Centre, Hamilton, Canada) and thawed on ice. Samples were diluted in PBS to specific concentrations (250-20,000PFU/mouse, as indicated in figure legends) and 25uL was administered intranasally

to each mouse. Animals were culled after various time-points following administration and as indicated in figure legends.

2.2 BALF Collection and Lung Tissue Processing

When mice were culled, lungs were washed twice with 0.3 ml PBS to collect bronchoalveolar lavage fluid (BALF). These samples were centrifuged at 12,000 RPM for 2 minutes at 4^{O}C, after which supernatants were collected as BALF and stored at -80 ^{O}C. Cell pellets from each sample were re-suspended and counted using Trypan Blue solution (Life Technologies, Burlington, ON). Cells were then cytocentrifuged and stained with Hema 3 Fixative Solutions (ThermoFisher Scientific) for differential cell analysis. After BALF collection, left lobe of lungs were perfused with 7ml 1xPBS to remove the remaining blood, followed by perfusion with 10% formalin fixative for 48 hours prior to being transferred and stored in 70% ethanol. For histological sections, lungs were embedded in paraffin, cut into 5µm sections and stained with H&E. The right lobes were extracted, immediately frozen in liquid nitrogen and stored in -80°C until further processing. Frozen tissue samples were crushed and equal portions were suspended in either radioimmunopercipiation (RIPA) buffer containing a protease inhibitor cocktail (Aprotinin, PMSF, Na_3VO_4, DTT) for protein or Trizol (ThermoFisher Scientific) for RNA. Protein samples were homogenized using a syringe/needle or homogenizer and centrifuged at 14,000 RPM for 20 minutes at 4°C. Supernatants were collected and stored at -80°C. 200uL of chloroform was added to Trizol samples after homogenization and centrifuged for 20 minutes. The aqueous phase was extracted and 500uL of isopropanol was added for

10 minutes at room temperature and centrifuged again. The supernatant was discarded and the pellet was washed with ethanol. After centrifugation, pellets were re-suspended in RNAse-free water and stored at -80°C until further analysis.

2.3 Cell Culture

2.3.1 He/A Mouse Lung Epithelial Cells (LA4)

LA4 cells were thawed from previously frozen-down vials and cultured under standard conditions (37°C and 5% CO_2) in Dulbecco's Modified Eagle's Medium/F12 (DMEM/F12) supplemented with 10% fetal-bovine serum (FBS), 1% Penicillin/Streptomycin and 1% L-Glutamine. Cells were passaged after reaching 80-90% confluency and used between passage 4-8 in various experiments. No experiment utilized cells beyond passage 8, however passage number prior to freezing is unknown.

2.3.2 C57Bl/6 Mouse Lung Epithelial Cells (TC-1)

TC1 cells were thawed from previously frozen-down vial (obtained from Dr. Brian Lichty's Laboratory) and cultured under standard conditions (37°C and 5% CO_2) in Roswell Park Memorial Institute medium (RPMI) supplemented with 10% fetal-bovine serum (FBS), 0.5% G418, 1% Hepes and 1% L-Glutamine. Cells were passaged after reaching 80-90% confluency and used at passage 4 in various experiments.

2.3.3 Primary Human Airway Epithelial Cells (A549)

A549 cells were thawed from previously frozen-down vial and cultured under standard conditions (37°C and 5% CO_2) in Alpha-MEM medium supplemented with 10% fetal-bovine serum (FBS), 1% Penicillin/Streptomycin and 1% L-Glutamine. Cells were

passaged after reaching 80-90% confluency and used between passage 4-8 in various experiments. No experiment utilized cells beyond passage 8, however passage number prior to freezing is unknown. The details of a specific time-course experiment using A549 cells and multiple cytokine stimulation treatments is outlined in the figure below.

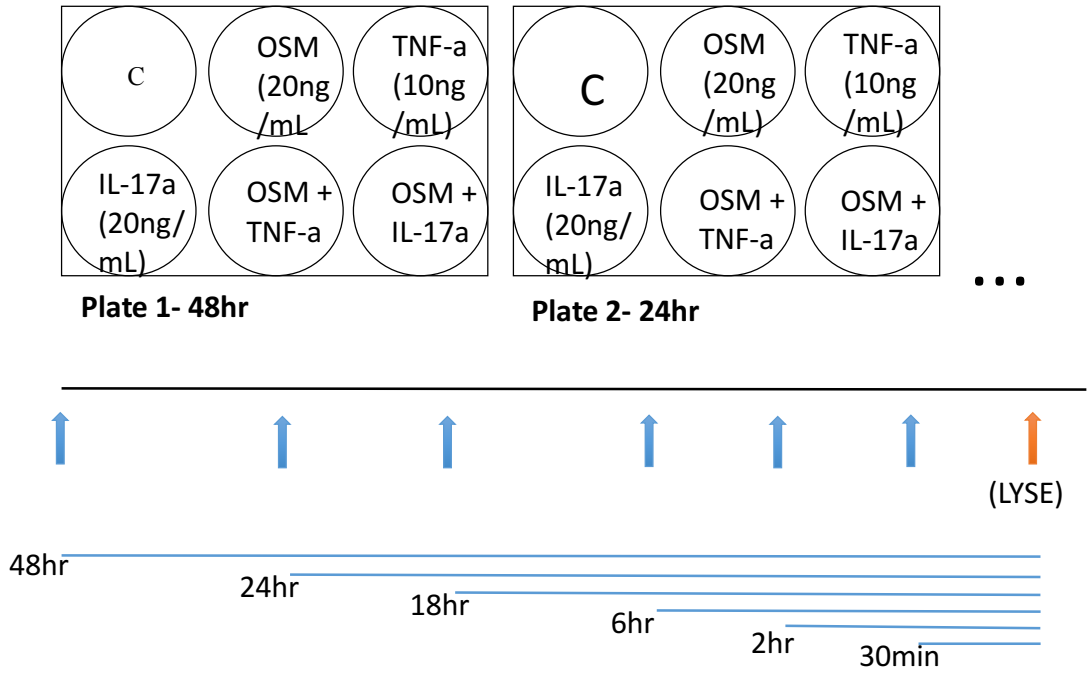

Figure A. A schematic diagram outlining the details of how the A549 time-course experiment was completed. Six 6-well plates were used in this experiment and cells were stimulated at various times. All cells were lysed at the same time.

2.3.4 Human Fetal Lung Fibroblasts (MRC-5)

MRC-5 cells were thawed from previously frozen-down vials and cultured under standard conditions (37°C and 5% CO_2) in Modified Eagle's Medium (DMEM) supplemented with 10% fetal-bovine serum (FBS), 1% Penicillin/Streptomycin and 1% L-Glutamine. Cells were passaged after reaching 80-90% confluency and used between passage 4-8 in various

experiments. No experiment utilized cells beyond passage 8, however passage number prior to freezing is unknown.

2.3.5 Human Primary Fibroblasts (HLF)

HLF cells were thawed from previously frozen-down vials and cultured under standard conditions (37°C and 5% CO_2) in Modified Eagle's Medium-15 (MEM-15) supplemented with 10% fetal-bovine serum (FBS), 1% Penicillin/Streptomycin and 1% L-Glutamine. Cells were passaged after reaching 80-90% confluency and used between passage 4-8 in various experiments. No experiment utilized cells beyond passage 8, however passage number prior to freezing is unknown.

2.3.6 Cytokine Stimulations

Cells were plated at a density ranging from 96,000 cells/well to 300,000 cells/well in 6-well plates or 3200 cells/well in 96-well plates, after being lifted off from 75mm^2 or 150mm^2 tissue culture plates using 0.5% Trypsin-EDTA diluted 10X with sterile PBS. After 24 hours of incubation at 37°C, cells were subjected to various cytokine stimulations (at varying doses and for specific time-points). Recombinant mouse or human cytokines were purchased from R&D Systems or PeproTech and prepared according to manufacturer's protocol.

2.3.7 In vitro Virus Infection

C10 or TC1 cells were plated at a density of 200,000 cells/well in 12-well plates, after being lifted off from 75mm^2 or 150mm^2 tissue culture plates using 0.5% Trypsin-EDTA diluted 10X with sterile PBS. Cells were then incubated overnight at 37°C. Following this incubations, cells were stimulated with recombinant mouse OSM at (5ng/mL) for 24 hours.

Frozen PR8 virus aliquots ($1.5x10^8$ PFU) were then thawed on ice and diluted to specific concentrations (MOI= 3 or 5) in flu-infection media (obtained from the Miller Laboratory). Stimulation media was then removed, cells were washed with PBS twice and 200ul of virus containing media was then added for 1 hour at 37°C. Virus containing media was then removed and 600-1000uL of fresh RPMI (supplemented with 10%FBS) media was added to wells. Supernatants were then collected for analysis after various time points as indicated within figure legends and inactivation reagent (paraformaldehyde) was added to each sample (1/100 dilution, provided by Miller lab). Samples were kept at 4°C for 24-48 hours and centrifuged at 10K rpm at 4°C for 10 min to remove debris. Samples were then stored at -80°C until analysis. Please refer to the diagram below detailing the experiment.

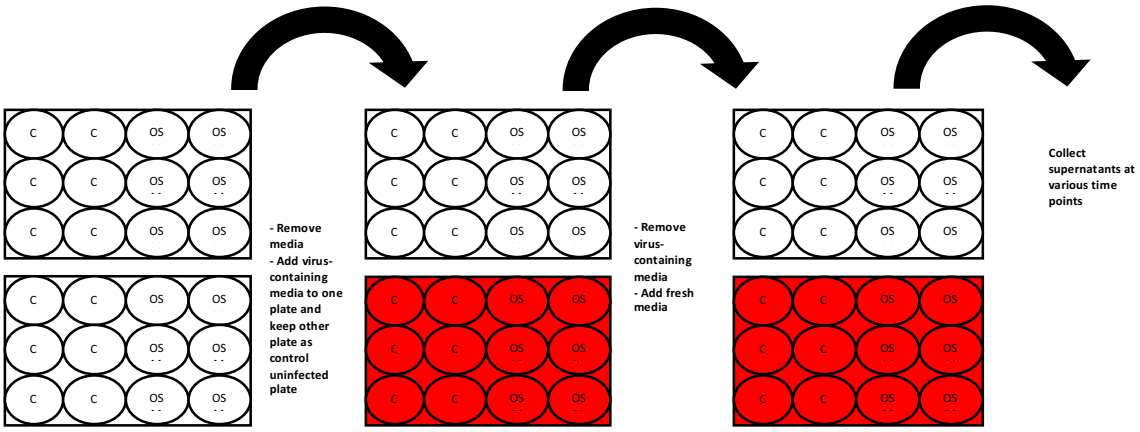

Figure B. Schematic diagram outlining *in vitro* virus-infection experiment. Cells stimulated with OSM (5ng/mL) for 24 hours prior to PR8 virus infection. Red plate = virus added, White plate = control uninfected plate.

2.3.8 Preparation of Cell Lysates

After experiment specific time-points and stimulations, supernatants were collected and

stored in -20°C and cells were washed twice with PBS. 200uL (for 6-well plate) of RIPA containing a protease inhibitor cocktail (30uL/mL Aprotonin, 5uL/mL sodium orthovanadate (Na_3VO_4), 5uL/mL phenylmethylsulfonyl fluoride (PMSF), and 1uL/mL diothioretiol (DTT)) was then added on top of cells on ice. Wells were then scrapped with cell scrappers and ~180uL of sample was collected in Eppendorf tubes and kept on ice for 1 hour at room temperature. Samples were then sheered using a 23G needle and syringe for approximately 30sec each and centrifuged for 10min at 4°C. Supernatants were collected and stored in -80°C for future analysis. Alternatively, RNA was isolated from cells following a detailed protocol from a commercially available PureLink mini RNA extraction kit (Life Technologies, Burlington, Canada).

2.4 Preparation of Lung Homogenates and RNA Extraction

Following sacrifice, a portion of mouse lung tissue was extracted, immediately frozen in liquid nitrogen and stored in -80°C until processed further. Frozen tissue samples were crushed and aliquoted in radioimmunopercipiation (RIPA) buffer for protein extraction (60%) or Trizol for RNA extraction (40%). RIPA samples were homogenized using a syringe/needle or homogenizer and centrifuged for 20 minutes at 4°C. Supernatants were collected and stored at -80°C. 200uL of chloroform was added to Trizol samples after homogenization and centrifuged for 20 minutes. Aqueous phase was extracted and 500uL of isopropanol was added for 10 minutes at room temperature and centrifuged again. The supernatant was discarded and the pellet was washed with ethanol. After centrifugation, pellets were re-suspended in RNAse-free water and stored at -80°C until analysis.

Protein concentration of cell lysates as well as whole lung homogenates were determined using Bradford Assay. Total cell lysates were diluted (1:32) and whole lung homogenates were diluted (1:100) in distilled water and compared to bovine serum albumin (BSA) standard (0-14ug BSA). 40uL of Bio-Rad Protein Assay (Bio-Rad, Hercules, CA, Cat# 500-0006) was added to each sample to make a 20% final concentration. The absorbance of each sample was determined using SpectroMax spectrometer at 595nm.

2.5 Western Blot Analysis

Whole lung homogenate or cell lysate samples were prepared using distilled water and and 5x reducing buffer (10% SDS, 25% 1M Tris (pH 6.8), 0.001% bromophenol blue, 5% 2-mercaptoethanol, 50% glycerol and ddH_2O) and boiled at 90°C for 5 minutes. Samples were then loaded onto SDS-PAGE gels (15-20ug protein/well) and separated by electrophoresis at 120V for 1 hour and transferred to nitrocellulose membranes at 400 mA for 1 hour by standard methods. Following blocking for 1 hour (TBS/Odyssey Blocking buffer – Mandal, Guelph, Canada), primary antibodies mouse IL-33 (R&D Systems Cat#AF3636), mouse Arg-1 (BD Biosciences Cat#610708), pSTAT3 (Cell Signaling Cat#9145), STAT3 (Cell Signaling Cat#4901), pSTAT6 (Cell Signaling Cat#9361), STAT6 (Santa Cruz #sc-981), pSTAT1 (Cell Signaling Cat#9171), STAT1 (Cell Signaling Cat#9172) and β-Actin (Santa Cruz Cat#sc-1616) were used to probe membranes overnight at 4°C. Blots (membranes containing protein) were washed the following day with TBS+0.15%Tween-20, and secondary antibodies (Anti-Goat; Mandel Scientific Cat# LIC92668074, Anti-Rabbit; Mandel Scientific Cat# LIC92632213, or Anti-Mouse; Mandel

Scientific, Cat#LIC92632212) were added for approximately 1 hour away from light. After 3 subsequent washes, blots were imaged using Odyssey LI-COR Imaging technologies. ImageJ software (National Institutes of Health) was used to analyze band intensity through densitometry. Band intensity was calculated by software and expressed as fold-change relative to control.

2.6 Immunohistochemistry

Histological sections were de-paraffinised, then treated with 0.5% peroxide in methanol for 10 minutes and blocked with 5% normal goat serum (NGS). Sections were then incubated with an anti-arginase-1 antibody (BD Biosciences Cat#610708) at a 1/100 dilution, followed by incubation with a biotinylated goat anti-mouse antibody (Vector Laboratories) at a 1/500 dilution. Sections were then treated with 1/50 dilution of streptavidin-peroxidase, developed in Nova Red peroxidase substrate (Vector Laboratories) and counterstained with hematoxylin.

2.7 Enzyme-Linked Immunosorbent Assay (ELISA)

Cytokine concentrations were measured in the supernatants of cell cultures or in the bronchoalveolar lavage fluid of mice using commercially available ELISA kits from R&D Systems. The limit of detection for the ELISAs are as follows: human and mouse MCP-1 IL-33-15.65 pg/mL; mouse OSM- 6.25 pg/mL, mouse IL-6- 15.65pg/mL.

2.8 Reverse-Transcription Polymerase Chain Reaction (RT-PCR)

Genomic DNA was removed from all RNA samples (Ambion DNA-free kit - Life Technologies, Burlington, ON- Cat. #AM1906 as directed by manufacturer's protocol) and RNA concentrations and contamination levels were determined using NanoVue spectrophotometer (General Electric, GE). Reverse transcription of RNA into complementary DNA (cDNA) was performed using Invitrogen Superscript II Reverse Transcriptase kit (Life Technologies, Burlington, Cat# 18064014). The resulting cDNA was diluted to 2 ng/ml and stored at -20°C. Samples were prepared in duplicates or triplicates in 96-well PCR plate (FroggaBio, North York, ON, Cat# 3426-00) with Taqman Universal Master Mix containing Uracil-N-glycosylase (UNG) and predetermined assay reagents (PDAR) purchased from Life Technologies (Burlington, ON) for mouse IL-33/IL-33R and Arg1/NOS2. PDAR for 18S was used as the endogenous control gene. Plates with prepared samples read and analyzed in ABI 7900HT Real-Time PCR System (Applied Biosystems, Foster City, CA). The resulting data was corrected to 18S threshold cycle value (CT value) and expressed at fold change relative to control. Protein-specific mRNA from cells or lung tissues were quantified using RT-PCR.

2.9 Statistical Analysis

GraphPad Prism version 5.0 or 6.0 for Macs (GraphPad Software, San Diego, CA) was for all statistical analyses. Figures represent mean values ± SEM. One- or Two-way analysis of variance (ANOVA), and either Tukey or Bonferroni post-hoc analyses were used to assess statistical differences between means for multiple groups. Difference between means were considered statistically significant at (Confidence Interval) CI of $P<0.05$.

CHAPTER 3

- REGULATION OF IL-33 AND ARGINASE-1 BY OSM IN MOUSE LUNG SYSTEMS -

AUTHOR'S PREFACE TO CHAPTER 3

Figures within this chapter have been modified and utilized in various publications or manuscript submissions. Figure 2 is incorporated into a published paper: **Richards, C.D, Izakelian, L. Dubey, A., Zhang, G., Wong, S., Kwofie, K., Qureshi, A., Botelho, F.** ***Regulation of Il-33 by OSM in mouse lung epithelial cells.*** **Mediators of Inflammation. August 2016.** Please be advised that the figure illustrated in this thesis is similar to the figure illustrated in the published paper and that the author of this thesis is also third author of the published paper cited above due to her work with regulation of IL-33 by OSM *in vitro* lung systems.

Additionally, many of the other results illustrated and described within this chapter have been used in a manuscript, submitted to Journal of Leukocyte Biology, titled "**Separate roles of IL-6 and Oncostatin M on mouse macrophage polarization *in vitro* and *in vivo***." The author of this thesis is also first author of the submitted manuscript.

CHAPTER 3

- REGULATION OF IL-33 AND ARGINASE-1 BY OSM IN MOUSE LUNG SYSTEMS -

3.1 *In vitro* Results in Mouse Lung Cells

Since IL-33 has been reported to be involved in augmenting the fibrotic outcome in mouse lung systems, initial experiments examined the regulation of this cytokine in response to OSM *in vitro* and *in vivo*. In order to accurately determine IL-33 detection by Western blot, comparison of *in vivo* lung samples from C57Bl/6 mice administered AdDel70 or AdOSM (Day 7) and unstimulated- or OSM-stimulated C10 cell lysates to varying amounts of recombinant mouse mature IL-33 protein (R&D Systems) was completed. **Figure 1A** demonstrates that IL-33 protein detected from control and AdOSM-treated animals, as well as unstimulated or OSM-stimulated C10 cells, is primarily full-length IL-33 at approximately 35kDa using a primary polyclonal IL-33 antibody (R&D Systems). Recombinant mature IL-33 appears at the expected molecular weight size of 18kDa and was not present in OSM-stimulated samples. In order to verify the quantification method by densitometry, a standard curve was created with increasing amounts of recombinant IL-33 and the corresponding signal value by densitometry, using Image Lite Studio (version 5.2). The resulting standard curve appeared linear, in which 1ng, 2ng, and 5ng of IL-33 protein showed proportionally increased band signal values (**Figure 1B**). These results confirm that OSM-induced IL-33 protein is primarily in its full-length form in this system and is consistent with previous data demonstrating nucleus-associated IL-33

expression in type 11 alveolar epithelial cells upon OSM stimulation[52].

Following preliminary experiments with BALB/c mouse lung epithelial cells (C10) by previous members of the laboratory, IL-33 production was then assessed after OSM stimulation in LA4 mouse lung epithelial cell line, derived from He/A mouse origin, in order to assess reproducibility in other cell lines. Specifically, LA4 cells were stimulated with 20ng/mL OSM, 20ng/mL TGF-β, 20ng/mL IL-17a or combinations of OSM and TGF-β or IL-17a for 18 hours. In **Figure 2A**, Western blots are shown for whole cell lysates probed for IL-33, phospho-STAT3, total STAT3, and β-Actin. IL-33 expression increased by approximately 5-fold in OSM-treated cells, compared to control. TGF-β and OSM treated cells produced less IL-33 protein (**Figure 2B**). Additionally, the effects of IL-17a on regulation of IL-33 was also studied based on previous findings in our laboratory demonstrating synergy between IL-17a and OSM in up-regulating IL-33 levels in human smooth muscle cells (data not shown). In contrast to the previous results, IL-17a alone did not induce IL-33 protein expression, and IL-17a in combination with OSM produced a similar level of IL-33 in cells treated with OSM alone. These experiments demonstrate the ability of OSM to up-regulate IL-33 protein expression in LA4 mouse lung epithelial cells.

The analysis was further expanded by assessing the effects of OSM on IL-33 protein regulation in the C57Bl/6 mouse lung epithelial cell line, TC1, obtained from a collaborator. This particular cell line has been previously shown to release IL-33 into cell culture supernatants following an Influenza A virus infection *in vitro* (Kearley et al., 2014) and therefore is another relevant cell line to test. An initial dose-response *in vitro* experiment showed increased levels of IL-33 protein by western blot following 24 hour

OSM stimulation of TC1 cells at 1 ng/mL, 5 ng/mL, 10 ng/mL and 20 ng/mL (**Figure 3A**). Phospho-STAT3 in these cells were also elevated upon OSM stimulation, consistent with previous results demonstrating STAT3 activation by OSM in lung stromal cells. These preliminary findings using this cell line suggests that OSM can prime these cells for increased intracellular IL-33 protein expression and a subsequent virus infection may cause exacerbated release.

3.2 *In Vitro* Results in Human Lung Cells

Figures 4-6 summarizes findings from preliminary *in vitro* experiments assessing IL-33 production after OSM stimulation in various human stromal lung cells. Due to the challenge in obtaining human primary type II alveolar epithelial cells, the readily available cancerous cell line, A549, was used instead to assess the effects of OSM on IL-33 expression in human type II alveolar epithelial cells. In the first experiment, A549 cells were plated at a density of approximately 100,000 cells/well in a 6-well plate using Alpha-MEM media supplemented with 10% FBS. The following day, cells were stimulated with 20ng/mL OSM, 10ng/mL TNF-α, or combination of OSM and TNF-α for 24 hours under standard conditions. TNF-α has previously been shown to regulate IL-33 in A549 cells and therefore was used as a comparator cytokine. **Figure 4A** shows the Western Blots for whole cell lysates probed for IL-33 (Nessy-1 primary Ab), phospho-STAT3, and β-Actin. Densitometry is shown in **Figure 4B.** A 3-fold increase in IL-33 protein expression was observed from cells treated with OSM alone, whereas there was a 7-fold increase in IL-33 from cells treated with both OSM and TNF-α, compared to control. IL-33 mRNA

expression was increased by 8-fold in OSM-treated cells and 14-fold higher in TNF-α-treated cells, compared to control (**Figure 4C**). However, insufficient RNA was isolated from the OSM and TNF-α sample, and therefore could not be analyzed by RT-qPCR.

Following preliminary results obtained from the A549 cells, a time-course experiment was performed to optimize the conditions for maximum IL-33 production. Approximately 300,000 cells/well were plated in 6-well plates under standard conditions for 24 hours prior to stimulation. Cells were stimulated with 20ng/mL OSM, 10ng/mL TNF-α, 20ng/mL IL-17a, or combinations of OSM and TNF-α or IL-17α for 30min, 2hr, 6hr, 18hr, or 24 hr. Whole cell lysates were prepared and assessed for IL-33 protein expression, as well as phosphorylation of STAT3 to verify OSM stimulation, by Western blot. IL-33 was not detectable at shorter time-points, however induced by 6 hours in OSM and TNF-α treated samples, and more apparent at 24 hours in all OSM treated samples (**Figure 5A**). Interestingly, IL-17a as well as TNF-α did not regulate IL-33 alone or in combination with OSM. Densitometry of the IL-33 band signal is summarized in **Figure 5B,** which demonstrates a clear time-dependent increase in OSM-induced IL-33 expression in A549, human type II alveolar epithelial cells. Phospho-STAT3 levels were induced in OSM treated samples, with the strongest signal appearing at 30 minutes following stimulation and still induced at 24hours post-stimulation (**Figure 5C**).

To determine if the band signal observed was consistent between two different primary antibodies, the 24hr and 48hr samples were re-run and probed for IL-33 using a monoclonal Nessy-1 antibody or polyclonal R&D antibody, as shown in **Figure 4D**. Both antibodies detected an IL-33 signal slightly below the 35kDa marker that was only present

in OSM treated samples. This signal is more pronounced in samples stimulated for 48hrs compared to shorter time points. Human IL-33 has been reported to be approximately 31kDa in size, which corresponds to the approximate size of the observed signal.

Next, similar experiments were conducted using human lung fibroblasts in order to determine if OSM could regulate IL-33 expression in other stromal cell types. In the first experiment, human fetal lung fibroblasts (MRC-5s) were cultured in DMEM medium supplemented with 10% FBS and plated at a density of 96,000 cells/well in a 6-well plate under standard conditions. Cells were then stimulated with increasing doses of OSM (0-20ng/mL) for 18 hours under standard conditions. IL-33 expression, measured by Western blot, remained constant for all treatments and did not increase in a dose-dependent manner (**Figure 6A**). As a positive control, phospho-STAT3 was present in the OSM treated samples and demonstrated cell responsiveness to OSM stimulation (**Figure 6A**). Additionally, human monocyte chemoattractant protein-1 (MCP-1) was measured in the supernatants based on previous experiments in the laboratory that demonstrated the ability of OSM to induce MCP-1 expression in cell culture supernatants of human smooth muscle cells. Consistent with previous results, a dose-dependent increase in MCP-1 was observed following OSM stimulation and therefore further validates cellular activation by OSM within this experiment (**Figure 6C**). A following experiment was performed to assess the synergy between OSM and TGF-β or IL-17a on regulating IL-33 expression in human lung cells, similar to the previous experiment with LA4 cells. In this experiment, cells were plated at a density of 96,000 cells/well in a 6-well plate under standard conditions. After 48 hours, cells were stimulated with OSM (20ng/mL), TGF-β (20ng/mL), IL-17a

(20ng/mL) or combinations of OSM and TGF-β or IL-17a for 18 hours. IL-33 protein expression was similar in all treatment groups as demonstrated by the Western blot in **Figure 6C**. Similarly, phosphorylation of STAT3 was present in OSM treated samples, verifying stimulation by OSM. In a parallel experiment, RNA was extracted and IL-33 gene expression was measured using RT-PCR. Levels of IL-33 mRNA varied for all treatment groups, except OSM and TGFβ (**Figure 6D**). For this sample, the comparative threshold values were undetermined, and therefore were below the detectable limit.

Following preliminary results from MRC-5 cells, primary human lung fibroblasts (HLF) were then used in a subsequent experiment. HLFs were grown in MEM/F15 media supplemented with 10% FBS and plated at a density of 96,000 cells/well in a 6-well plate under standard conditions. After 48 hours, cells were stimulated with increasing doses of OSM (0-40ng/mL) for 18 hours. IL-33 protein expression were similar in all treatment groups and did not increase in a dose-dependent manner, according to the Western Blot results shown in **Figure 6E**, although activation of STAT3 was observed for all groups stimulated with OSM. In **Figure 6F**, MCP-1 levels from culture supernatants were analyzed using ELISA. Results indicated an increase in MCP-1 following OSM stimulation in a dose-dependent manner.

Overall, these experiments confirm that OSM up-regulated IL-33 protein expression in human and mouse alveolar epithelial cells in comparison to other cell-types, such as human lung fibroblasts.

3.2 *In Vivo* Results

OSM is part of the IL-6 family and shares many downstream signaling effects with IL-6, such as activation of the STAT3 signalling pathway. Laboratory has previously shown that OSM can induce IL-6 expression in mouse lung systems, and therefore may be contributing to the observed effect on IL-33 expression. Thus, further characterization of the OSM/IL-33 pathway *in vivo* was completed by comparing the effects of OSM and IL-6 on IL-33 regulation.

In an experiment comparing OSM and IL-6 overexpression *in vivo*, C57Bl/6 mice were endotracheally administered adenovirus control vector (AdDel70) or adenovirus encoding OSM (AdOSM) or IL-6 (AdIL-6) to induce transient pulmonary overexpression of the corresponding cytokines. At day 7, mice were euthanized and bronchoalveolar lavage fluid (BAL) and lung tissue was extracted for further analysis. IL-33 protein expression was significantly up-regulated in lung homogenates of four mice overexpressing OSM (**Figure 7A**)**.** However, this same induction was not observed for mice administered AdIL-6. Densitometry in **Figure 7B** shows a slight increase in IL-33 relative to control vector for AdIL-6-treated mice, however this was very low compared to the 20-fold increase in AdOSM-treated animals ($p<0.0001$). An increase in phospho-STAT1 signal was observed in both AdOSM and AdIL-6-treated mice, compared to control. AdIL-6 (but not AdOSM) also increased total amounts of STAT1 protein (**Figure 7A**). Assessment of total lung mRNA showed there was approximately a 20-fold increase in IL-33 mRNA from AdOSM-treated mice, whereas there was only a 7-fold increase in AdIL-6 treated mice, compared to the AdDel70 control vector (**Figure 7D**). The IL-33 receptor (IL-33R/ST2) mRNA

expression also followed a similar pattern, with an increased expression in mice treated with AdOSM and only a slight increase in mice treated with AdIL-6 (**Figure 7D**). In order to determine whether the induction of IL-33 was sustained past 7 days, a subsequent experiment was performed on C57Bl/6 mice and culled animals at Day 7 and Day 14. The OSM-induced IL-33 signal was still elevated at Day 14 following vector administration, as observed by Western blot in whole lung homogenates (**Figure 7E**). Additionally, this increase in IL-33 protein was sustained to Day 21 post-administration (in house data not shown). However, IL-33 protein levels were lower at Day 14 compared to Day 7, suggesting that IL-33 regulation by OSM peaks at 7-days post-administration (**Figure 7F**).

Following analysis of IL-33 *in vivo*, the regulation of Arg-1 regulation by OSM was then examined. Previous studies showed that pulmonary overexpression of OSM induces Arg-1 expression and Arg-1^+ cells in C57Bl/6 mouse lungs[25], which is correlated to increased IL-33 expression. Arg-1 expression was compared between mice treated with AdOSM or AdIL-6. Confirming overexpression of vector-encoded cytokines in the system, we observed increased levels of OSM or IL-6 in the BALF of mice treated with AdOSM or AdIL-6 (respectively) was observed (**Figure 8A and 8B**). AdOSM induced IL-6 expression in BALF as previously published[25], but levels were not as high in AdIL-6 treatments. OSM protein levels were not detectable in BALF of AdIL-6 nor Addel70 treated mice. Arg-1^+ cells were elevated in the lung tissue of mice intubated with AdOSM, but not by AdIL-6, as assessed by immunohistochemistry (**Figure 8C**). Expression of Arg-1 was primarily localized to cells resembling macrophage morphology within the alveolar spaces. Similarly, western blot analysis of whole lung homogenates demonstrated an

induction of Arg-1 protein signal (50-fold) in the lungs of mice treated with AdOSM, compared to AdDel70 or AdIL-6 (**Figure 8D and 8E**). Two bands were observed by Western blot using the Arg-1 primary antibody, which has been previously reported as two isoform variants of Arg-1 protein[80]. We also observed increased phosphorylation of STAT3 in total lung extracts was also observed upon overexpression of OSM or IL-6 (**Figure 8F**) further indicating that sufficient levels of OSM or IL-6 were present to induce biological effects. Arg-1 mRNA levels were significantly increased in total lung homogenates of mice treated with AdOSM, whereas homogenates from AdIL-6 treated mice showed no detectable levels above AdDel70 control (**Figure 8G**), consistent with Arg-1 protein data. iNOS (Nos2) mRNA levels in lung homogenates among the three treatment groups were similar and detected at significantly lower levels compared to Arg-1. Combined, this data suggests that overexpression of OSM *in vivo* promoted elevation of Arg-1 expressing cells, whereas IL-6 overexpression did not.

Other products in the cytokine milieu present in the BALF of mice administered AdDel70, AdOSM and AdIL-6 were also assessed. Over-expression of OSM resulted in elevated levels of IL-4, IL-13, IL-5, eotaxin-1 (CCL-11) and eotaxin-2 (CCL24) (**Supplementary Figure 2A-E)** as well as IL-6 (shown in **Figure 8B)**. In contrast, AdIL-6 administration led to increased levels of IFN-γ, monokine-induced by interferon-gamma (MIG/CXCL9), and interferon-gamma inducible protein-10 (IP-10/CXCL10) in BALF compared to mice receiving the control vector (AdDel70) or AdOSM (**Supplementary Figure 2F-I**). Both AdOSM and AdIL-6 treated mice showed increased levels of the neutrophil chemoattractant, KC chemokine (CXCL1) (**Figure 2J**). These results indicate

that OSM overexpression led to the up-regulation of Th2-skewed cytokines, while IL-6 overexpression induced a cytokine profile more towards a Th1-associated inflammatory microenvironment.

Since OSM up-regulates IL-6 expression *in vivo,* it was next assessed whether IL-6 was required for AdOSM-induced Arg-1+ macrophage accumulation or IL-33 expression by using IL-$6^{-/-}$ mice. IL-$6^{-/-}$ and wild-type mice were administered AdDel70 and AdOSM and lung tissue was extracted for mRNA, protein and histological analysis at day 7 following vector administration. Upon over-expression of OSM, IL-$6^{-/-}$ mice demonstrated complete attenuation of Arg1 protein signal and mRNA levels within whole lung homogenates, compared to wild-type mice which showed an approximately 100-fold increase in Arg1 protein signal (**Figure 9A, B, D**). In contrast to Arg1, OSM-induced IL-33 protein expression was not regulated by IL-6 *in vivo*. Il-33 protein signal was increased upon OSM overexpression by approximately 5-fold increase within whole lung homogenates and was similar between wild-type and IL-$6^{-/-}$ mice (**Figure 9A, C**). Similarly, IL-33 mRNA levels were induced by approximately 15-fold following OSM overexpression in both wild-type and IL-$6^{-/-}$ animals (**Figure 9E**). Overall, these results suggest that OSM-induced Arg-1 protein is dependent on IL-6 expression, while up-regulation of IL-33 is not.

These *in vivo* results were consistent with *in vitro* data (experiment performed by Ehab Ayaub in Dr. Ask's group) using bone-marrow derived macrophages. BMDMs were stimulated for 24 hours with M1 (IFNγ/LPS) and M2 (IL-4/IL-13) cytokine cocktails (as previous [81]) to skew M1 and M2 macrophage phenotypes, and tested in combination with

varying doses of recombinant OSM, IL-6, and another gp130 cytokine comparator, LIF. After 30 hours of cytokine stimulation, polarization of macrophages toward the Arg-1 expressing M2 phenotype was assessed by measuring changes in arginase activity in parallel to a typical M1 macrophage phenotype product nitric oxide (NO). Results indicated increased arginase enzymatic activity in BMDMs stimulated with IL-4/IL-13 (**Supplementary Figure 2A**). OSM, IL-6 or LIF stimulation alone were not sufficient to elevate arginase activity. While neither OSM nor LIF (at 5 or 50 ng/ml) could modulate IL-4/IL-13 (M2 stimuli) -induced arginase-1, IL-6 further elevated Arg-1 activity in a dose dependent manner. In the same cells, IFNγ/LPS stimulus markedly enhanced NO levels. Neither IL-6, OSM or LIF stimulation alone elevated NO levels, nor did they modulate the response to IFNγ/LPS (**Supplementary Figure 2B**). In contrast to BMDMs, alveolar macrophages were not responsive to IL-14/IL-13 stimulation with respect to elevation of arginase activity (**Supplementary Figure 2C**). However, in the presence of IL-6, alveolar macrophages demonstrated an enhanced M2 phenotype, albeit the response was markedly lower than that in BMDM (OSM had no affect, data not shown). Alveolar macrophages showed increases in NO levels in response to the M1 cytokine cocktail, although there was no effect of IL-6 on this phenotype (**Supplementary Figure 2D**).

To verify the currently used IL-33 detection methods, such as Western blot antibodies and ELISA Duoset kits, IL-33$^{-/-}$ animals were obtained from MedImmune (Dr. R. Kolbeck) and analyzed as a negative control. IL-33$^{-/-}$ mice were endotracheally administered AdDel70 control vector or AdOSM for 7 and 14 days and parallel experiments were performed using wild-type mice for comparison. **Figure 10A** shows a complete

absence of IL-33 protein expression in IL-33$^{-/-}$ mice (C57Bl/6 background) as assessed by Western blot. Phospho-STAT3 was measured as a positive control to demonstrate OSM activity in the IL-33 deficient animals. Following analysis of whole-lung homogenates, BALFs from C57Bl/6 wild-type and IL-33$^{-/-}$ mice were assessed for IL-33 and OSM to verify OSM activity after adenovirus administration. Interestingly, IL-33$^{-/-}$ mice produced less OSM at day 7 in comparison to wild-type mice administered AdOSM. These results indicate a potential role for IL-33 in regulating endogenous OSM expression in C57Bl/6 mice, however future studies are needed to explore this possibility. At day 7, IL-33 signals detected by ELISA in the BALF are significantly decreased in both wild-type and IL-33$^{-/-}$ mice treated with AdOSM (**Figure 10C**). This could indicate non-specific binding of the IL-33 ELISA since a signal was observed in AdDel70-treated IL-33$^{-/-}$ mice, and therefore indicated a concern for future analysis using this method of detection. Due to the large variation and reduction in IL-33 signal by ELISA within AdOSM-treated animals, it was postulated that the presence of proteases or competitive inhibitors within the BALF may be interfering with the ability to detect IL-33. Therefore, various optimization experiments were performed in order to provide a rationale for these results. By spiking 3 concentrations (62.5pg/mL, 125pg/mL and 250pg/mL) of the IL-33 standard curve from the ELISA with various BAL samples from AdDel70 or low and high dose of AdOSM-treated mice and comparing the OD(450nm) values, results indicated that high dose AdOSM-BAL had a small and not major inhibitory effect within the ELISA (**Figure 10D**). Overall, these results suggest that there is no strong effect of the BALF on inhibiting IL-33 signal within the ELISA (R&D) that is being used.

Following optimization experiments for the IL-33 R&D ELISA, we then tested lung homogenate samples and cell lysates were tested, which were prepared using RIPA buffer. This buffer contains the reducing agent sodium dodecyl sulfate (SDS), which at high concentrations can interfere with the antibody interactions within an ELISA. However, RIPA buffer utilized for these samples was prepared with 0.1% SDS, which others have used in this assay and at low concentrations considered to not effect the ELISA results overtly. Therefore, the lung homogenates of the IL-33$^{-/-}$ samples were first assessed at a 1:200 dilutions. IL-33 levels detected were markedly increased in AdOSM-treated wild-type mice, compared to IL-33$^{-/-}$ AdOSM-treated mice (**Figure 11A**). Background or non-specific signal for IL-33 within the IL-33$^{-/-}$ animal samples were observed, which were also present in AdDel70-treated wild-type control animal samples. Therefore, within the lung homogenates there is non-specific background using this ELISA when measuring IL-33 protein. Following a similar protocol, OSM levels were measured within the lung homogenates using the R&D mouse specific ELISA. OSM levels were similar in both AdDel70 and AdOSM treated animals, in both the wild-type and IL-33$^{-/-}$ samples. These results suggest that OSM levels at 7-days following vector administration was no longer elevated within this experiment, however levels appear similar between both mouse strains, which is inconsistent with results obtained from analyzing the BALF, which showed decreased OSM levels within IL-33$^{-/-}$ animals. Overall, since OSM levels appear similar in the tissue homogenates, we can further analysis of the phenotypic differences between the two mouse strains were possible. Interestingly, complete attenuation of OSM-induced Arg-1 signal in the lung homogenates of IL-33 deficient mice was observed, as assessed by

Western blot (**Figure 11C and D**). This data suggests that IL-33 was required for OSM-induced Arg-1 expression, in addition to the previously reported requirement for IL-6 and IL-4/13 signalling. This enables speculation that IL-33 may regulate Th2 cytokines required for Arg-1 induction in the presence of OSM-induced lung inflammation, however further experimentation is needed to investigate this possibility.

Next, the IL-33 ELISA detection method was utilized to analyze several other samples. Initial experiments were completed using the Mammalian protein extraction reagent (MPER) which had been previously used to lyse cells for use in ELISAs. However, experiments using this lysis buffer in the C10 epithelial cell line produced 10 times less protein detected (in house data). In one experiment, C10 cells were cultured at 200,000 cells/well and stimulated with OSM (5ng/mL) for 24 hours and lysed using the MPER buffer (200uL with 50nM of NaCl). These cell lysates were used in the IL-33 R&D ELISA at a 1:2 and 1:20 dilution (**Figure 12A**). Approximately, 750pg/mg of protein was detectable following OSM stimulation, and this trend was consistent with the Western blot detection method. Additionally, in a parallel experiment, C10 cells (200,000 cells/well) were cultured and stimulated with OSM (5ng/mL) and lysed using RIPA buffer. Using these samples in the ELISA at a 1:50 dilution, we were able to detect 4000pg/mg of IL-33 from cells stimulated with OSM (**Figure 12B**). IL-33 levels from lung homogenates prepared in RIPA buffer from previous experiments was also assessed, including. we first IL-33 from lung homogenates from Balb/c mice treated with AdDel70, AdOSM low dose ($2x10^7$ PFU) or high dose ($5x10^7$ PFU) at Day 2. At a 1:200 dilution in the ELISA, a dose-dependent increase in IL-33 protein upon was observed AdOSM treatment (**Figure 12C**).

Following these results, OSM levels with the lung homogenates were assessed by ELISA, and these samples demonstrated a robust increase in OSM protein in lung tissue from mice treated with high dose AdOSM at day 2 (**Figure 12D**). Comparing IL-33 and OSM levels by ELISA C57Bl/6 mice to Balb/c mice treated with AdDel70 or AdOSM (Day 7), IL-33 levels were markedly up-regulated in both C57Bl/6 and BALB/c mice treated AdOSM, however there was significantly less IL-33 in Balb/c mice (**Figure 12E**). Additionally, OSM was elevated upon AdOSM treatment in Balb/c mice at 7 days post-vector administration, whereas OSM levels were similar to control in C57BL/6 mice (**Figure 12F**).

3.4 Figures and Figure Legends

Figure 1. Immunoblot analysis detects increases in full-length pro-IL-33 in response to OSM. (A) Lung tissue homogenate protein from 3 individual BALB/c mice treated with AdDel70 (lanes 1-3) or AdOSM vector (lanes 4-6), or C10 alveolar epithelial cell protein lysates from unstimulated (lane 7) or OSM-stimulated cells (treated with 5 ng/ml OSM for 18 hours, lane 8) were separated by 12% SDS-PAGE. Blots were probed for IL-33 (top panel) and β-Actin (bottom panel). Lanes 9 and 10 contained samples of 1 ng and 2 ng (respectively) recombinant mature IL-33 (R&D systems). BLUeye molecular weight marker migration is shown on the left. (B) Standard curve generated to determine quantitative value of IL-33 band signal.

Figure 1

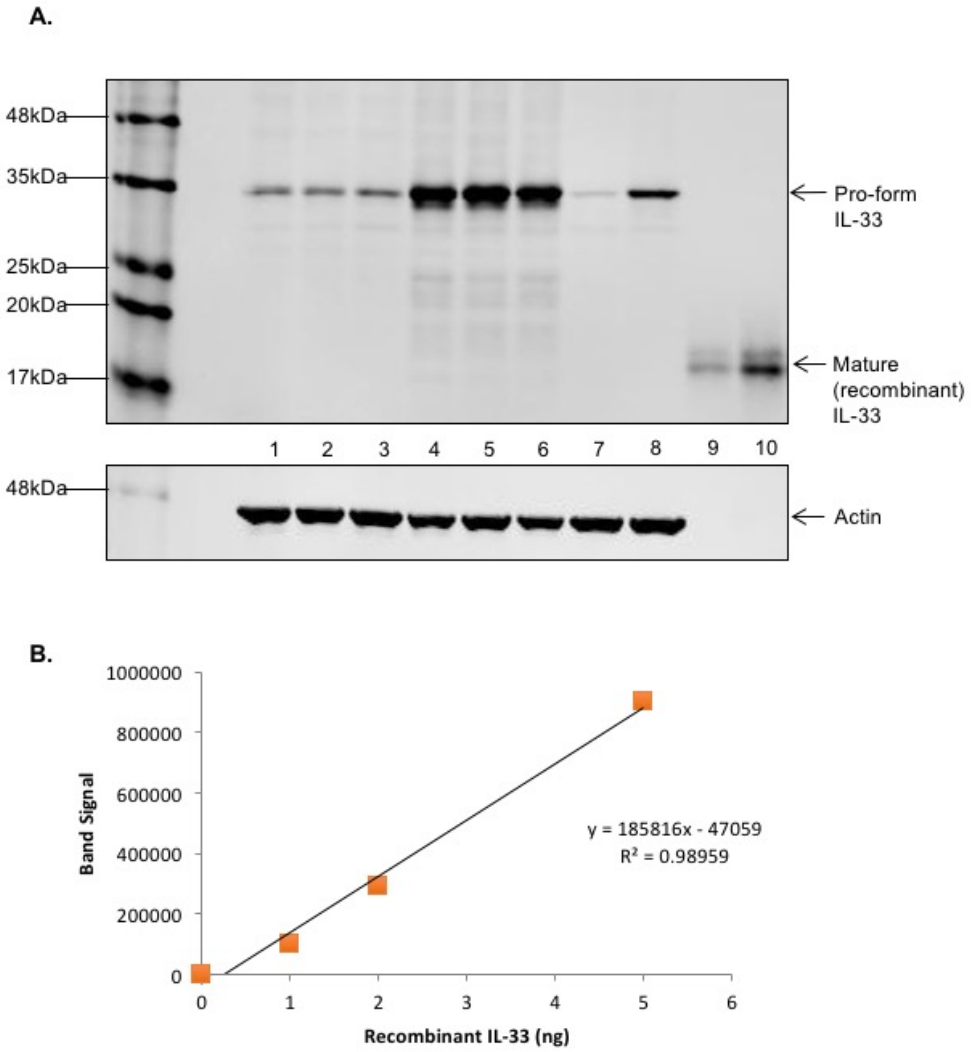
A.
48kDa
35kDa
25kDa
20kDa
17kDa
Pro-form IL-33
Mature (recombinant) IL-33
1 2 3 4 5 6 7 8 9 10
48kDa
Actin
B.
Band Signal
1000000
800000
600000
400000
200000
0
y = 185816x - 47059
R² = 0.98959
0 1 2 3 4 5 6
Recombinant IL-33 (ng)

Figure 2. Regulation of IL-33 by OSM and other cytokines in LA4 mouse lung epithelial cells. LA4 cells were stimulated with 20ng/mL OSM, 20ng/mL TGF-β, 20ng/mL IL-17a or combinations. 18 hours after stimulation, whole cell lysates were prepared using RIPA buffer. (A) Samples were probed for IL-33 (R&D Systems) pSTAT3 (Cell Signalling), STAT3 (Cell signalling) and β-Actin (Santa Cruz). Densitometry was completed for IL-33 (B) and pSTAT3 (C) signals using Image Studio Lite and corrected for β-Actin or STAT3, respectively. Representative blot from three independent experiments. (*Modified from publication: Richards, et al., Regulation of IL-33 by OSM in mouse lung epithelial cells, Mediators of Inflammation, 2016*)

Figure 2

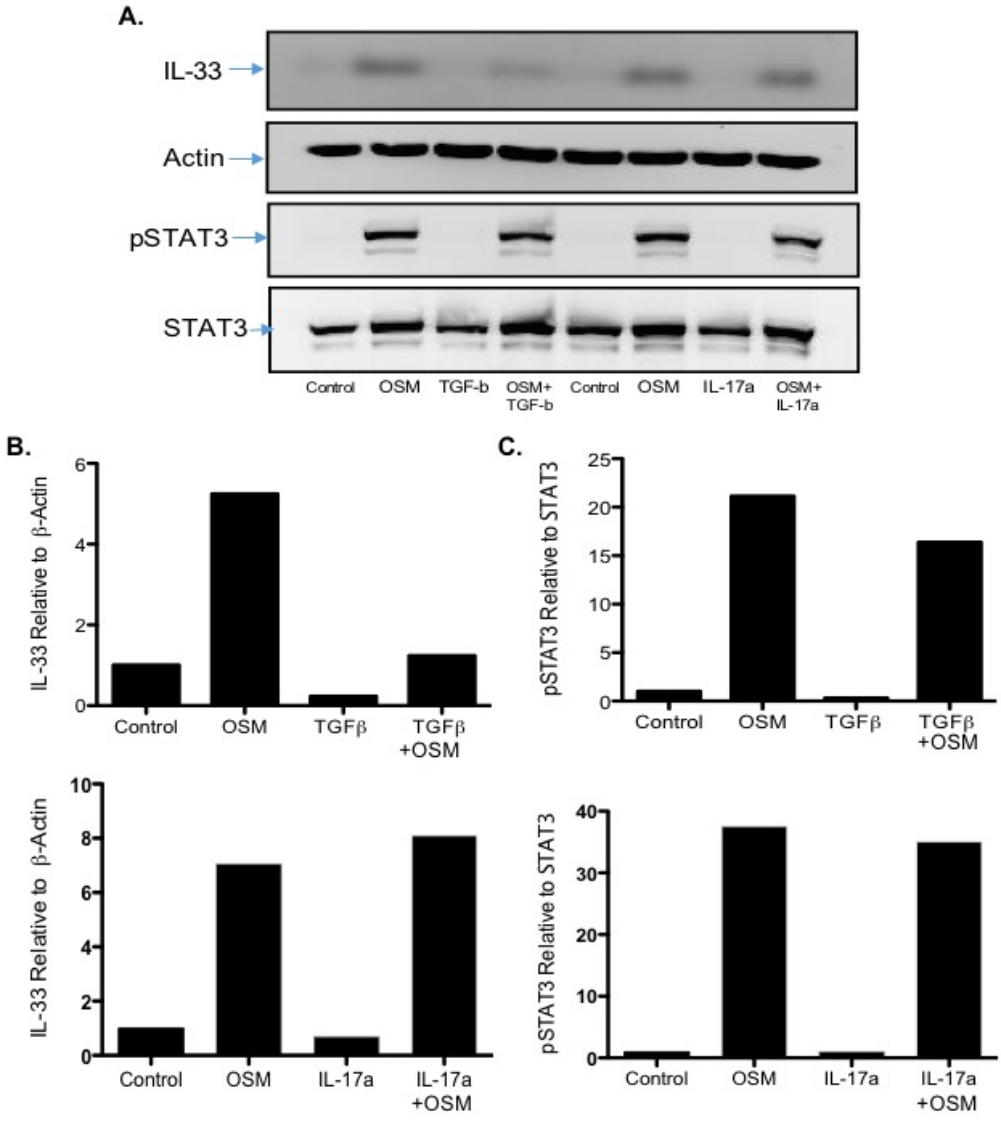
A.
IL-33
Actin
pSTAT3
STAT3
Control
OSM
TGF-b
OSM+ TGF-b
Control
OSM
IL-17a
OSM+ IL-17a
B.
IL-33 Relative to β-Actin
Control
OSM
TGFβ
TGFβ +OSM
C.
pSTAT3 Relative to STAT3
Control
OSM
TGFβ
TGFβ +OSM
IL-33 Relative to β-Actin
Control
OSM
IL-17a
IL-17a +OSM
pSTAT3 Relative to STAT3
Control
OSM
IL-17a
IL-17a +OSM

Figure 3. Up-regulation of IL-33 by OSM in TC1 mouse lung epithelial cell lysates. (A) TC-1 cells were cultured (100,000 cells/well) and stimulated with varying doses of mouse recombinant OSM for 24 hours. Lysates were collected and probed for IL-33 (R&D) and pSTAT3 (cell-signalling) by Western Blot. Duplicates are shown here but experiment was completed in quadruplicates. (B) Quantification of IL-33 signal corrected to β-Actin and represented as a fold-change relative to control.

Figure 3

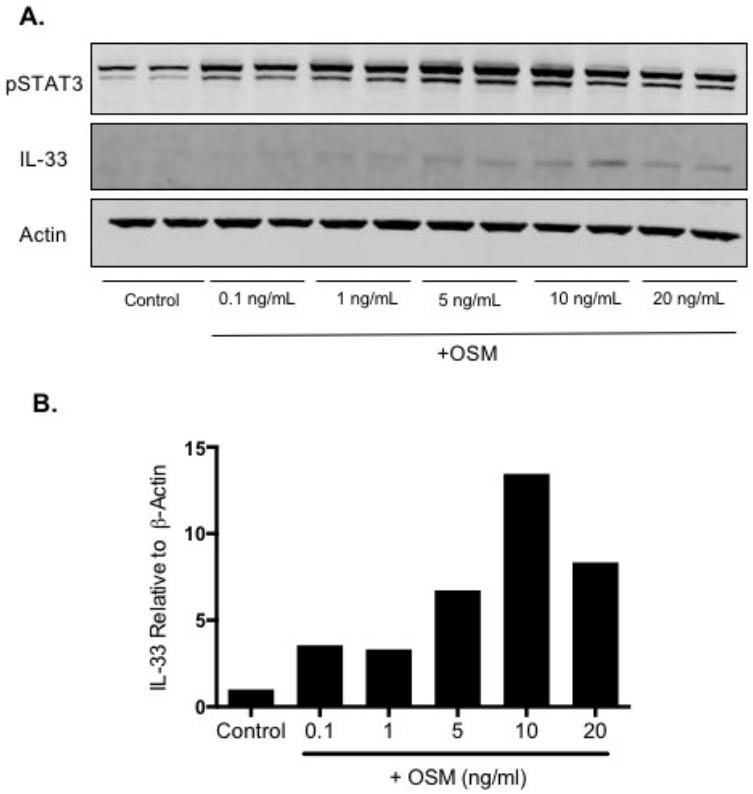
A.
pSTAT3
IL-33
Actin
Control
0.1 ng/mL
1 ng/mL
5 ng/mL
10 ng/mL
20 ng/mL
+OSM
B.
IL-33 Relative to β-Actin
15
10
5
0
Control
0.1
1
5
10
20
+ OSM (ng/ml)

Figure 4. Regulation of IL-33 by OSM and other cytokines in Human Type 2 Alveolar Epithelial Cells (A549). A549 cells cultured (150,000 cells/well) in a 6 well-plate were stimulated with OSM (20ng/mL) TNF-α (10ng/mL) or combinations for 24 hours. (A) Western Blot analysis of IL-33 (Nessy-1), pSTAT3 (Cell Signalling) and β-Actin (Santa cruz) from cell lysates. (B) Densitometry of IL-33 signal was completed using Image Studio Lite. (C) IL-33 mRNA expression from a parallel experiment by qPCR. (D) A549 cells stimulated with OSM (20ng/mL), TNF-α (10ng/mL), IL-17a (20ng/mL), 48 hours and probed for IL-33 using two different antibodies.

Figure 4

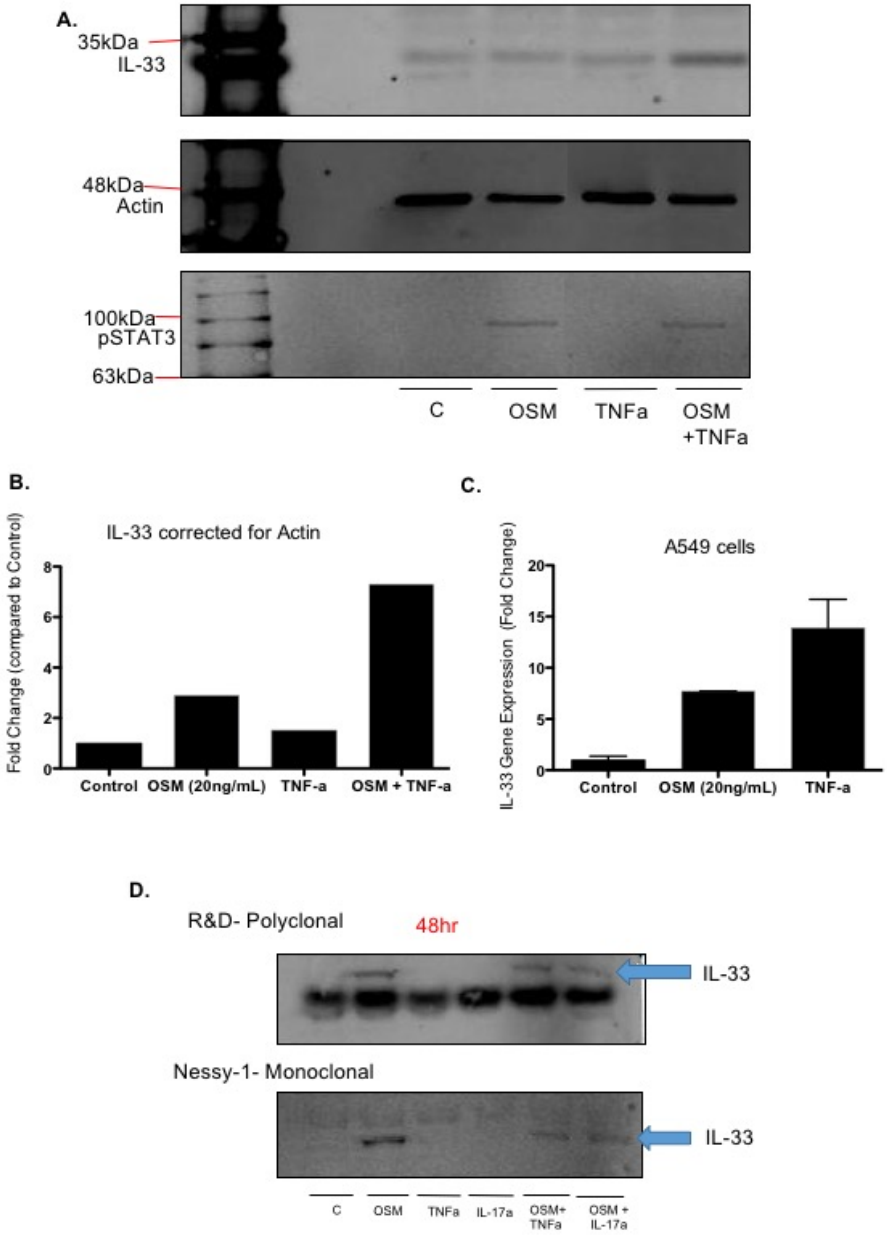
A.
35kDa
IL-33
48kDa
Actin
100kDa
pSTAT3
63kDa
C
OSM
TNFa
OSM
+TNFa
B.
IL-33 corrected for Actin
Fold Change (compared to Control)
Control
OSM (20ng/mL)
TNF-a
OSM + TNF-a
C.
A549 cells
IL-33 Gene Expression (Fold Change)
Control
OSM (20ng/mL)
TNF-a
D.
R&D- Polyclonal
48hr
IL-33
Nessy-1- Monoclonal
IL-33
C
OSM
TNFa
IL-17a
OSM+
TNFa
OSM +
IL-17a

Figure 5. Time-dependent regulation of IL-33 by OSM and other cytokines in Human Type 2 Alveolar Epithelial Cells (A549). (A) 300,000 cells/well in 6 well-plates were stimulated with OSM (20ng/mL), TNF-α (10ng/mL), IL-17a (20ng/mL), or combinations for 30min, 2, 6 and 24 hours. (B) Western Blot analysis of IL-33 (Nessy-1), pSTAT3 (Cell Signalling), STAT3 (Cell Signalling) and β-Actin (Santa Cruz) from cell lysates. Densitometry of (B) IL-33 and (C) pSTAT3 signal was completed using Image Studio for 30min, 2 hours, 6 hours and 24 hour samples.

Figure 5

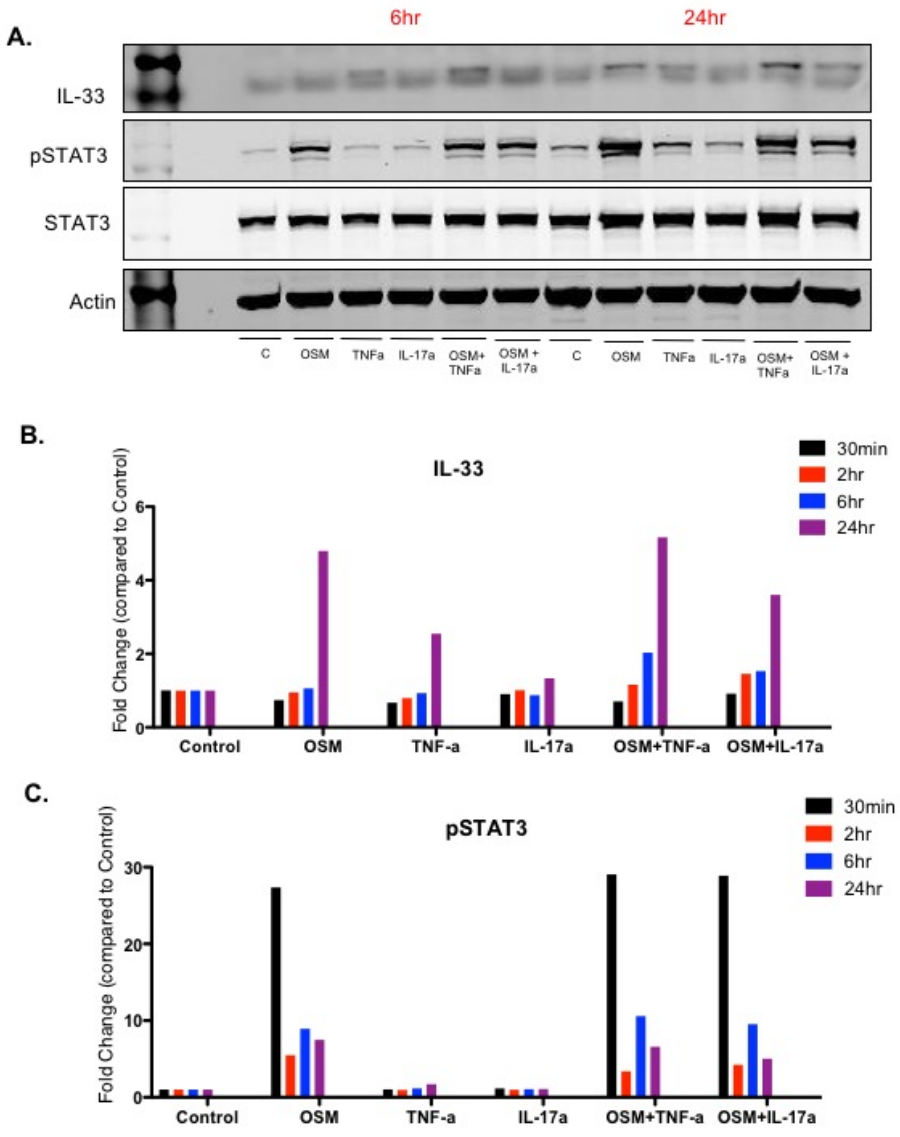
A.
6hr
24hr
IL-33
pSTAT3
STAT3
Actin
C
OSM
TNFa
IL-17a
OSM+ TNFa
OSM + IL-17a
B.
IL-33
30min
2hr
6hr
24hr
Fold Change (compared to Control)
Control
OSM
TNF-a
IL-17a
OSM+TNF-a
OSM+IL-17a
C.
pSTAT3

Figure 6. Regulation of IL-33 by OSM and other cytokines in Human Lung Fibroblasts (MRC-5 and HLF). MRC-5 Cells were stimulated with increasing doses of OSM for 18 hours. (A) Western Blot analysis of IL-33 (R&D Systems) and pSTAT3 (Cell Signalling) from cell lysates. (B) MCP-1 levels measured using ELISA (R&D). (C) Western blot analysis of IL-33 in cell lysates stimulated with OSM (20ng/mL), TGF-β (20ng/mL), IL-17a (20ng/mL) or combinations for 18 hours. (D) mRNA analysis (qPCR) of IL-33 from parallel experiment. (E) Western blot analysis of IL-33 (R&D) and (F) pSTAT3 (cell signalling) from HLF cell lysates stimulated with increasing doses of OSM for 18 hours. MCP-1 levels measured by ELISA in supernatants.

Figure 6

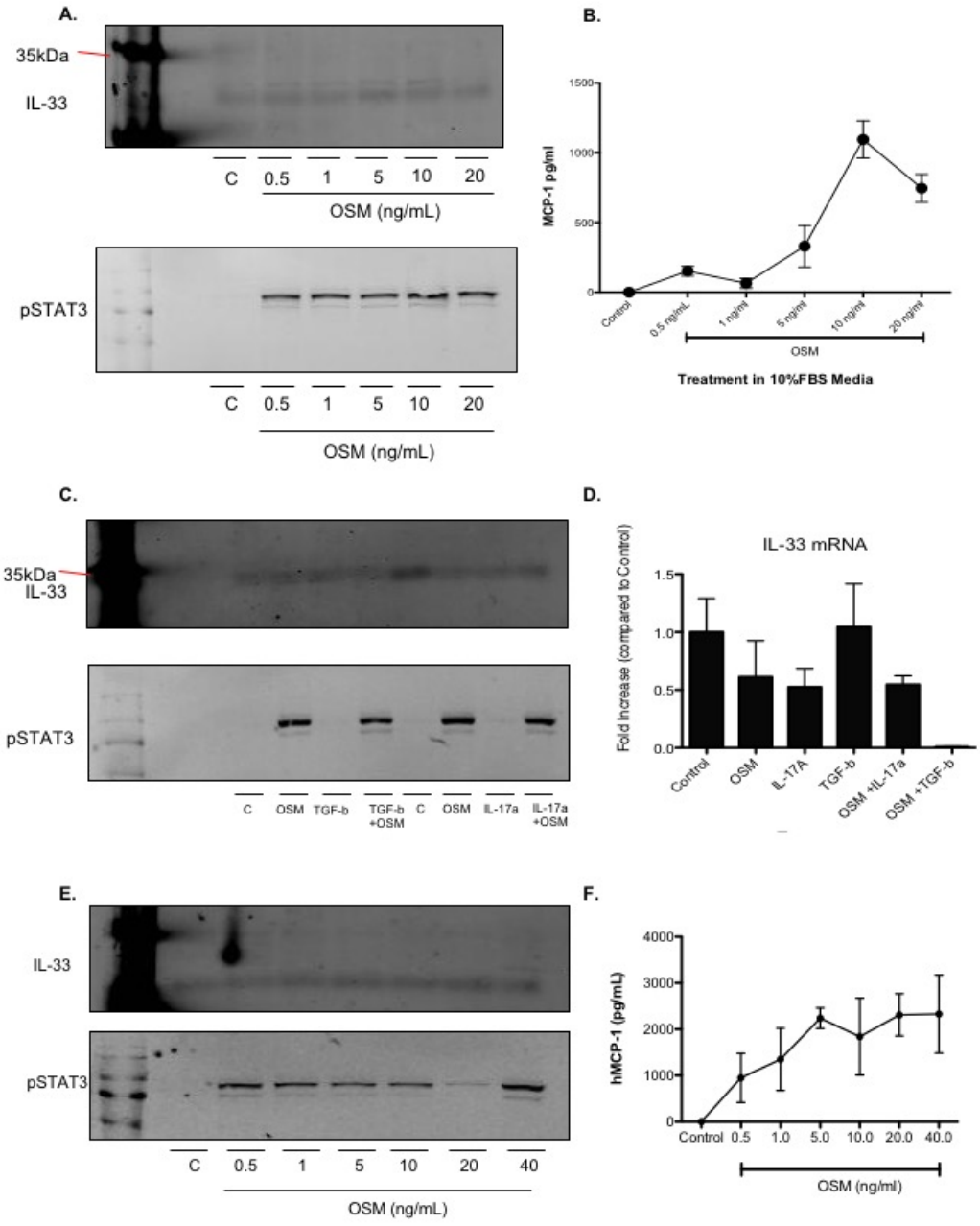
A.
35kDa
IL-33
C 0.5 1 5 10 20
OSM (ng/mL)
pSTAT3
C 0.5 1 5 10 20
OSM (ng/mL)
B.
MCP-1 pg/ml
1500
1000
500
0
Control
0.5 ng/mL
1 ng/ml
5 ng/ml
10 ng/ml
20 ng/ml
OSM
Treatment in 10%FBS Media
C.
35kDa
IL-33
pSTAT3
C OSM TGF-b TGF-b +OSM C OSM IL-17a IL-17a +OSM
D.
IL-33 mRNA
Fold Increase (compared to Control)
1.5
1.0
0.5
0.0
Control
OSM
IL-17A
TGF-b
OSM +IL-17a
OSM +TGF-b
E.
IL-33
pSTAT3
C 0.5 1 5 10 20 40
OSM (ng/mL)
F.
hMCP-1 (pg/mL)
4000
3000
2000
1000
0
Control 0.5 1.0 5.0 10.0 20.0 40.0
OSM (ng/ml)

Figure 7. Overexpression of OSM induces IL-33 protein and mRNA expression. C57bl/6 mice were administered AdDel70 ($1x10^8$ PFU), AdOSM ($5x10^7$ PFU) or AdIL-6 ($3x10^7$ PFU) (n=5/group) and culled at day 7. (A) Western Blot analysis of lung homogenates (n=4/treatment) probed for IL-33, β-Actin, pSTAT1, STAT1. (B) Quantification of IL-33 signal corrected to β-Actin and represented as fold-changes relative to AdDel70 control. (C) IL-33 levels in lung homogenates measured by ELISA (R&D). (D) Gene expression levels of IL-33 and IL-33R/ST2 from lung RNA (n=5/treatment) assessed by qPCR. (E) Western Blot analysis of lung homogenates from C57Bl/6 mice administered AdDel70 or AdOSM and culled at day 7 or 14 (n=3/treatment) probed for IL-33, β-Actin and pSTAT3. (F) Quantification of IL-33 signal corrected to β-Actin and represented as fold-changes relative to AdDel70 day 7 control. Statistics were completed using a one-way ANOVA for multiple comparisons and subsequent Tukey's post-hoc analysis (p*<0.05; p****<0.0001)

Figure 7

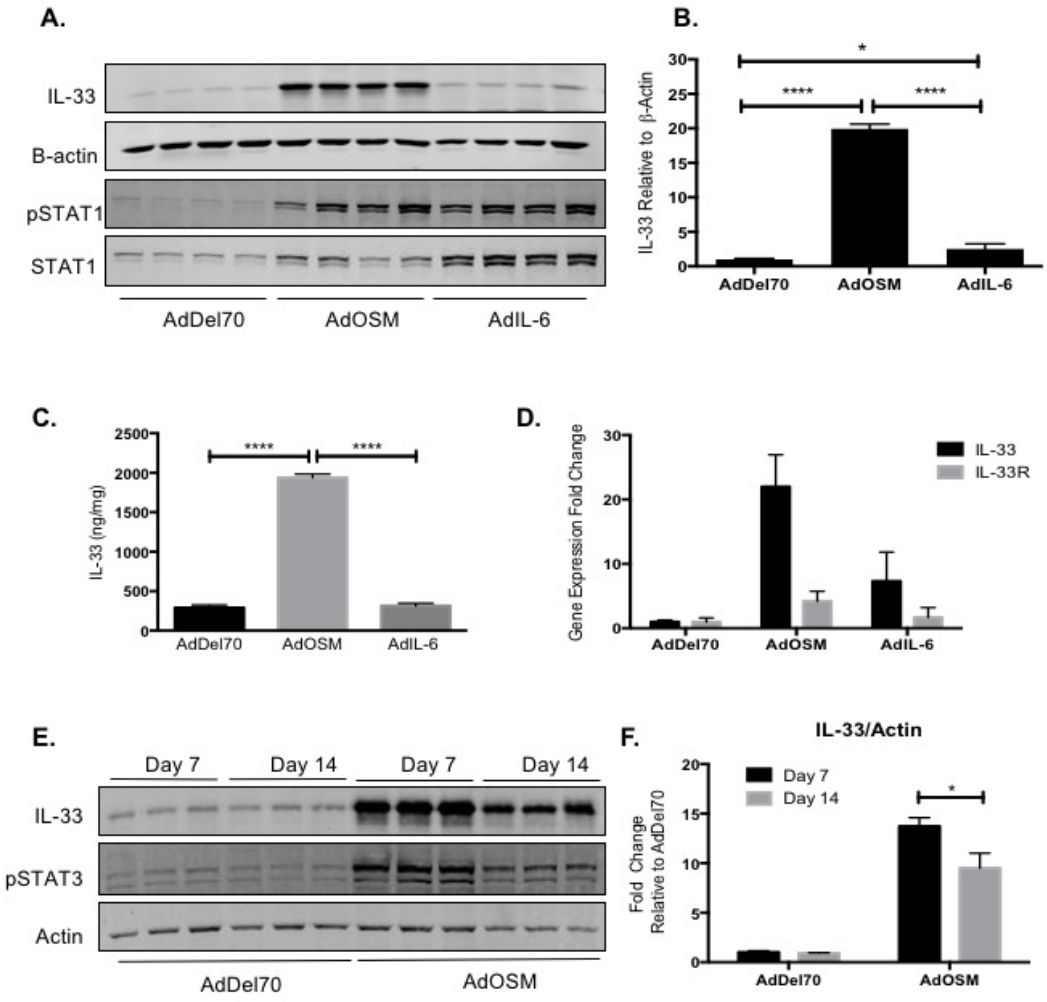
A.
IL-33
B-actin
pSTAT1
STAT1
AdDel70
AdOSM
AdIL-6
B.
IL-33 Relative to β-Actin
*
****
****
AdDel70
AdOSM
AdIL-6
C.
IL-33 (ng/mg)
****
****
AdDel70
AdOSM
AdIL-6
D.
Gene Expression Fold Change
IL-33
IL-33R
AdDel70
AdOSM
AdIL-6
E.
Day 7
Day 14
Day 7
Day 14
IL-33
pSTAT3
Actin
AdDel70
AdOSM
F.
IL-33/Actin
Day 7
Day 14
*
Fold Change Relative to AdDel70
AdDel70
AdOSM

Figure 8. Overexpression of OSM induces Arg1 protein and mRNA expression. C57bl/6 mice were endotracheally administered AdDel70 control vector ($1x10^8$ PFU), AdOSM ($5x10^7$ PFU) or AdIL-6 ($3x10^7$ PFU) (n=5/group) and culled at day 7. IL-6 (A) and OSM (B) levels in the BALF by ELISA (R&D). (C) Representative images of immunohistochemistry for Arg1. (D) Western Blot analysis of lung homogenates (n=4/treatment) probed for Arg1, β-Actin, pSTAT3 and STAT3. (E) Quantification of Arg1 and (F) pSTAT3 signal corrected to β-Actin or STAT3, respectively, using Image Studio software analysis of signals in (D). (G) Gene expression levels of Arg1 and iNOS from lung RNA (n=5/treatment) assessed by RT-qPCR. Statistics were completed using a one-way ANOVA for multiple comparisons and subsequent Tukey's post-hoc analysis (p*<0.05; p**<0.01; p***<0.001; p****<0.0001)

Figure 8

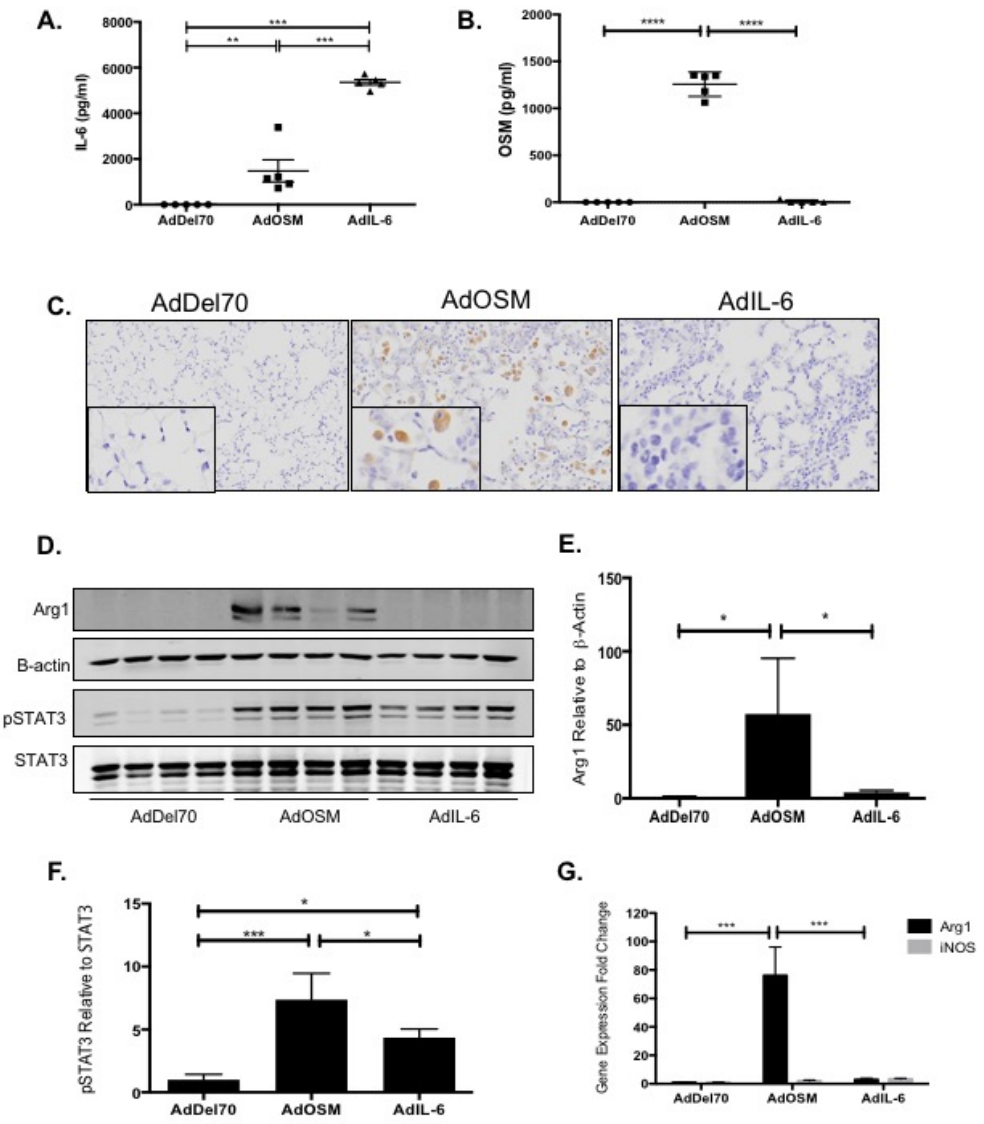
A.
IL-6 (pg/ml)
8000
6000
4000
2000
0
***
**
***
AdDel70
AdOSM
AdIL-6
B.
OSM (pg/ml)
2000
1500
1000
500
0
****
****
AdDel70
AdOSM
AdIL-6
C.
AdDel70
AdOSM
AdIL-6
D.
Arg1
B-actin
pSTAT3
STAT3
AdDel70
AdOSM
AdIL-6
E.
Arg1 Relative to β-Actin
150
100
50
0
*
*
AdDel70
AdOSM
AdIL-6
F.
pSTAT3 Relative to STAT3
15
10
5
0
*
***
*
AdDel70
AdOSM
AdIL-6
G.
Gene Expression Fold Change
120
100
80
60
40
20
0
***
***
Arg1
iNOS
AdDel70
AdOSM
AdIL-6

Figure 9. IL-6 is necessary for OSM-induced arginase-1 protein expression, but not IL-33 protein expression, *in mouse lung tissue.* C57Bl/6 wild-type or IL-$6^{-/-}$ mice were endotracheally administered AdDel70 control vector ($5x10^7$PFU/mouse) or AdOSM ($5x10^7$PFU/mouse) and culled at day 7. (A) Western blot analysis of Arg1, IL-33, pSTAT3, STAT3 and β-Actin from whole lung homogenates. Quantification of Arg1 (B) and IL-33 (C) bands corrected to β-Actin, using Image Studio and represented as fold-changes relative to AdDel70 control. Arg-1 (D) and IL-33 (E) mRNA levels were measured using qPCR and represented as fold-changes relative to AdDel70 control. Statistics were completed using a one-way ANOVA for multiple comparisons and subsequent Tukey's post-hoc analysis (*$p<0.05$; ****:$p<0.0001$).

Figure 9

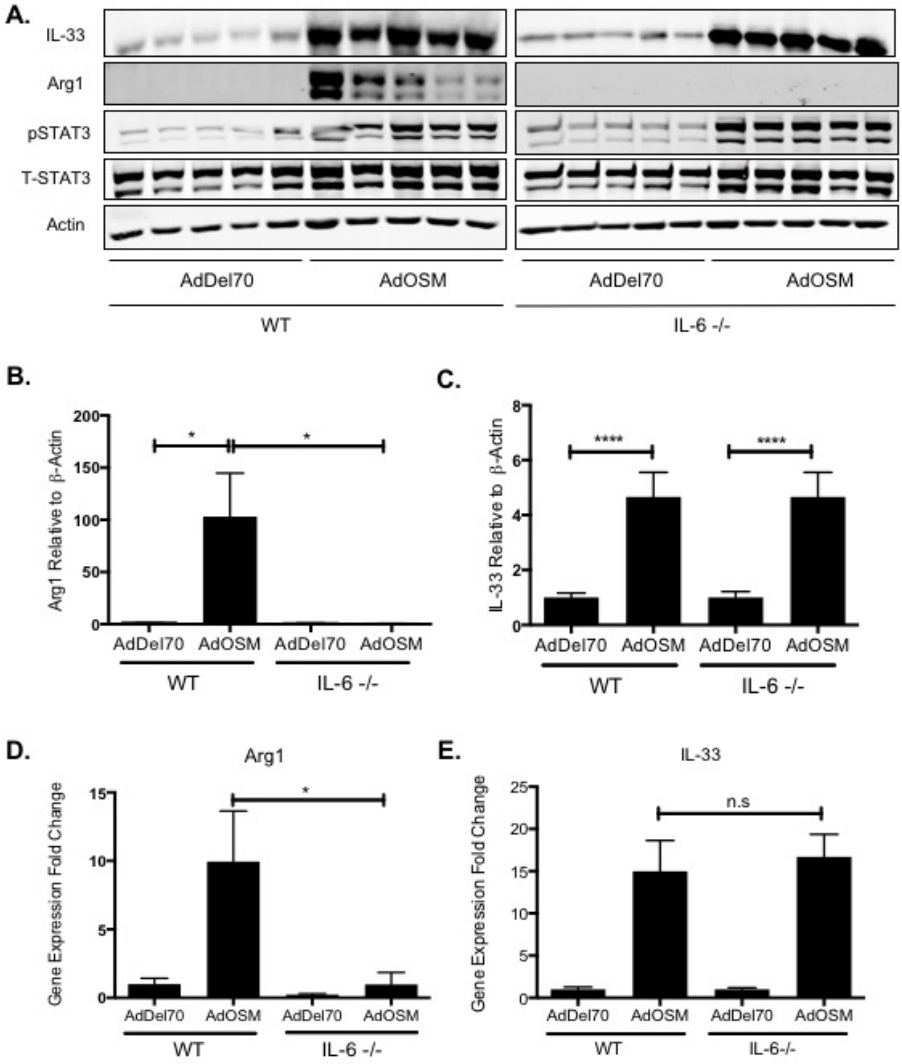
A.
IL-33
Arg1
pSTAT3
T-STAT3
Actin
AdDel70
AdOSM
AdDel70
AdOSM
WT
IL-6 -/-
B.
Arg1 Relative to β-Actin
200
150
100
50
0
*
*
AdDel70
AdOSM
AdDel70
AdOSM
WT
IL-6 -/-
C.
IL-33 Relative to β-Actin
8
6
4
2
0
****
****
AdDel70
AdOSM
AdDel70
AdOSM
WT
IL-6 -/-
D.
Arg1
Gene Expression Fold Change
15
10
5
0
*
AdDel70
AdOSM
AdDel70
AdOSM
WT
IL-6 -/-
E.
IL-33
Gene Expression Fold Change
25
20
15
10
5
0
n.s
AdDel70
AdOSM
AdDel70
AdOSM
WT
IL-6-/-

Figure 10. Regulation of IL-33 in wild-type or IL-33$^{-/-}$ mice upon overexpression of OSM in lung tissue and BAL. (A) Western Blot analysis of IL-33 (R&D) from C57Bl/6 whole lung homogenates (7 days). IL-33 (B) and OSM (C) levels in the BALF of C57Bl/6 WT or IL-33$^{-/-}$ mice administered with AdDel70 or AdOSM (7 days). (D) OD values for IL-33 standard curve concentrations 62.5 pg/mL, 125 pg/mL and 250 pg/mL spiked with 25uL PBS, AdOSM (2x10^8 pfu), AdOSM (5x10^7 pfu), AdDel70 (1x10^8 pfu), or the Mammalian Protein Extraction Reagent (MPER) lysis buffer compared to recombinant IL-33 standard alone (STD). Statistics were completed using a one-way ANOVA for multiple comparisons and subsequent Tukey's post-hoc analysis (*$p<0.05$, **$p<0.01$).

Figure 10

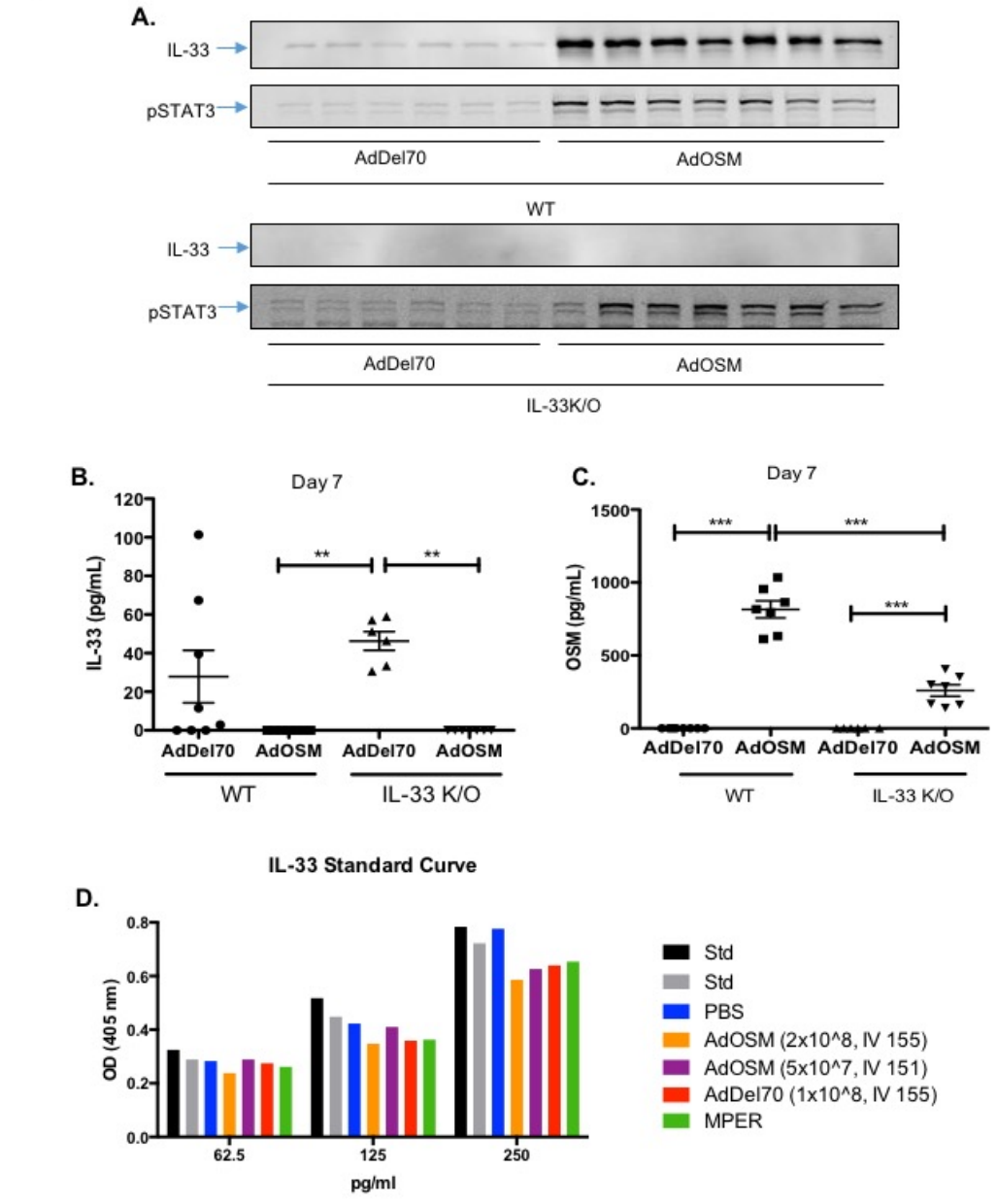
A.
IL-33
pSTAT3
AdDel70
AdOSM
WT
IL-33
pSTAT3
AdDel70
AdOSM
IL-33K/O
B.
Day 7
IL-33 (pg/mL)
120
100
80
60
40
20
0
**
**
AdDel70
AdOSM
AdDel70
AdOSM
WT
IL-33 K/O
C.
Day 7
OSM (pg/mL)
1500
1000
500
0
***
***
***
AdDel70
AdOSM
AdDel70
AdOSM
WT
IL-33 K/O
IL-33 Standard Curve
D.
OD (405 nm)
0.8
0.6
0.4
0.2
0.0
62.5
125
250
pg/ml
Std
Std
PBS
AdOSM (2x10^8, IV 155)
AdOSM (5x10^7, IV 151)
AdDel70 (1x10^8, IV 155)
MPER

Figure 11. IL-33 is required for OSM-induced Arg-1 expression in mouse lung tissue. C57Bl/6 wild-type or IL-33$^{-/-}$ female mice intubated with AdDel70 or AdOSM (5x10^7PFU/mouse) and culled at day 7. IL-33 (A) and OSM (B) levels in lung homogenates measured by ELISA (R&D). (C) Whole lung homogenates probed for Arginase-1 (BD Biosciences) and β-Actin (Santa Cruz) by Western blot. (D) Quantification of Arg-1 signal corrected to β-Actin and represented as a fold-change relative to AdDel70 wild-type treated mice. Statistics were completed using a two-way ANOVA for multiple comparisons and subsequent Bonferroni post-hoc analysis (****$p<0.0001$, ***$p<0.001$).

Figure 11

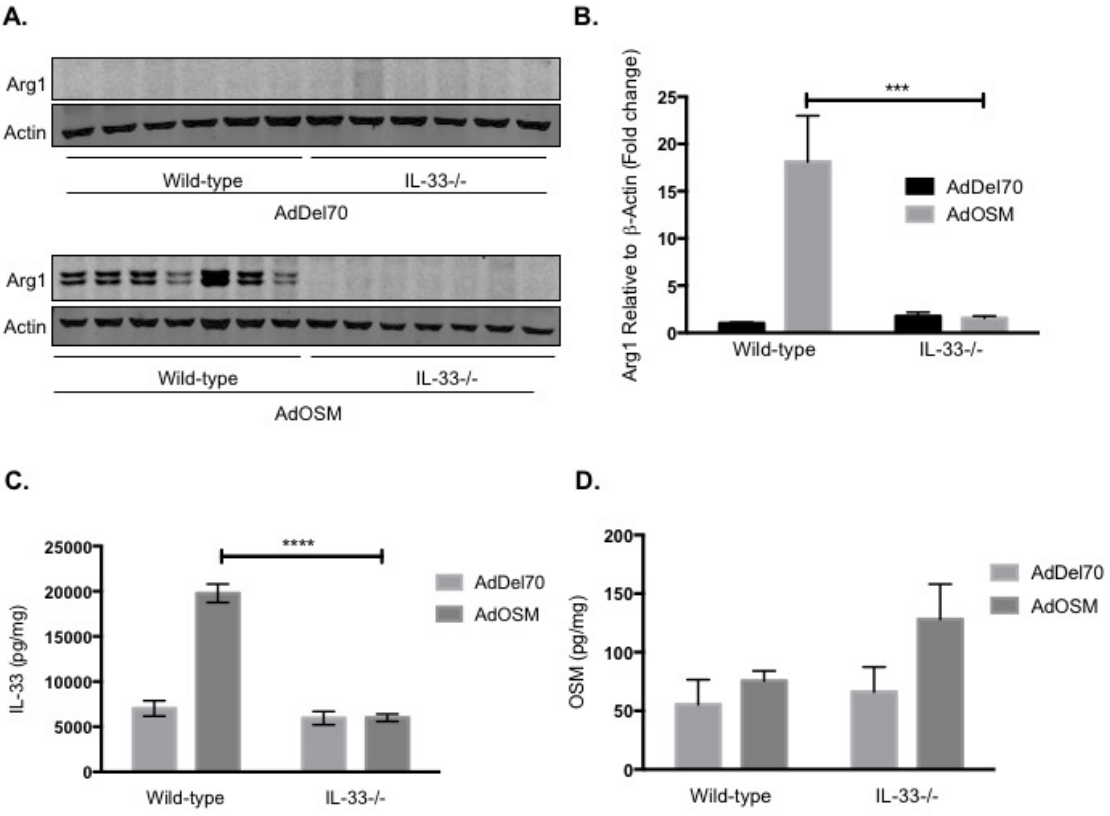
A.
Arg1
Actin
Wild-type
IL-33-/-
AdDel70
Arg1
Actin
Wild-type
IL-33-/-
AdOSM
B.
Arg1 Relative to β-Actin (Fold change)
***
AdDel70
AdOSM
Wild-type
IL-33-/-
C.
IL-33 (pg/mg)
****
AdDel70
AdOSM
Wild-type
IL-33-/-
D.
OSM (pg/mg)
AdDel70
AdOSM
Wild-type
IL-33-/-

Figure 12. IL-33 and OSM protein concentrations using the R&D ELISA. (A) C10 mouse lung epithelial cells (200,000 cells/well) were stimulated with OSM (5ng/mL) for 24 hour, lysed using the MPER lysis buffer (200uL) and assessed for IL-33 protein using an ELISA at 1:2 or 1:20 dilutions. (B) C10 cell lysates prepared using RIPA buffer following stimulation with OSM (5ng/mL) for 24hrs and used in the IL-33 ELISA at 1:50 dilution. Lung homogenates from BALB/c naïve, AdDel70 or AdOSM-treated mice (Day 2) measured for IL-33 (C) and OSM (D) at 1:200 or 1:50 dilution using their respective ELISAs. Lung homogenates from C57Bl/6 and BALB/c mice treated with AdDel70 or AdOSM (Day 7) and measured for IL-33 (E) and OSM (F) at 1:200 (IL-33) and 1:50 (OSM) dilutions using their respective ELISA kits. Statistics were completed using a one-way ANOVA for multiple comparisons and subsequent Tukey's post-hoc analysis (*$p<0.05$, **$p<0.01$, ***$p<0.001$, ****$p<0.0001$).

Figure 12

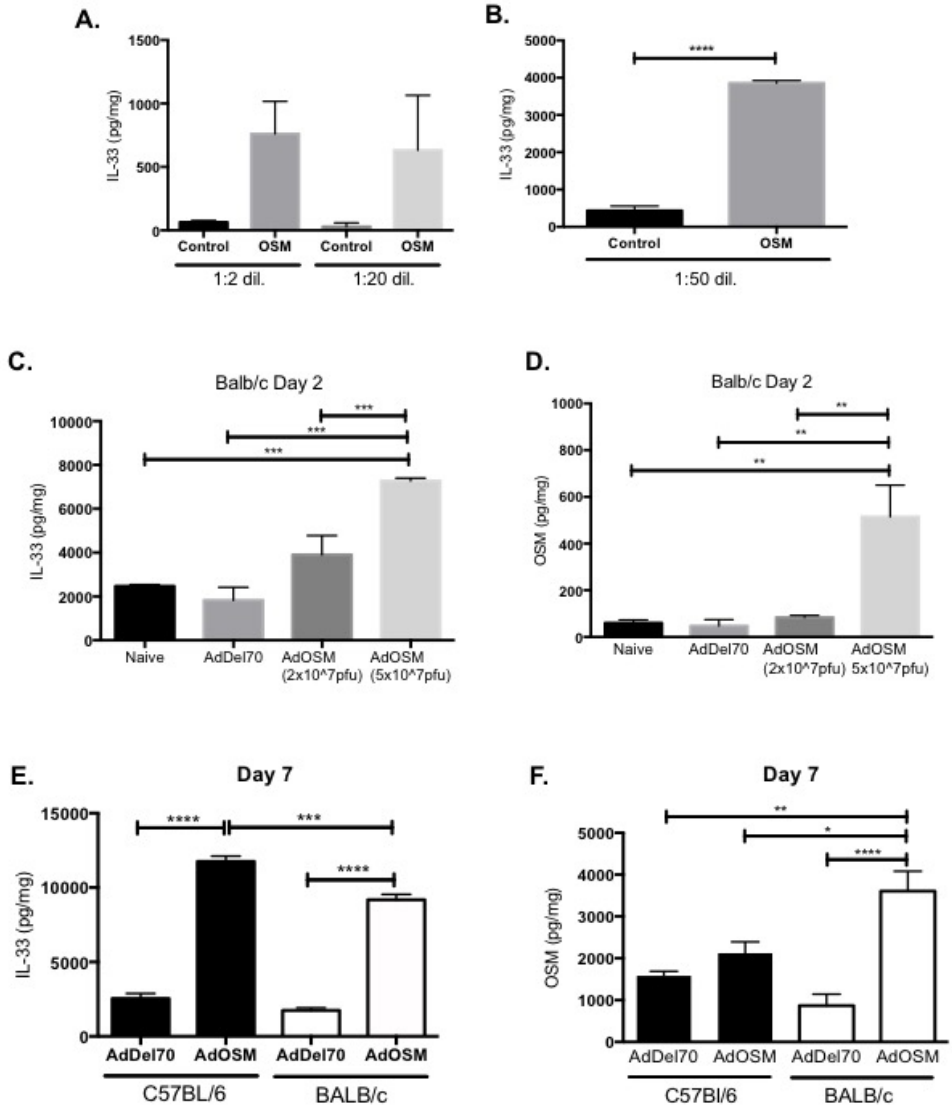
A.
IL-33 (pg/mg)
1500
1000
500
0
Control
OSM
Control
OSM
1:2 dil.
1:20 dil.
B.
IL-33 (pg/mg)
5000
4000
3000
2000
1000
0
****
Control
OSM
1:50 dil.
C.
Balb/c Day 2
IL-33 (pg/mg)
10000
8000
6000
4000
2000
0
***
***
***
Naive
AdDel70
AdOSM (2x10^7pfu)
AdOSM (5x10^7pfu)
D.
Balb/c Day 2
OSM (pg/mg)
1000
800
600
400
200
0
**
**
**
Naive
AdDel70
AdOSM (2x10^7pfu)
AdOSM 5x10^7pfu)
E.
Day 7
IL-33 (pg/mg)
15000
10000
5000
0
****
***
****
AdDel70
AdOSM
AdDel70
AdOSM
C57BL/6
BALB/c
F.
Day 7
OSM (pg/mg)
5000
4000
3000
2000
1000
0
**
*
****
AdDel70
AdOSM
AdDel70
AdOSM
C57Bl/6
BALB/c

Supplementary Figure 1. Overexpression of OSM and IL-6 produce unique inflammatory microenvironments in the lung. C57Bl/6 mice were endotracheally administered AdDel70 control vector ($1x10^8$ PFU), AdOSM ($5x10^7$ PFU) or AdIL-6 ($3x10^7$ PFU) (n=5/group) vectors and culled at day 7. Levels of IL-4 (A), IL-13 (B), IL-5 (C), Eotaxin-2 (D), Eotaxin (E), IFNγ (F), IP-10 (G), MIG (H), MCP-1 (I) and KC (J) were measured in BALF using cytokine-specific ELISAs or Eve Technology Murine Discovery Assay (AdDel70- circles, AdOSM- squares, AdIL-6- triangles). Statistics were completed using a one-way ANOVA for multiple comparisons and subsequent Tukey's post-hoc analysis (where p*<0.05; p**<0.01; p***<0.001; p****<0.0001 indicates a statistically significant difference between indicated groups. (*Used in the manuscript, "Separate roles of IL-6 and Oncostatin M on mouse macrophage polarization in vitro and in vivo" submitted to Journal of Leukocyte Biology*)

Supplementary Figure 1

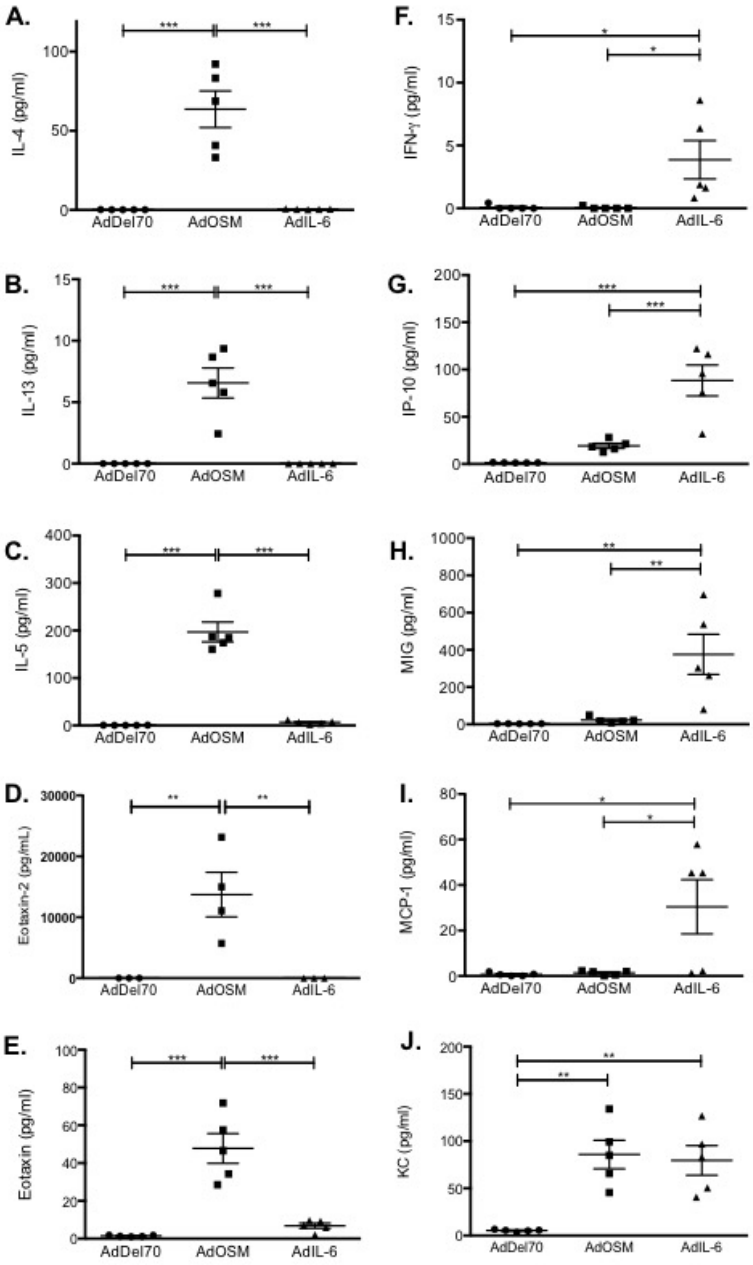

Supplementary Figure 2. IL-6, but not OSM or LIF, enhances murine macrophage arginase enzymatic activity. BMDMs and primary alveolar macrophages isolated from naïve C57BL6 mice were cultured for 24 hours with M2 and M1 cytokine cocktails (M2: IL-4 + IL-13; M1: LPS + IFNγ) alone or in combination with the indicated gp130 cytokines. (A) Arginase activity from cell lysates and (B) nitric oxide levels are shown in supernatants of BMDMs. (C) Arginase activity and (D) nitric oxide levels in primary alveolar macrophages retrieved from naïve C57Bl/6 mice. Bars represent mean ± SEM from 4 replicates per group and graph is representative of two independent experiments. Statistics completed using one-way ANOVA and Tukey's post-hoc analysis, p*<0.05; p**<0.01; P***<0.001. (*Experiment completed by Ehab Ayaub in the Ask group and used in the manuscript, "Separate roles of IL-6 and Oncostatin M on mouse macrophage polarization in vitro and in vivo" submitted to Journal of Leukocyte Biology*)

Supplementary Figure 2

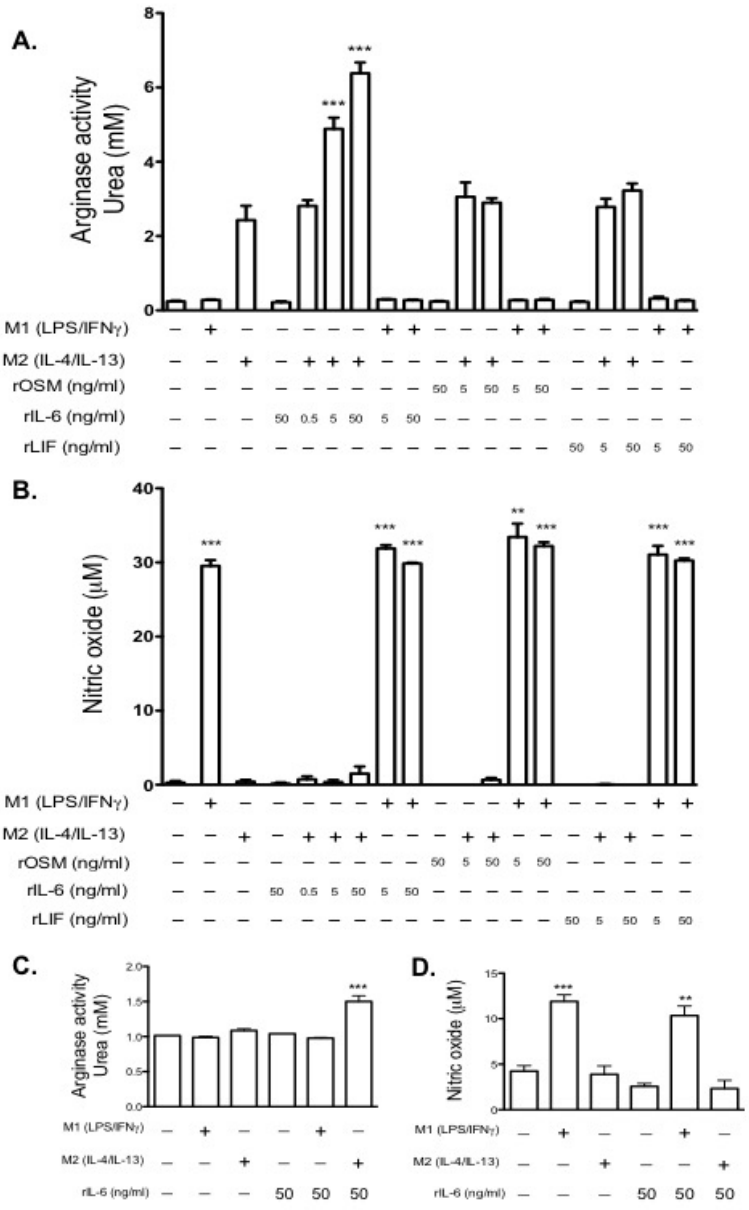

CHAPTER 4

- IL-33 REGULATION BY OSM FOLLOWING INFLUENZA A VIRUS INFECTION *IN VITRO* AND *IN VIVO* -

4.1 *In vitro* Results

In order to determine if OSM can prime lung cells for exacerbated IL-33 release following a PR8 virus infection, the C10 Balb/c cell line was used to perform a preliminary experiment *in vitro*. C10 cells were stimulated with OSM (5ng/mL) for 24 hours and then infected using flu-infection media at an MOI of 0.01 or MOI of 5 for 1 hour at 37°C. Virus media was removed and fresh RPMI media (serum-containing) was added to each well (600uL). After 2, 24 and 48 hours of incubation, 180uL of supernatants were collected at each time-point and assayed for IL-33 using the R&D ELISA. Interestingly, control cells not infected with influenza virus showed increased levels of IL-33 in the supernatants compared to uninfected cells stimulated with OSM (**Figure 13A**). Contrary to the hypothesis, Influenza A virus infection *in vitro* led to decreased basal levels of IL-33 released within the culture supernatants, when comparing levels of uninfected control cells to infected control cells (**Figure 13A and B**). Although basal levels of IL-33 detected in supernatants were reduced upon virus infection *in vitro*, prior stimulation with OSM led to increased levels of IL-33 release in a time-dependent manner, albeit low levels were detected (**Figure 13B**). Cells infected with PR8 at an MOI of 0.01 and incubated for 48 hours showed similar results in which preceding OSM stimulation led to higher levels of IL-33 within culture supernatants, suggesting that OSM can prime the cells for increased

release of IL-33 following virus infection (**Figure 13C**). Whole cell lysates (uninfected cells) showed increased IL-33 protein following OSM stimulation and therefore acts as a positive control to demonstrate that the cells were stimulated and intracellular IL-33 protein was induced (**Figure 13D**). IL-33 protein release within the same cell culture supernatants was also assessed by Western blot analysis. Supernatants were pooled from 4 replicates of each group (12uL each) and added to loading buffer (12uL) and boiled for 5 min at 90°C. 45uL of each sample was then loaded onto a 12% SDS-PAGE gel and standard Western blot protocol was followed. Results demonstrated the IL-33 was detected using this method, although ELISA data suggested very low levels of protein within the supernatants. Additionally, we detected an increase in IL-33 protein signal for samples pre-stimulated with OSM at 48-hour post-infection (**Figure 13E**), similar to the trend observed using the ELISA. A non-specific band appeared at approximately 60kDa in size and is shown in **Figure 13E** in order to demonstrate even loading for all samples, although this is not a precise control and will need to be repeated with a specific control antibody. Therefore, these findings suggest that the Western blot method of detection and ELISA method of detection were useful for measuring IL-33 release within cell culture supernatants.

4.2 Influenza A Virus Infection in the Absence of OSM Receptor Signalling

In order to determine if OSM has an important role in regulating IL-33 in the presence of an influenza virus infection, several *in vivo* experiments were performed utilizing OSM-receptor-deficient mice. Firstly, wild-type and $OSMR^{-/-}$ mice (n=4/group) were infected with a low dose of Influenza A/Puerto Rico/8/1934 H1N1 (PR8) virulent

virus ($2.5x10^2$ PFU) and various outcomes were assessed at Day 7. OSM levels in the BALF were induced following virus infection in both wild-type and $OSMR^{-/-}$ mice but were significantly greater in $OSMR^{-/-}$ animals (**Figure 14A**). Similarly, IL-6 levels were elevated following virus infection and there was also a trend toward a decrease in $OSMR^{-/-}$ animals BALF samples compared to wild-type (**Figure 14B**). Interestingly, IL-33 levels in the BALF was induced following virus infection, however BALF IL-33 was significantly reduced in $OSMR^{-/-}$ infected animals (**Figure 14C**). This suggests OSMR-signalling may play a role in IL-33 regulation in the context of a virus infection. Additionally, using the IL-33 and OSM ELISA detection method, OSM and IL-33 levels in the lung homogenates were decreased following virus infection in both wild-type and $OSMR^{-/-}$ mice (**Figure 14D and 14E**). This result was confirmed using the Western Blot detection method for IL-33, which also shows a decrease in IL-33 protein within lung homogenates of infected mice (**Figure 14F**). Assessing the histopathology, there was evidence of increased immune cell infiltration following virus infection in both wild-type and $OSMR^{-/-}$ mice, however differential cell counts of the BALF cells indicated a higher macrophage percentage and lower neutrophil percentage within the $OSMR^{-/-}$ animals (Representative images in **Figure 15A, 15B, 15C**). This suggests that OSMR-signalling may have an effect on immune cell accumulation to the lung during a virus infection. This corresponded to increase in macrophage total counts and neutrophil total counts (**Figure 15D and 15E**). There was undetectable levels of lymphocytes and eosinophils (data not shown). After observing these effects, assessment of IL-33 and OSM regulation was explored using a higher dose of the virus and earlier time-points.

Using the PR8 virus, wild-type or OSMR$^{-/-}$ mice were infected with 1000 PFU/mouse and culled at day 2, 4 and 7 to assess various outcomes. OSM levels were induced in the BALF by day 2, maintained at day 4 and then reduced back to basal levels by day 7 (**Figure 16A**). This trend was consistent in both wild-type and OSMR$^{-/-}$ animals. IL-6 levels in the BALF showed a time-dependent increase in both wild-type and OSMR$^{-/-}$ animals, however, IL-6 was significantly reduced in OSMR$^{-/-}$ at day 7 compared to wild-type (**Figure 16B**). IL-33 levels in the BALF by ELISA showed a similar trend to OSM, where it was elevated at day 2 and then returned to basal levels by day 7, in both wild-type and OSMR$^{-/-}$ animals (**Figure 16C**). Reduction of IL-33 BALF levels in OSMR$^{-/-}$ following low dose infection was not observed when animals were administered a high dose of the virus. Assessing the total lung homogenates by ELISA, IL-33 and OSM levels showed very similar trends. IL-33 and OSM were reduced following virus infection in a time-dependent manner, however there was a slight increase in IL-33 and OSM in OSMR$^{-/-}$ animals at day 2 following infection, which then returned to normal by day 4 and further reduced by day 7 (**Figure 16D and 16E**). These results were in contrast to the western blot data of the same lung homogenates. By Western blot, there was an induction of IL-33 following virus infection in wild-type animals at day 2, which was absent in the OSMR$^{-/-}$ animals (**Figure 17A**). At day 4 following infection, IL-33 levels were not regulated in the lung tissue as assessed by western blot (**Figure 17B**). However, by day 7, IL-33 levels were significantly reduced to lower levels than naïve animals, which is consistent with the ELISA data and suggests that the virus infection may be inhibiting IL-33 production in the lung at day 7 (**Figure 17C**). The weights of the mice at day 0, 2, 4, and 7 post-infections were also

assessed. These results demonstrate that both wild-type and OSMR$^{-/-}$ mice infected with influenza A showed a similar significant weight reduction by day 4 post-infection, which was maintained until day 7 (**Figure 16F**).

Assessment of the histopathology revealed that there was increased immune cell infiltration in a time-dependent manner for both wild-type and OSMR$^{-/-}$ animals. Although H&E staining suggested more enhanced immune cell infiltration in wild-type mice following infection, compared to OSMR$^{-/-}$ (**Figure 18A**), this observation will have to be verified by quantification methods. However, according to the differential cell count data of BALF cells, there was a statistically significant increase in macrophage percentage and decrease in neutrophil percentage at Day 7 within OSMR$^{-/-}$ infected mice, suggesting a role for OSMR signalling in immune cell recruitment during virus infection (**Figure 18B and 18C**). This corresponded to increase in macrophage total counts and neutrophil total counts (**Figure 18D and 18E**). There was undetectable levels of lymphocytes and eosinophils (data not shown) in BALF samples. These results were consistent with animals infected at a lower dose of the virus.

In order to determine if these results were reproducible within Influenza A virus variants, similar experiments were performed utilizing a different strain of the virus. Influenza A/FM/1/47 H1N1 non-virulent strain was used to infect wild-type mice with low ($2x10^4$ PFU) and high doses ($1x10^5$ PFU) and animals were culled at day 2 and 4 post-infection. Assessment of the BALF revealed elevated levels of OSM at both low and high dose at both time-points compared to Day 0 (naïve), as well as a time-dependent and dose-dependent increase in IL-6 levels (**Figure 19A and 19B**). However, the IL-33 BALF levels

were varied and these concentrations were below the detection limit of the ELISA and therefore unreliable (**Figure 19C**). Within the lung homogenates, we observed a dose-dependent increase in IL-33 levels by Western Blot for both Day 2 and Day 4 following virus infection (**Figure 20A, 20B, 20C, and 20D**). The differential cell counts revealed robust decrease in macrophage percentage (increase in total numbers, data not shown) and increase in neutrophil percentage (increase in total numbers, data not shown) at day 2 and 4 following virus infection and for both low and high doses (**Figure 20E, 20F, 20G and 20H**). Lymphocytes and eosinophils were undetectable (data not shown). Following this preliminary experiment in wild-type mice, a comparison to $OSMR^{-/-}$ mice was completed for both the low and high dose of the virus at Day 7. Assessment of the BALF cytokines revealed that OSM and IL-6 levels were increased following a virus infection in wild-type mice. Interestingly, OSM was robustly up-regulated following virus infection in a dose-dependent manner in $OSMR^{-/-}$ mice, compared to wild-type animals (**Figure 21A**). Similarly, IL-6 was also significantly up-regulated in $OSMR^{-/-}$ animals following high dose infection (**Figure 21B**). IL-33 levels in BALF were variable and below the limit of detection (LoD – 15.625pg/mL) (**Figure 21C**). Analysis of lung homogenates showed decreased levels of IL-33 and OSM protein levels following virus infection at both the low and high dose of virus, which is consistent with results from mice infected with the more virulent PR8 strain (**Figure 21D and 21E**). Overall, the histopathology (specifically BALF differentials) revealed a dose-dependent increase in immune cell infiltration for both the wild-type and $OSMR^{-/-}$ animals at 7-days post-virus infection (**Figure 22**), but no obvious difference between wild-type and $OSMR^{-/-}$ mice.

4.3 Influenza A virus infection in the presence of elevated levels of OSM

Subsequent experiments assessed the effects of OSM priming on the lung microenvironment *in vivo*, in order to determine if OSM could exacerbate IL-33 release following a virus infection. In an initial experiment C57Bl/6 mice were intubated with AdOSM and then infected with Influenza A/PR8 virus. Specifically, wild-type C57Bl/6 mice were pre-treated with AdDel70 control vector or AdOSM ($5x10^7$ PFU/mouse) until day 7, followed by intranasal infection with Influenza A/PeurtoRico/8/1934 (250 PFU) virus for 2 days (**Figure 23A** for schematic of experiment). Animals were culled at Day 9 and BALF and lung tissue was collected for cell differential and cytokine analysis. The weight of the mice at Day 0 and Day 9 were similar within all treatment groups (data not shown). OSM levels were elevated in the BALF of mice pre-treated with AdOSM alone at Day 9, indicating effective vector intubation (**Figure 23B**). As observed in previous *in vivo* experiments, virus infection alone led to increased OSM levels in the BALF at Day 2 post-infection (**Figure 23B**). In comparison to naïve animals, IL-33 protein in the BALF measured by ELISA was also elevated at Day 2 post-infection, however levels were attenuated in mice pre-treated with AdOSM (**Figure 23C**). Similarly, in animals that were uninfected with PR8, AdDel70 at Day 9 led to increased levels of IL-33 in the BALF, while AdOSM at Day 9 showed levels similar to naïve animals (**Figure 23C**). Next, lung tissue samples were analyzed on two different Western blots in order to load appropriate controls on the same blot. **Figure 24A** shows samples from naïve animals compared to animals treated with PR8 virus alone or adenovirus vectors alone and **Figure 24D** shows samples

from animals treated with adenovirus vectors alone compared to mice that were pre-treated with adenovirus and then infected with influenza A. In contrast to results obtained from the BALF compartment, IL-33 protein was up-regulated in the whole lung tissue of mice treated with AdOSM at Day 9 alone or Day 2 post-virus infection with pre-treatment of AdOSM, to a similar level as assessed using Densitometry (**Figure 24A, 24B, 24D and 24E**). Similar to IL-33, Arg-1 protein was up-regulated following AdOSM treatment alone, as well as with a subsequent virus infection at Day 2 post-infection (**Figure 24A, 24D, 24C and 24F**). Therefore, this data suggests that OSM can prime the lung for IL-33 and Arg-1 induction in the lung tissue, however IL-33 is either not released into the BALF or undetectable by using this ELISA. No difference was observed on AdOSM-induced effects by PR8 at this time-point.

Histopathological analysis of lung tissue demonstrated increased immune cell infiltration and inflammation following AdOSM treatment or co-infection with AdOSM and subsequent PR8 infection at Day 2 post-infection (**Supplementary Figure 3, four mice/group**). Upon analysis of immune cell differentials within the BALF, animals infected with influenza A had generally increased number of macrophages, lymphocytes, and neutrophils within the BALF (**Figure 25A, 25B, 25C, 25E, 25F, 25G**). However, in comparison to these immune cells, the total number and percentage of eosinophil infiltration was significantly decreased in mice pre-treated with AdOSM and co-infected with PR8 (Day 2) in comparison to AdOSM treatment alone (**Figure 25D and 25H**).

To determine the effects of co-infection with AdOSM and PR8 at a later time-point, the experiment was repeated by analyzed at Day 5 post-PR8 infection. Specifically, wild-

type C57Bl/6 mice were pre-treated with AdDel70 control vector or AdOSM ($5x10^7$ PFU/mouse), followed by intranasal infection at Day 7 with Influenza A/PeurtoRico/8/1934 (250 PFU) virus for a further 5 days (**Figure 26A** for schematic of experiment). Animals were culled at Day 12 and BALF and lung tissue was collected for cell differential and protein analysis. The weights of the mice were also measured at Day 0 and at Day 12, and demonstrated a reduction in body weight of approximately 20% for mice treated with Influenza A 5-days post-infection, indicating that the PR8 virus had the expected affect on the mice (**Figure 26B**). An increase in OSM levels was evident within the BALF of mice pre-treated with AdOSM alone at Day 12, albeit lower levels than those at Day 9 (**Figure 26C**). Additionally, Influenza A virus infection alone led to increased OSM levels in the BALF at Day 5 post-infection, while AdOSM-PR8 co-infection showed significantly higher levels of OSM in comparison to mice treated with influenza A virus alone or AdOSM alone (**Figure 26C**). BALF associated IL-33 protein was also elevated at Day 5 post-influenza infection, however levels were attenuated in mice pre-treated with AdOSM (**Figure 26D**). Similarly, in animals treated with AdDel70 alone at Day 12 showed approximately 50pg/mL of IL-33 protein, while a subsequent virus infection led to approximately 150pg/mL of IL-33 protein within the BALF (**Figure 26D**). Analysis of total lung homogenates by Western blot in **Figure 27A** shows samples from naïve animals compared to animals treated with virus alone or adenovirus alone and **Figure 27D** shows samples from animals treated with adenovirus alone compared to mice that were pre-treated with adenovirus and then infected with influenza A. Similar to prior results (**Figure 9**), IL-33 protein was markedly up-regulated in the whole lung tissue of mice treated with AdOSM

at Day 12 alone (**Figure 27A, 27B and 27C**). Interestingly, animals pre-treated with AdOSM showed decreased levels of IL-33 following a subsequent PR8 virus infection for 5 days (**Figure 27B and 27C**). This results are consistent with previous *in vivo* data showing a reduction in IL-33 protein within the lung homogenates of mice infected with the PR8 virus for 7 days (**Figure 14D and 16D**). Additionally, Arg-1 protein was robustly up-regulated following AdOSM treatment alone at Day 12, however was attenuated in mice that received a subsequent PR8 virus infection at Day 5 post-infection (**Figure 27B and 27D**). Overall, this data suggests that OSM can prime the lung for IL-33 and Arg-1 up-regulation, while a subsequent PR8 virus infection for 5 days led to attenuated levels of both proteins within the lung tissue.

Analysis of lung tissue histology demonstrated an apparent increased immune cell infiltration and inflammation following AdOSM treatment or co-infection with AdOSM and subsequent PR8 infection at Day 5 post-infection (**Supplementary Figure 4, four mice/group**). Analysis of immune cell differentials within the BALF showed increased number of macrophages, lymphocytes, and neutrophils within the BALF (**Figure 28A, 28B, 28C, 28E, 28F, 28G**) of animals infected with PR8 Influenza A (Day 5). Similar to 2-days post-influenza infection results, the total number and percentage of eosinophil infiltration was significantly decreased in mice pre-treated with AdOSM followed by subsequent PR8 infection in comparison to AdOSM treatment alone (**Figure 28D and 28H**) at the Day 12.

4.4 Figures and Figure Legends

Figure 13. IL-33 release from mouse lung epithelial cells following virus infection *in vitro*. C10 cells OSM (5ng/mL) for 24 hours prior to PR8 virus infection (MOI of 0.01 or 5) for 1 hour. (A) IL-33 levels within supernatants of uninfected control or OSM stimulated cells at 2, 24 and 48 hours. (B) IL-33 levels within supernatants of virus infected cells (MOI=5) at 2, 24 and 48 hours measured by ELISA (R&D limit of detection = 15.625 pg/mL). (C) IL-33 measured in supernatants of cells infected at MOI of 0.01 after 24 hours. (D) IL-33 levels in whole cell lysates measured by ELISA (R&D). (E) Supernatants of *in vitro* infected samples with PR8 virus at an MOI of 5 for 24 and 48 hours probed for IL-33 by Western. Non-specific band is shown as a control for loading. Red lines indicate LOD of the IL-33 ELISA at 15.625pg/mL.

Figure 13

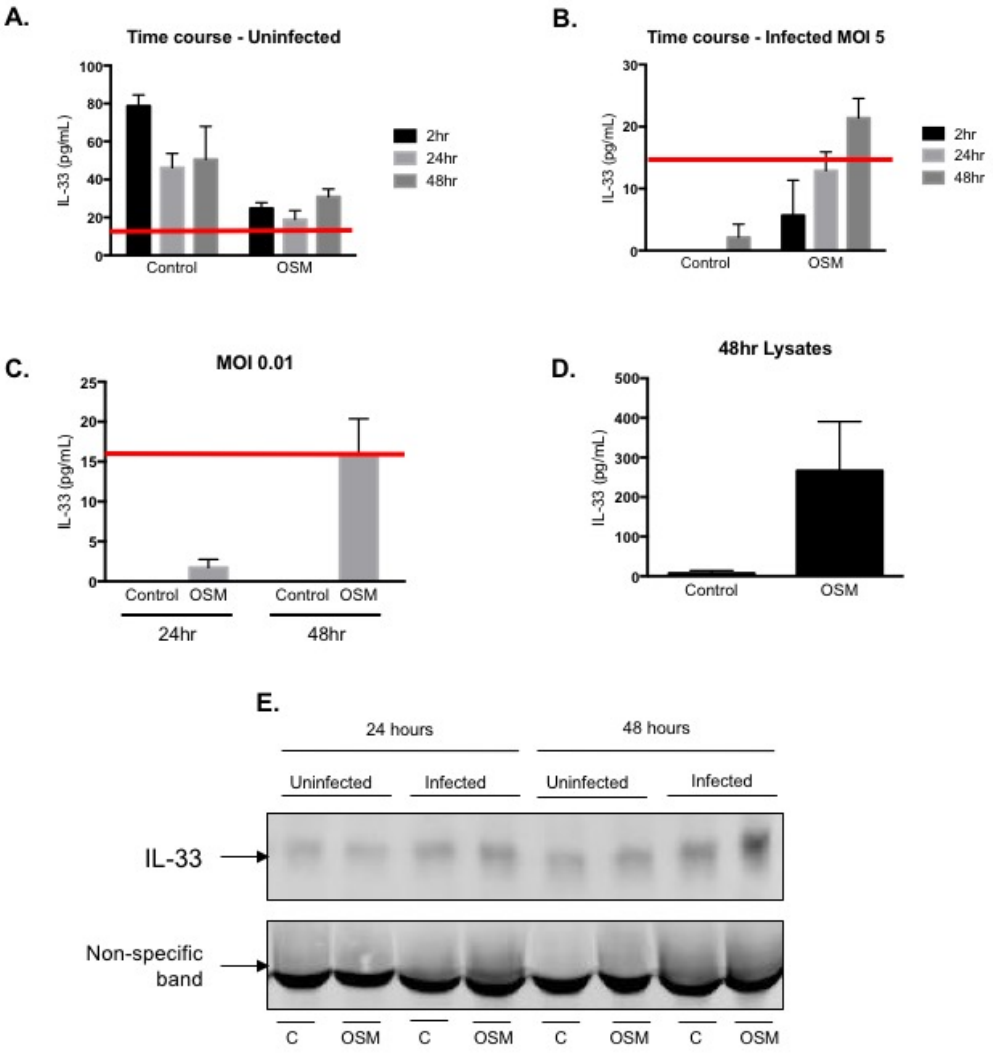
A.
Time course - Uninfected
IL-33 (pg/mL)
100
80
60
40
20
0
Control
OSM
2hr
24hr
48hr
B.
Time course - Infected MOI 5
IL-33 (pg/mL)
30
20
10
0
Control
OSM
2hr
24hr
48hr
C.
MOI 0.01
IL-33 (pg/mL)
25
20
15
10
5
0
Control OSM
Control OSM
24hr
48hr
D.
48hr Lysates
IL-33 (pg/mL)
500
400
300
200
100
0
Control
OSM
E.
24 hours
48 hours
Uninfected
Infected
Uninfected
Infected
IL-33
Non-specific band
C
OSM
C
OSM
C
OSM
C
OSM

Figure 14. Effect of OSMR signalling on cytokine levels in the BAL or lung homogenates following Influenza A/PR8-infection. C57Bl/6 wild-type and $OSMR^{-/-}$ mice were infected with a low dose ($2.5x10^2$ PFU/mouse) of the PR8 strain of Influenza A virus and culled at day 7 (n=4 mice/treatment). OSM (A), IL-6 (B) and IL-33 (C) levels in the bronchoalveolar lavage fluid. OSM (D) and IL-33 (E) levels in the lung homogenates using respective ELISAs at 1:50 and 1:200 dilutions. (F) Lung homogenates probed for IL-33 and β-Actin by Western blot. Statistics were completed using a two-way ANOVA and Bonferroni post-hoc analysis, where $p^*<0.05$ and $p^{***}<0.001$.

Figure 14

Low Dose – PR8

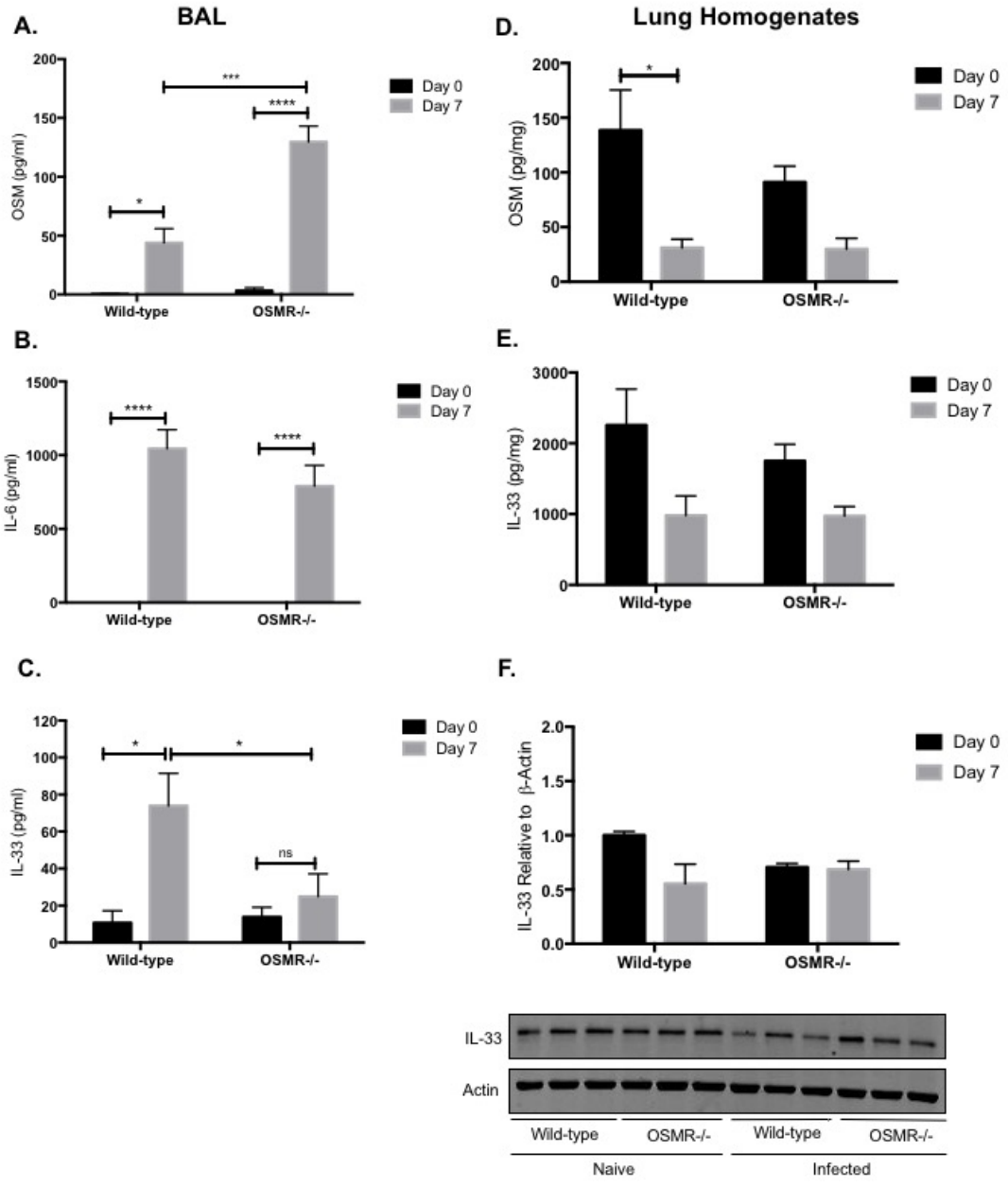

Figure 15. Effect of OSMR signalling on histopathology and immune cell infiltration following Influenza A/PR8-infection. C57Bl/6 wild-type and $OSMR^{-/-}$ mice were infected with a low dose ($2.5x10^2$ PFU/mouse) of the PR8 strain of Influenza A virus and culled at day 7 (n=4 mice/treatment). (A) Histopathology (H&E staining) of paraffin-embedded formalin-fixed lung tissue. Macrophage percentage (B) and neutrophil percentage (C) of cells within the bronchoalveolar lavage fluid. Total macrophage count (D) and total neutrophil count (E) within the bronchoalveolar lavage fluid. Statistics completed using GraphPad Prism by one-way ANOVA and Tukey's post-hoc analysis, where $p^*<0.05$.

Figure 15

Low Dose – PR8

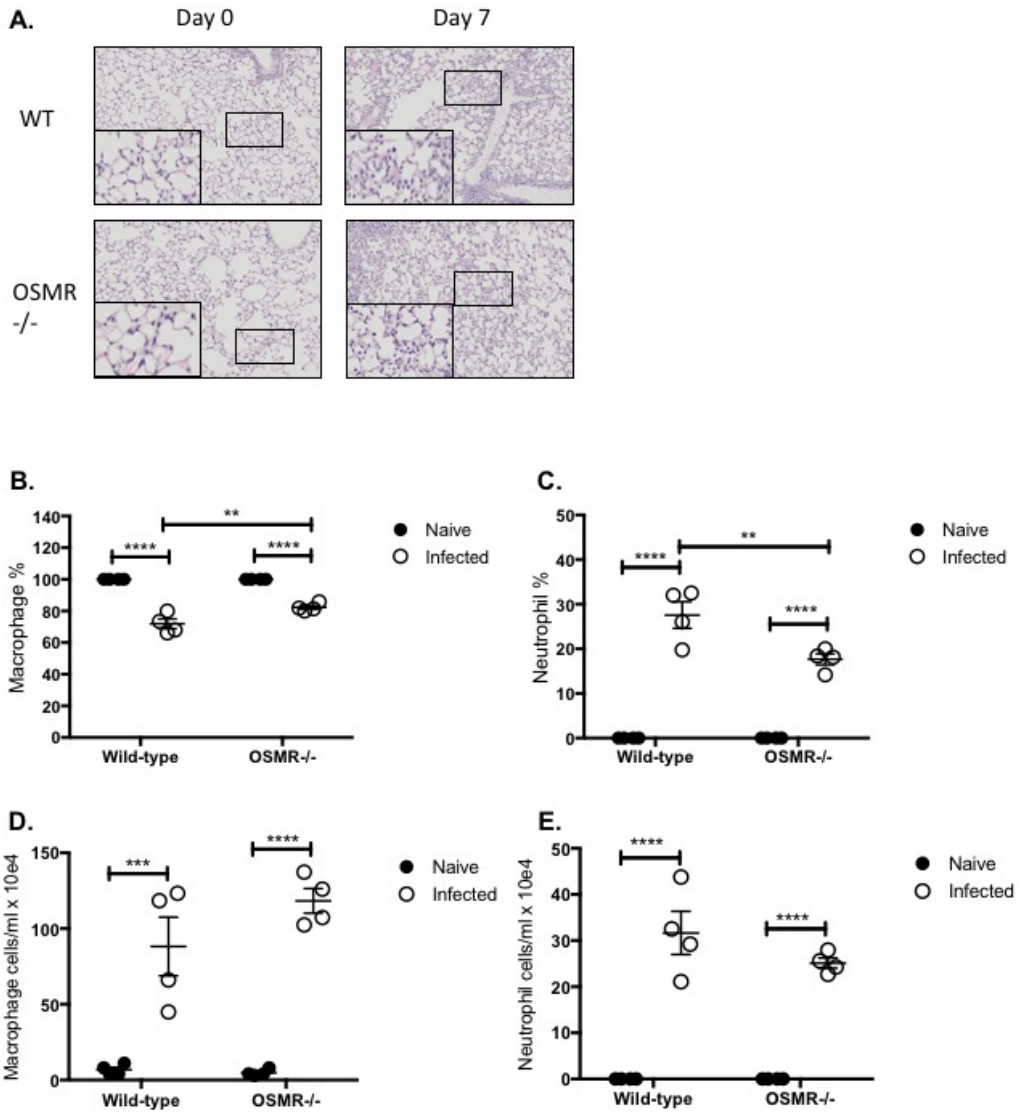

Figure 16. Effect of OSMR signalling on cytokine levels in the BAL or lung homogenates following Influenza A/PR8-infection at Day 7. C57Bl/6 wild-type and $OSMR^{-/-}$ mice were infected with a high dose ($1x10^3$ PFU/mouse) of the PR8 strain of Influenza A virus and culled at 2, 4, and day 7 (n=4 mice/treatment). OSM (A), IL-6 (B) and IL-33 (C) levels in the bronchoalveolar lavage fluid. OSM (D) and IL-33 (E) levels in the lung homogenates using respective ELISAs at 1:50 and 1:200 dilutions. (F) Weights of mice following Day 2, 4, and 7-days post-infection with influenza. Statistics were completed using a two-way ANOVA and Tukey's post-hoc analysis, where p*<0.05 and p***<0.001, indicates a statistically significant difference from naïve to treatment groups within the same mouse strain (i.e WT naïve vs WT day 2) and p#<0.05, indicates a statistically significant difference between strains of the same treatment group (i.e WT day 2 vs $OSMR^{-/-}$ day 2).

Figure 16 High Dose – PR8

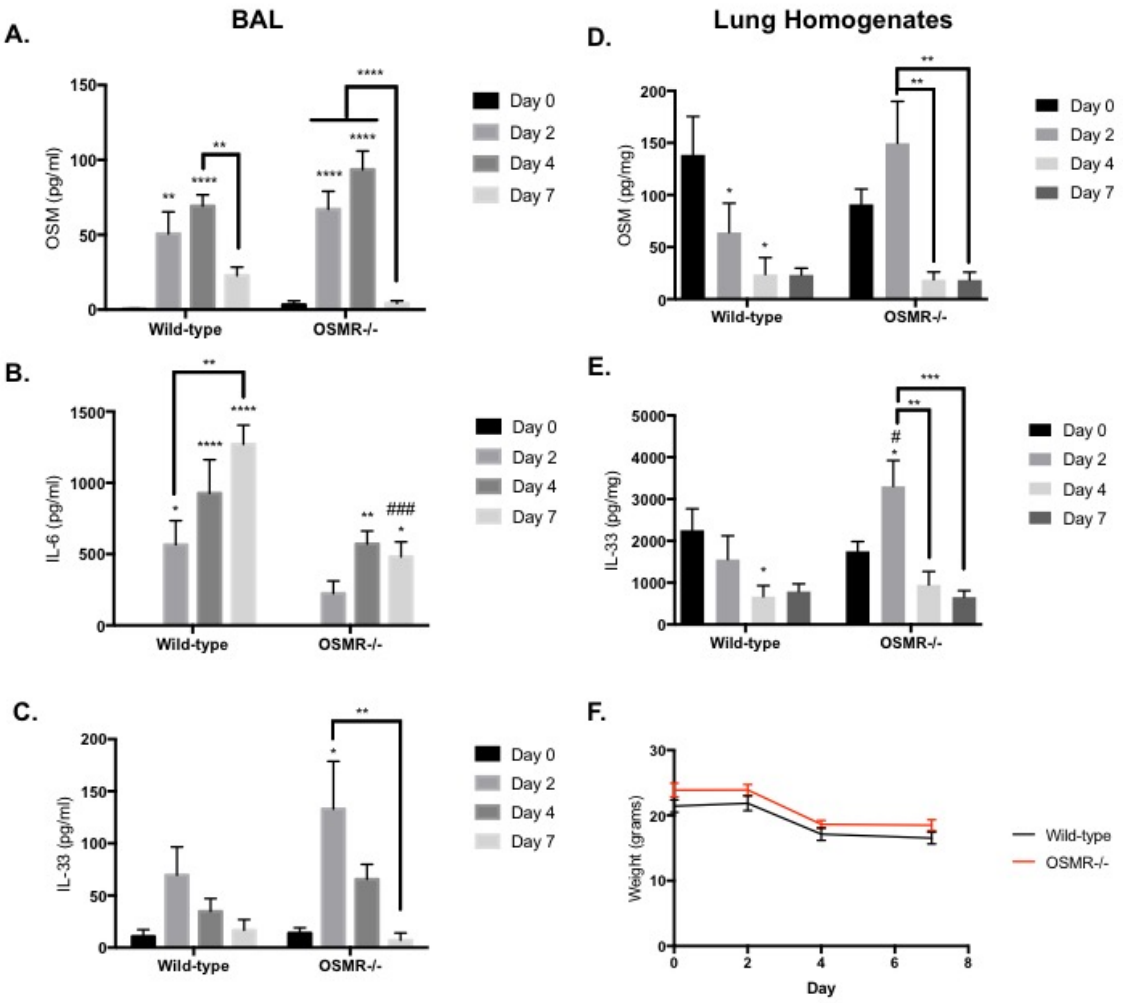

Figure 17. Effect of OSMR signalling on IL-33 levels in lung homogenates following Influenza A/PR8-infection. C57Bl/6 wild-type and $OSMR^{-/-}$ mice were infected with a high dose ($1x10^3$ PFU/mouse) of the PR8 strain of Influenza A virus and culled at day 2, 4 and 7 (n=4 mice/treatment). Lung homogenates probed for IL-33, β-Actin, and pSTAT3 by Western blot from mice administered virus and culled on day 2 (A), day 4 (B) and day 7 (C). Quantification of IL-33 Western blot signal corrected for β-Actin from day 2 (D), day 4 (E) and day 7 (F). Naïve samples on each gel were the same for each blot. Statistics were completed using a two-way ANOVA and Bonferroni post-hoc analysis, where $p^*<0.05$ and $p^{***}<0.001$.

Figure 17

High Dose – PR8

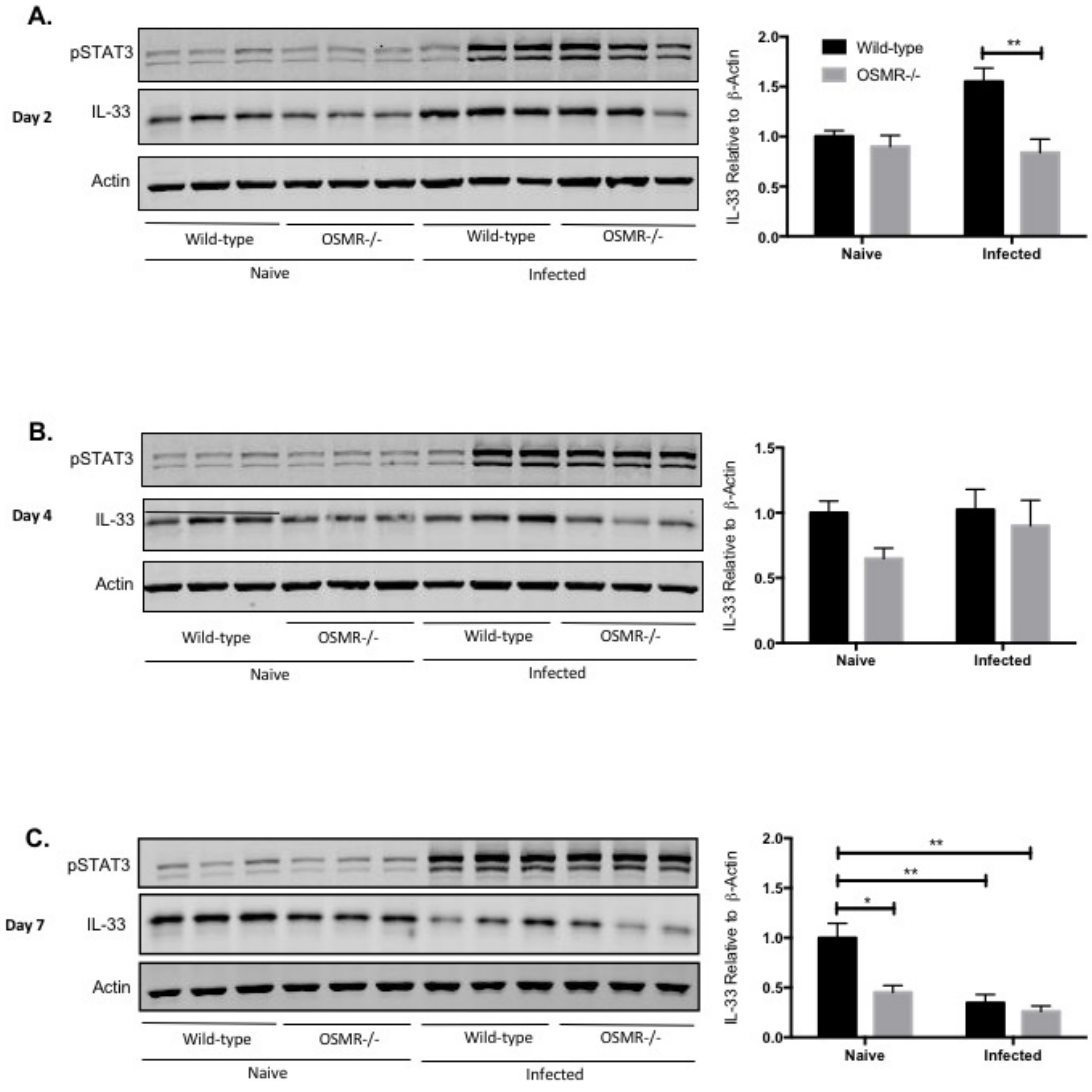

Figure 18. Effect of OSMR signalling on histopathology and immune cell infiltration following Influenza A/PR8-infection. C57Bl/6 wild-type and $OSMR^{-/-}$ mice were infected with a high dose ($1x10^3$ PFU/mouse) of the PR8 strain of Influenza A virus and culled at day 2, 4, and 7 (n=4 mice/treatment). (A) Histopathology (H&E staining) of paraffin-embedded formalin-fixed lung tissue. Macrophage percentage (B) and neutrophil percentage (C) of cells within the bronchoalveolar lavage fluid (Day 7). Total macrophage count (D) and total neutrophil count (E) within the bronchoalveolar lavage fluid (Day 7). Statistics completed using GraphPad Prism by one-way ANOVA and Tukey's post-hoc analysis, where $p^*<0.05$.

Figure 18

High Dose – PR8

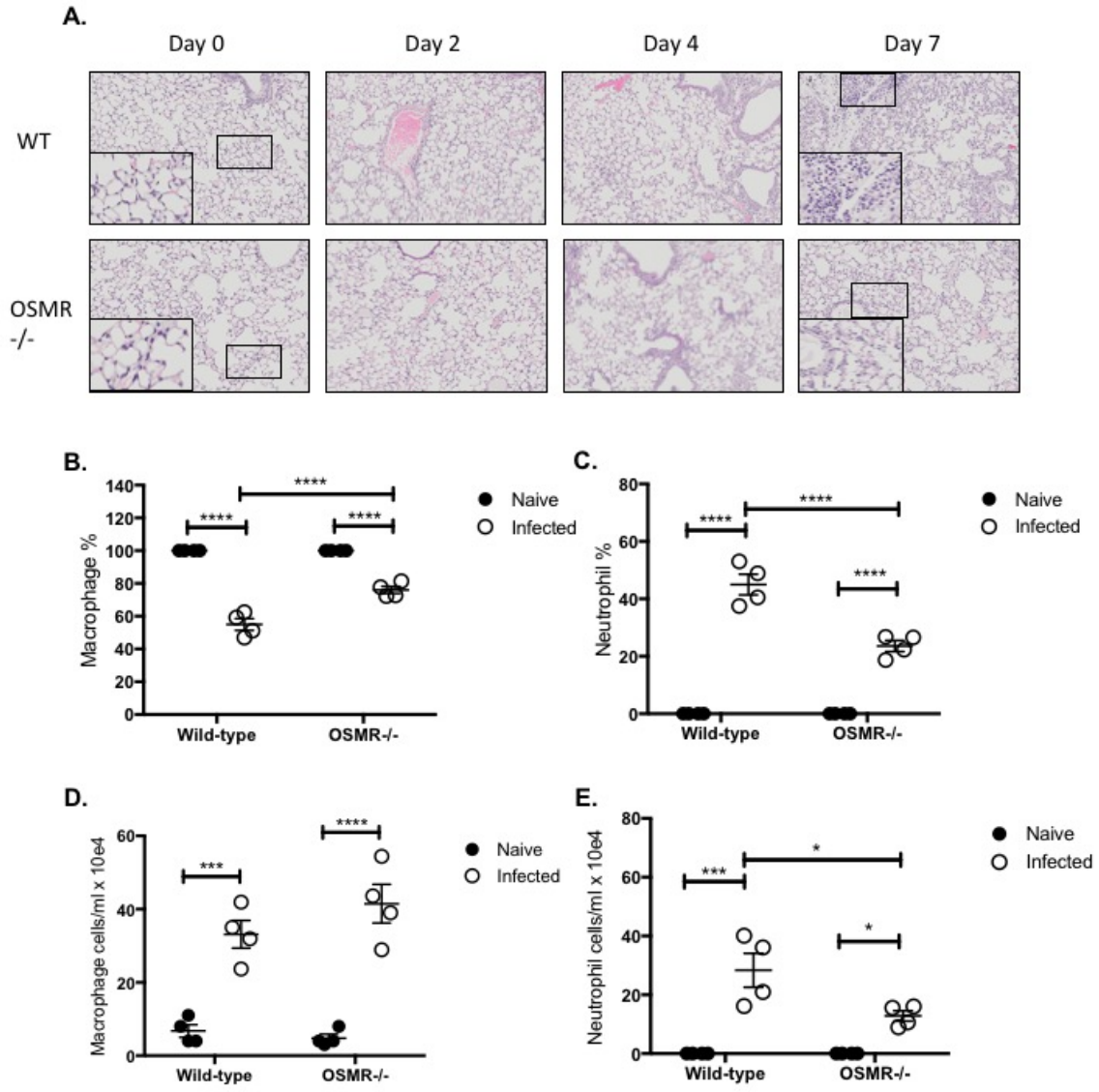

Figure 19. Cytokine levels in the BAL of C57Bl/6 mice following Influenza A/FM/1/47-infection. C57Bl/6 wild-type mice were infected with a low ($2x10^4$ PFU/mouse) and high dose ($1x10^5$ PFU/mouse) of the FM/1/47 strain of Influenza A virus and culled at day 2 and 4 (n=4 mice/treatment). OSM (A), IL-6 (B) and IL-33 (C) levels in the bronchoalveolar lavage fluid. Statistics were completed using a one-way ANOVA and Tukey's post-hoc analysis, where p*<0.05 and p***<0.001. represents a statically significant difference between treatment groups and the mean of the 2 groups of naïve mice (day 0).

Figure 19

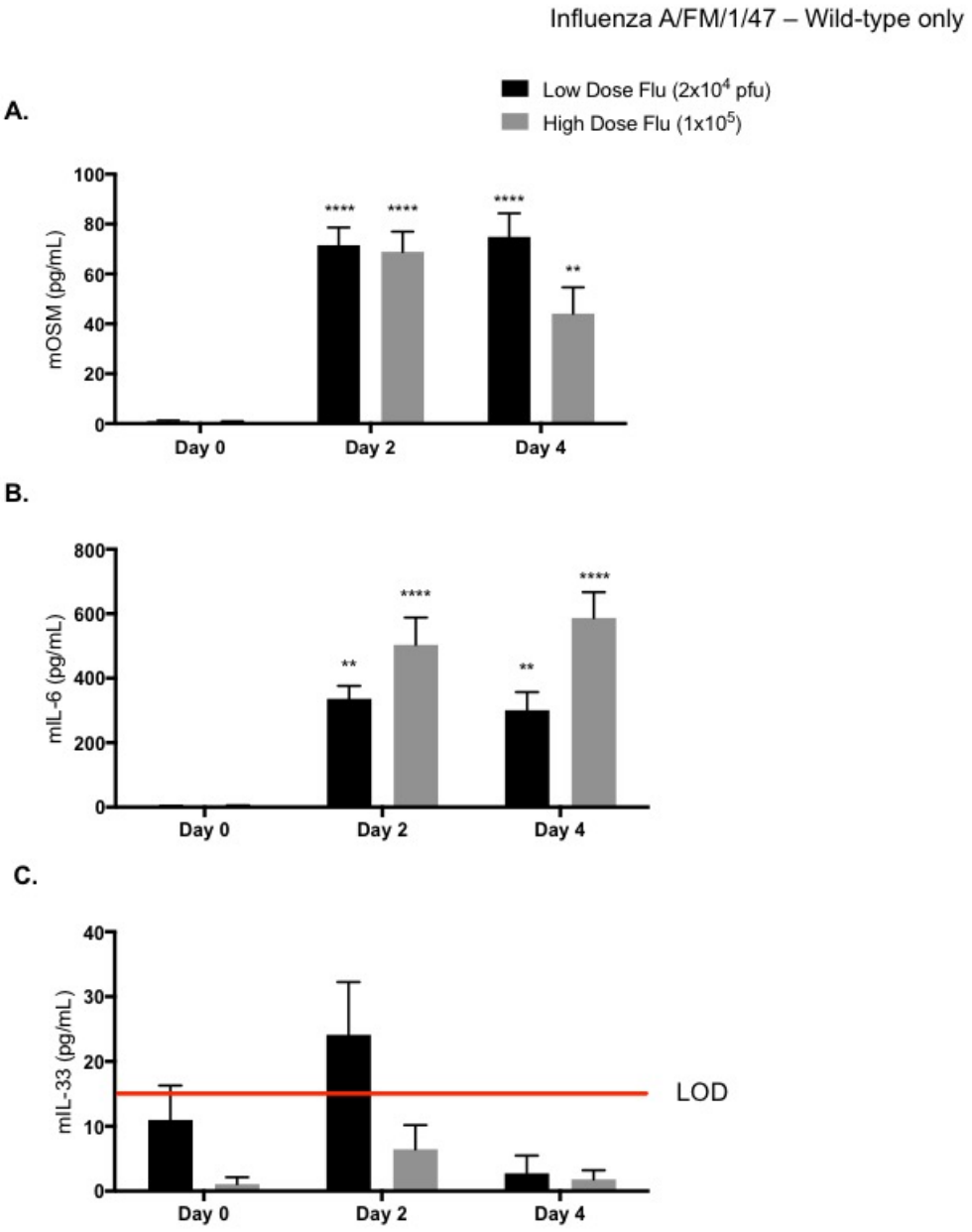
Influenza A/FM/1/47 – Wild-type only
Low Dose Flu (2x10^4 pfu)
High Dose Flu (1x10^5)
A.
mOSM (pg/mL)
100
80
60
40
20
0
****
****
****
**
Day 0
Day 2
Day 4
B.
mIL-6 (pg/mL)
800
600
400
200
0
**
****
**
****
Day 0
Day 2
Day 4
C.
mIL-33 (pg/mL)
40
30
20
10
0
LOD
Day 0
Day 2
Day 4

Figure 20. Regulation of IL-33 and immune cell infiltration in C57Bl/6 mice following Influenza A/FM/1/47-infection. C57Bl/6 wild-type mice were infected with a low ($2x10^4$ PFU/mouse) and high dose ($1x10^5$ PFU/mouse) of the FM/1/47 strain of Influenza A virus and culled at day 2 and 4 (n=4 mice/treatment). (A, C) Lung homogenates were probed for IL-33, pSTAT3 and β-Actin by Western Blot. Quantification of IL-33 signal using Image Studio for Day 2 (B) and Day 4 (D). Macrophage percentage (E, G) and neutrophil percentage (F, H) of cells within the bronchoalveolar lavage fluid at day 2 and day 4. Statistics were completed using a one-way ANOVA and Tukey's post-hoc analysis, where $p^*<0.05$.

Figure 20

Influenza A/FM/1/47 – Wild-type only

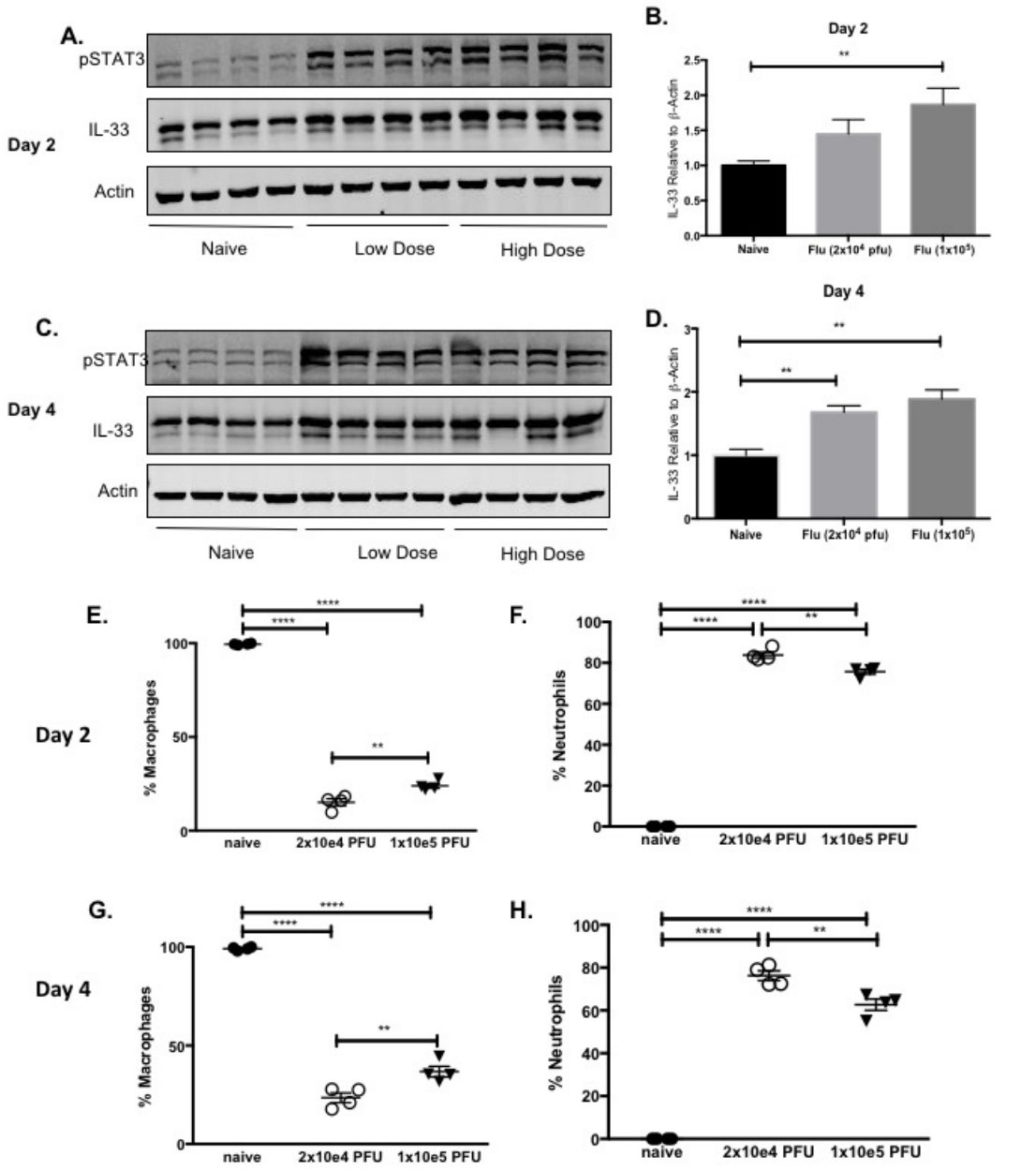

Figure 21. Effect of OSMR signalling on cytokine levels in the BAL or lung homogenates following Influenza A/FM/1/47-infection. C57Bl/6 wild-type and OSMR$^{-/-}$ mice were infected with a low ($2x10^4$ PFU/mouse) and high dose ($1x10^5$ PFU/mouse) of the FM/1/47 strain of Influenza A virus and culled at day 7 (n=4 mice/treatment). OSM (A), IL-6 (B) and IL-33 (C) levels in the bronchoalveolar lavage fluid. OSM (D) and IL-33 (E) levels in the lung homogenates using respective ELISAs at 1:50 and 1:200 dilutions. Statistics were completed using a two-way ANOVA and Tukey's post-hoc analysis, where p*<0.05 and p***<0.001, indicates a statistically significant difference from naïve to treatment groups within the same mouse strain (i.e WT naïve vs WT day 2) and p#<0.05, indicates a statistically significant difference between strains of the same treatment group (i.e WT day 2 vs OSMR$^{-/-}$ day 2).

Figure 21 Influenza A/FM/1/47 – Wild-type and OSMR-/- (Low and High Dose)

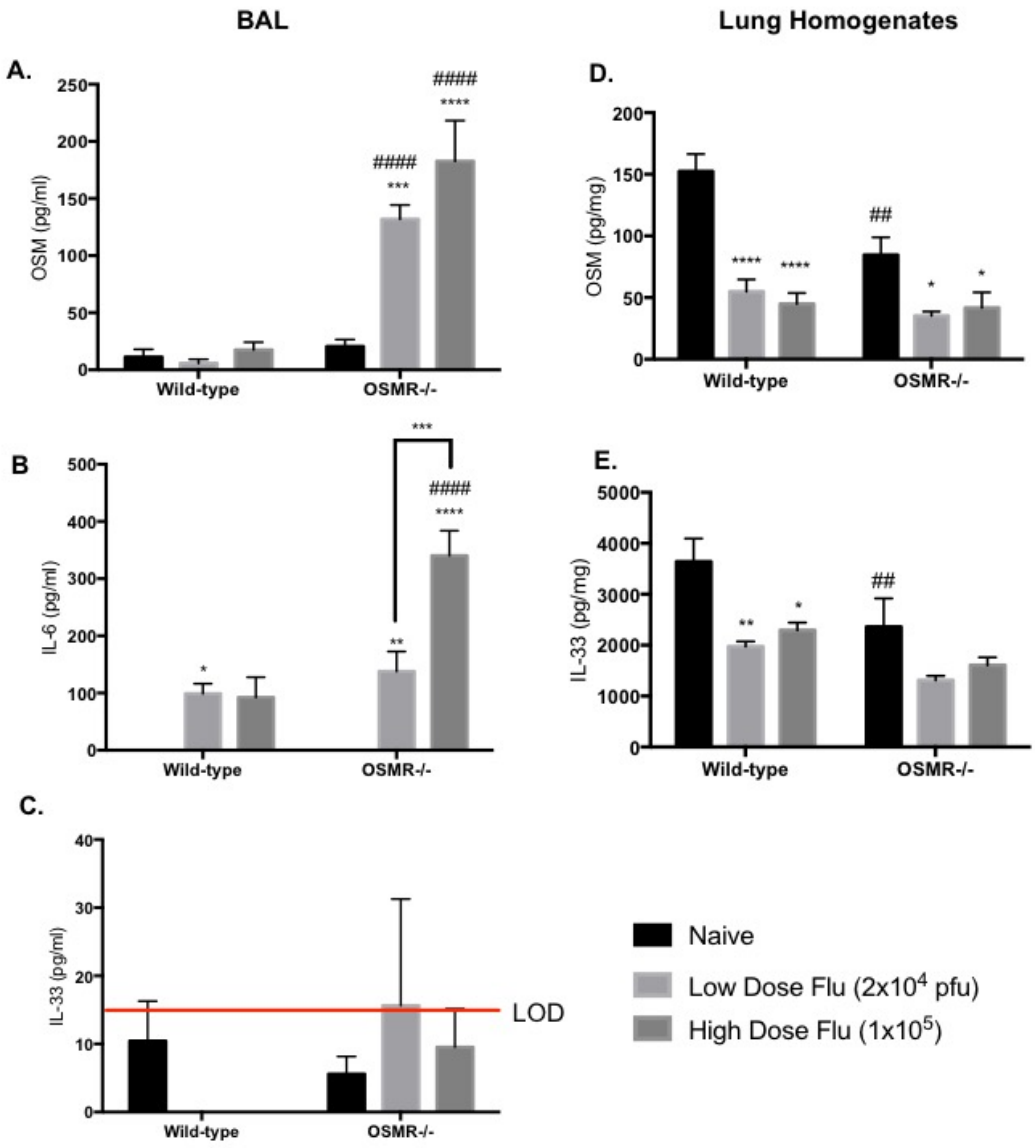

Figure 22. Effect of OSMR signalling on histopathology and immune cell infiltration following Influenza A/FM/1/47-infection. C57Bl/6 wild-type and $OSMR^{-/-}$ mice were infected with a low ($2x10^4$ PFU/mouse) and high dose ($1x10^5$ PFU/mouse) of the FM/1/47 strain of Influenza A virus and culled at day 7 (n=4 mice/treatment). Histopathology (H&E staining) of paraffin-embedded formalin-fixed lung tissue (A). Macrophage percentage (B) and neutrophil percentage (C) of cells within the bronchoalveolar lavage fluid (Day 7). Total macrophage count (D) and total neutrophil count (E) within the BALF (Day 7). Statistics completed using GraphPad Prisim by one-way ANOVA and Tukey's post-hoc analysis, where $p^*<0.05$.

Figure 22 Influenza A/FM/1/47 – Wild-type and OSMR-/- (Low and High Dose)

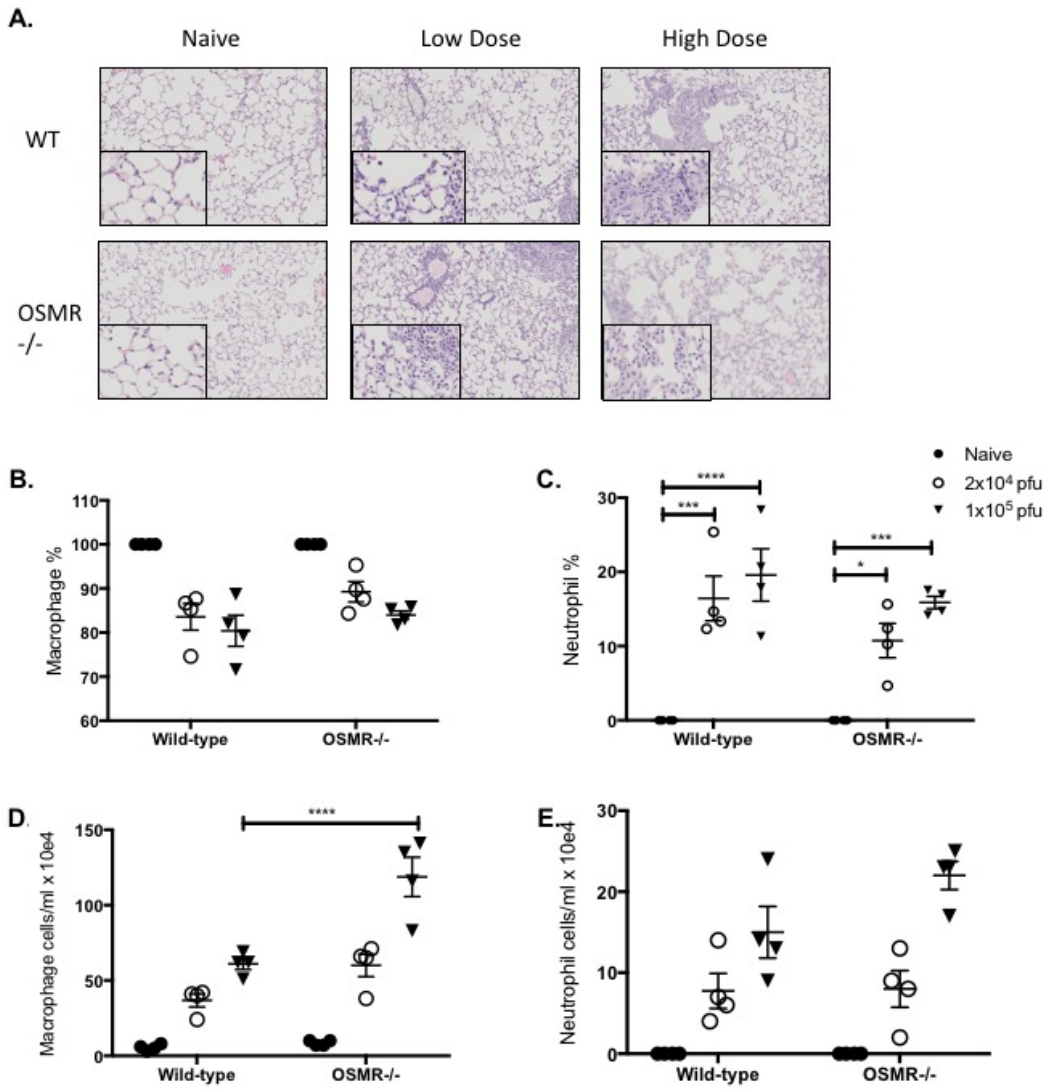

Figure 23. Cytokine levels in the BAL following co-infection. Wild-type C57Bl/6 mice pre-treated with AdDel70 or Ad OSM ($5x10^7$ PFU/mouse for 7 days) and then infected with Influenza A (PR8) virus for 2 days. (A) Schematic figure outlining the details of the experiment. (B) OSM and (C) IL-33 measured by ELISA (R&D) in the bronchoalveolar lavage fluid of mice pre-treated with AdDel70 or AdOSM and then infected with PR8 virus (250 PFU/mouse).

Figure 23

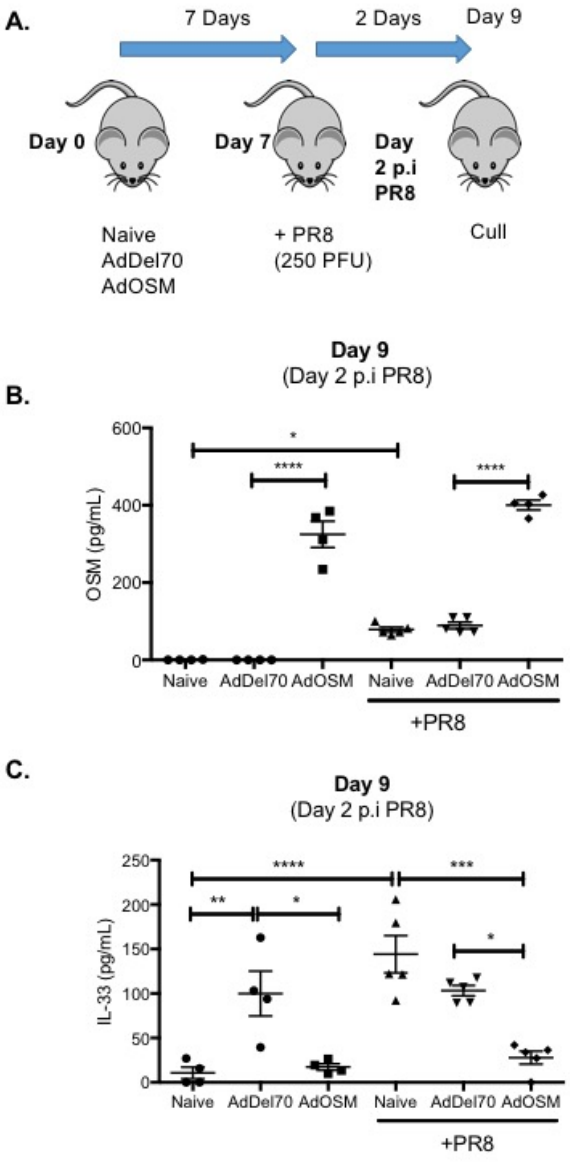
A.
7 Days
2 Days
Day 9
Day 0
Day 7
Day 2 p.i PR8
Naive
AdDel70
AdOSM
+ PR8 (250 PFU)
Cull
B.
Day 9
(Day 2 p.i PR8)
OSM (pg/mL)
600
400
200
0
Naive
AdDel70
AdOSM
Naive
AdDel70
AdOSM
+PR8
C.
Day 9
(Day 2 p.i PR8)
IL-33 (pg/mL)
250
200
150
100
50
0
Naive
AdDel70
AdOSM
Naive
AdDel70
AdOSM
+PR8

Figure 24. Regulation of IL-33 and Arg1 in lung tissue of co-infected mice. (A) Whole lung homogenates of naïve mice, PR8 virus-infected (2 days) mice and control AdDel70 and AdOSM-treated (9 days) mice probed for IL-33 (R&D), pSTAT3 (Cell Signalling) and β-Actin (Santa Cruz) by Western blot. (D) Whole lung homogenates of control AdDel70 and AdOSM-treated (9 days) mice and mice pre-treated with AdDel70 and AdOSM (7 days) followed by PR8 virus infection (2 days) probed for IL-33 (R&D), pSTAT3 (Cell Signalling) and β-Actin (Santa Cruz) by Western blot. (B-C, E-F) Quantification of IL-33 signal corrected to β-Actin and represented as a fold-change relative to naïve or AdDel70 samples.

Figure 24

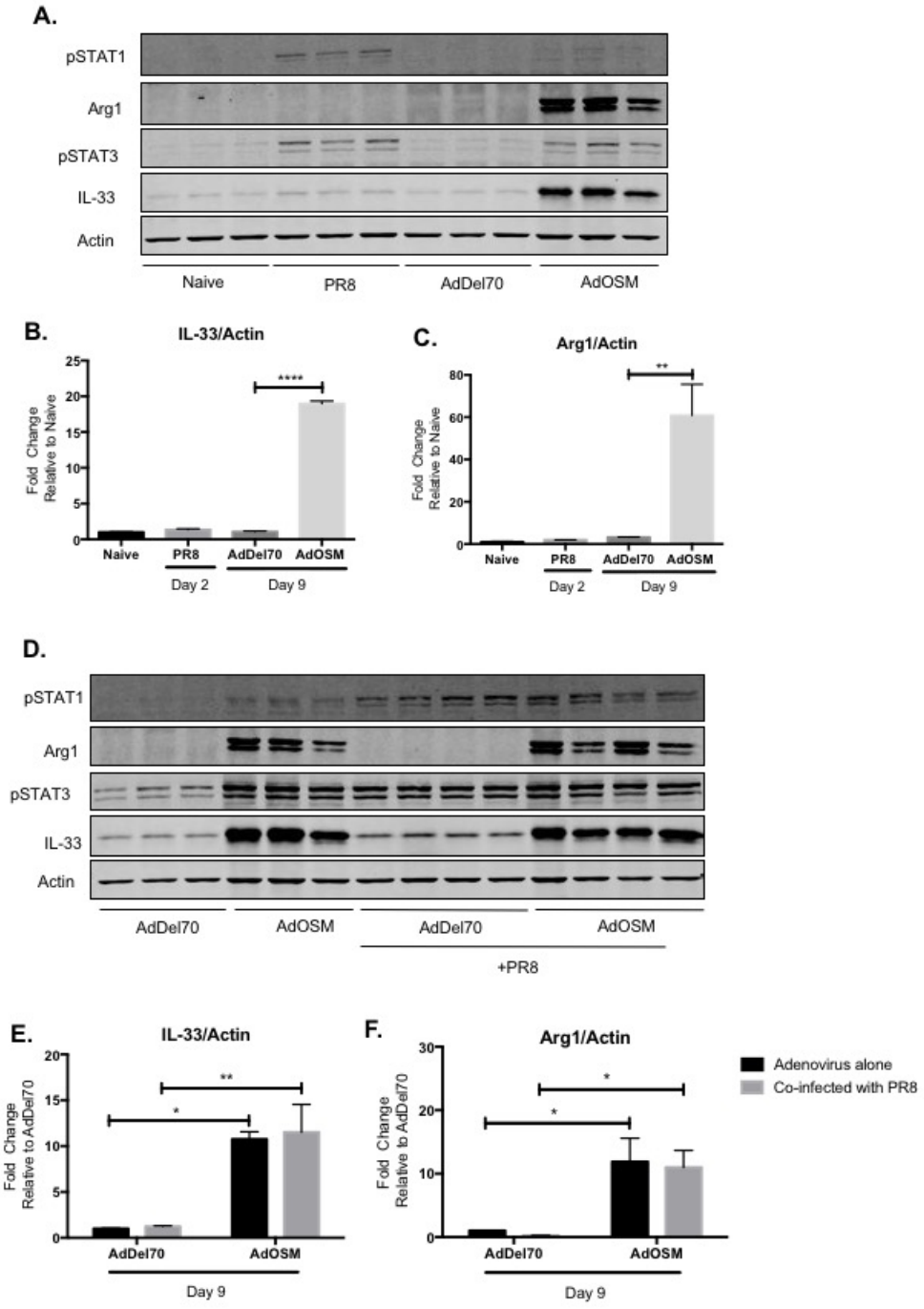
A.
pSTAT1
Arg1
pSTAT3
IL-33
Actin
Naive
PR8
AdDel70
AdOSM
B.
IL-33/Actin
Fold Change Relative to Naive
****
Naive
PR8
AdDel70
AdOSM
Day 2
Day 9
C.
Arg1/Actin
Fold Change Relative to Naive
**
Naive
PR8
AdDel70
AdOSM
Day 2
Day 9
D.
pSTAT1
Arg1
pSTAT3
IL-33
Actin
AdDel70
AdOSM
AdDel70
AdOSM
+PR8
E.
IL-33/Actin
Fold Change Relative to AdDel70
**
*
AdDel70
AdOSM
Day 9
F.
Arg1/Actin
Fold Change Relative to AdDel70
*
*
AdDel70
AdOSM
Day 9
Adenovirus alone
Co-infected with PR8

Figure 25. Differential cell counts from co-infected mice (2 days). Wild-type C57Bl/6 mice pre-treated with AdDel70 or AdOSM ($5x10^7$ PFU/mouse for 7 days) and then infected with Influenza A (PR8) virus for 2 days. BALF cell percentages of A) macrophages, B) neutrophils, C) lymphocytes and D) eosinophils. BALF total cell counts for E) macrophages, F) neutrophils, G) lymphocytes, and H) eosinophils.

Figure 25

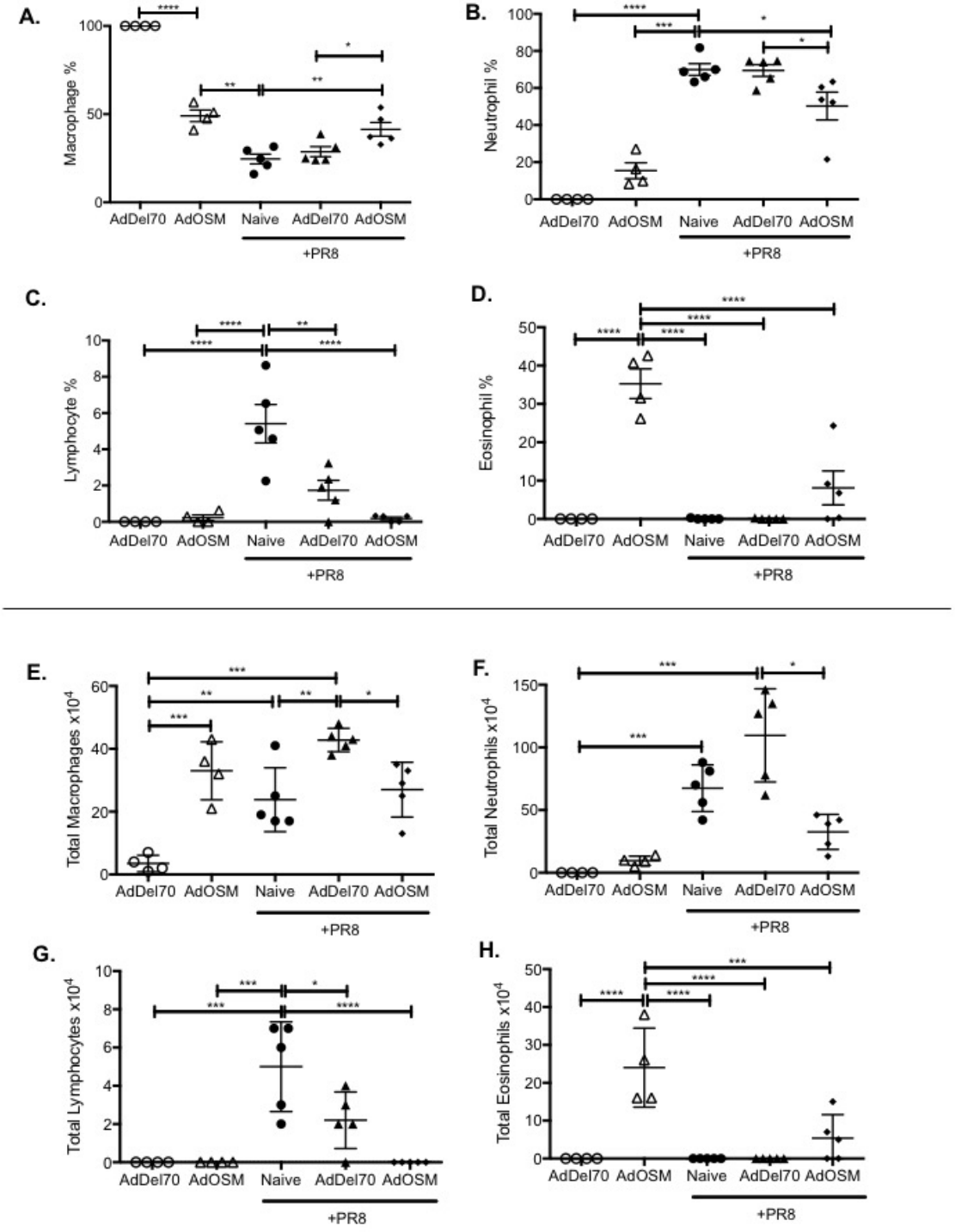
A.
Macrophage %
B.
Neutrophil %
C.
Lymphocyte %
D.
Eosinophil %
E.
Total Macrophages x10^4
F.
Total Neutrophils x10^4
G.
Total Lymphocytes x10^4
H.
Total Eosinophils x10^4
AdDel70
AdOSM
Naive
AdDel70
AdOSM
+PR8

Figure 26. Cytokine levels in the BAL following co-infection. Wild-type C57Bl/6 mice pre-treated with AdDel70 or AdOSM ($5x10^7$ PFU/mouse for 7 days) and then infected with Influenza A (PR8) virus for 5 days. (A) Schematic figure outlining the details of the experiment. (B) Weights (in grams) of mice at Day 0 and at Day 2 following influenza A virus infection. (A) OSM and (B) IL-33 measured by ELISA (R&D) in the bronchoalveolar lavage fluid of mice pre-treated with AdDel70 or AdOSM and then infected with PR8 virus (250 PFU/mouse).

.

Figure 26

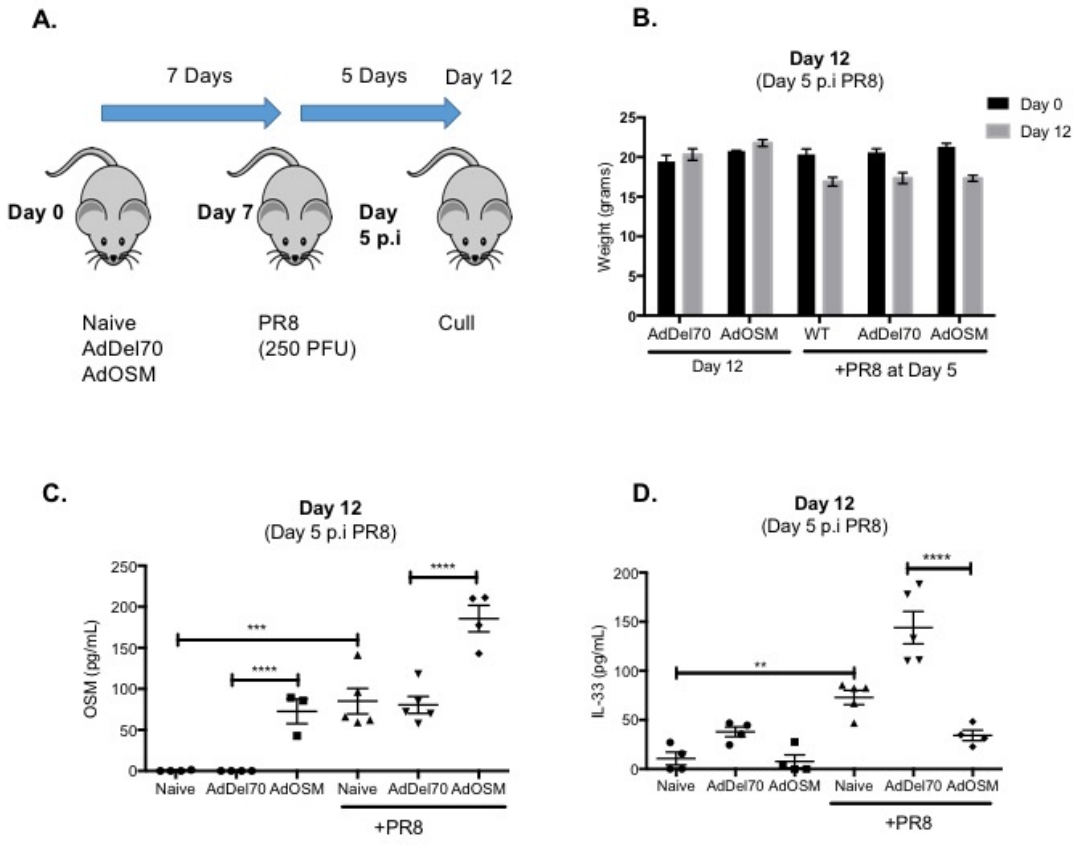
A.
7 Days
5 Days
Day 12
Day 0
Day 7
Day 5 p.i
Naive
AdDel70
AdOSM
PR8
(250 PFU)
Cull
B.
Day 12
(Day 5 p.i PR8)
Day 0
Day 12
Weight (grams)
AdDel70
AdOSM
WT
AdDel70
AdOSM
Day 12
+PR8 at Day 5
C.
Day 12
(Day 5 p.i PR8)
OSM (pg/mL)
Naive
AdDel70
AdOSM
Naive
AdDel70
AdOSM
+PR8
D.
Day 12
(Day 5 p.i PR8)
IL-33 (pg/mL)
Naive
AdDel70
AdOSM
Naive
AdDel70
AdOSM
+PR8

Figure 27. Regulation of IL-33 and Arg1 in lung tissue of co-infected mice. Wild-type C57Bl/6 mice pre-treated with AdDel70 or AdOSM ($5x10^7$ PFU/mouse for 7 days) and then infected with Influenza A (PR8) virus for 5 days. (A) Whole lung homogenates of naïve mice, PR8 virus-infected (2 days) mice and control AdDel70 and AdOSM-treated (12 days) mice probed for IL-33 (R&D), pSTAT3 (Cell Signalling) and β-Actin (Santa Cruz) by Western blot. (B) Whole lung homogenates of control AdDel70 and AdOSM-treated (12 days) mice and mice pre-treated with AdDel70 and AdOSM (7 days) followed by PR8 virus infection (2 days) probed for IL-33 (R&D), pSTAT3 (Cell Signalling) and β-Actin (Santa Cruz) by Western blot. (D) Quantification of IL-33 signal corrected to β-Actin and represented as a fold-change relative to AdDel70 uninfected samples.

Figure 27

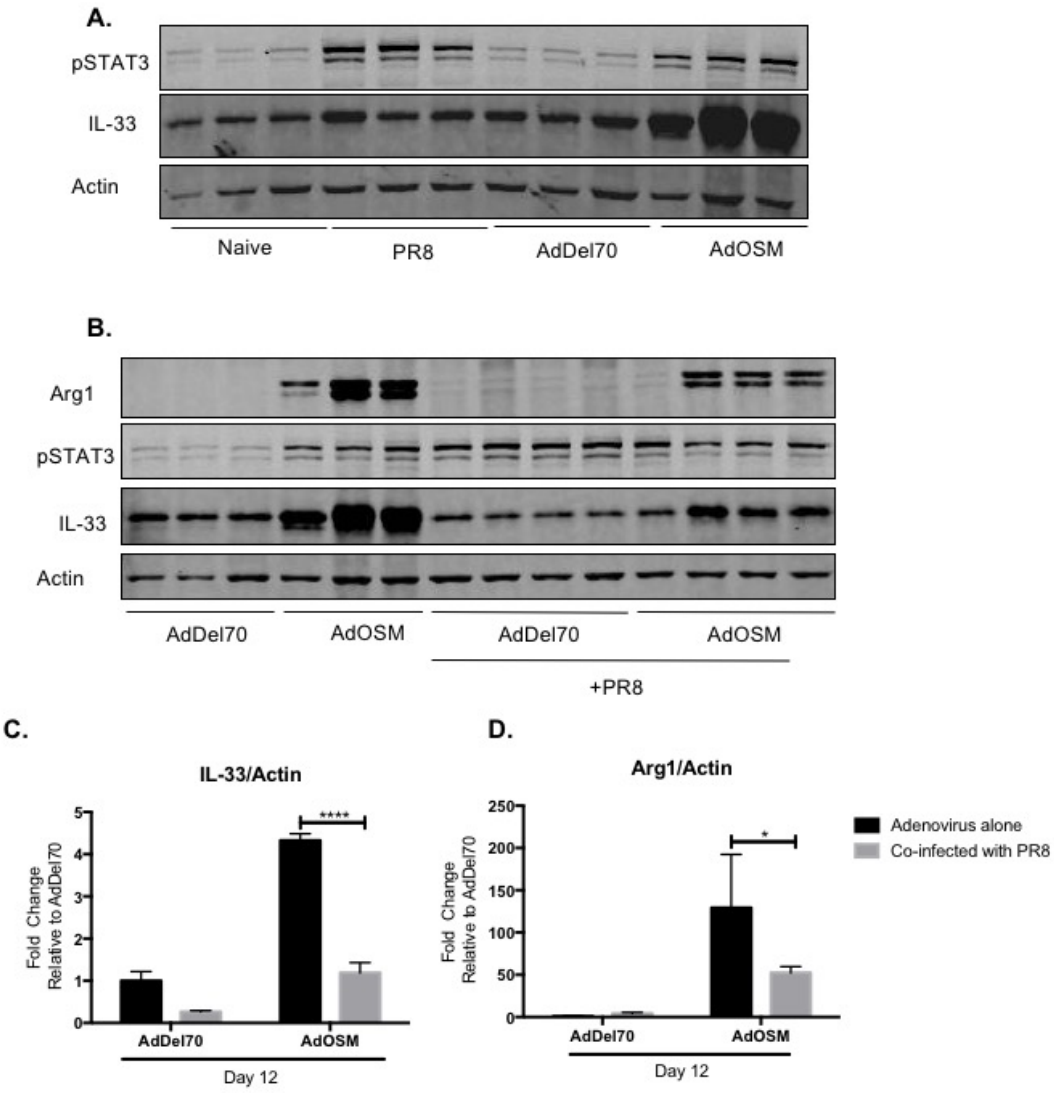
A.
pSTAT3
IL-33
Actin
Naive
PR8
AdDel70
AdOSM
B.
Arg1
pSTAT3
IL-33
Actin
AdDel70
AdOSM
AdDel70
AdOSM
+PR8
C.
IL-33/Actin
Fold Change Relative to AdDel70
****
AdDel70
AdOSM
Day 12
D.
Arg1/Actin
Fold Change Relative to AdDel70
*
AdDel70
AdOSM
Day 12
Adenovirus alone
Co-infected with PR8

Figure 28. Differential cell counts from co-infected mice (5 days). Wild-type C57Bl/6 mice pre-treated with AdDel70 or AdOSM ($5x10^7$ PFU/mouse for 7 days) and then infected with Influenza A (PR8) virus for 5 days. BALF cell percentages of A) macrophages, B) neutrophils, C) lymphocytes and D) eosinophils. BALF total cell counts for E) macrophages, F) neutrophils, G) lymphocytes, and H) eosinophils.

Figure 28

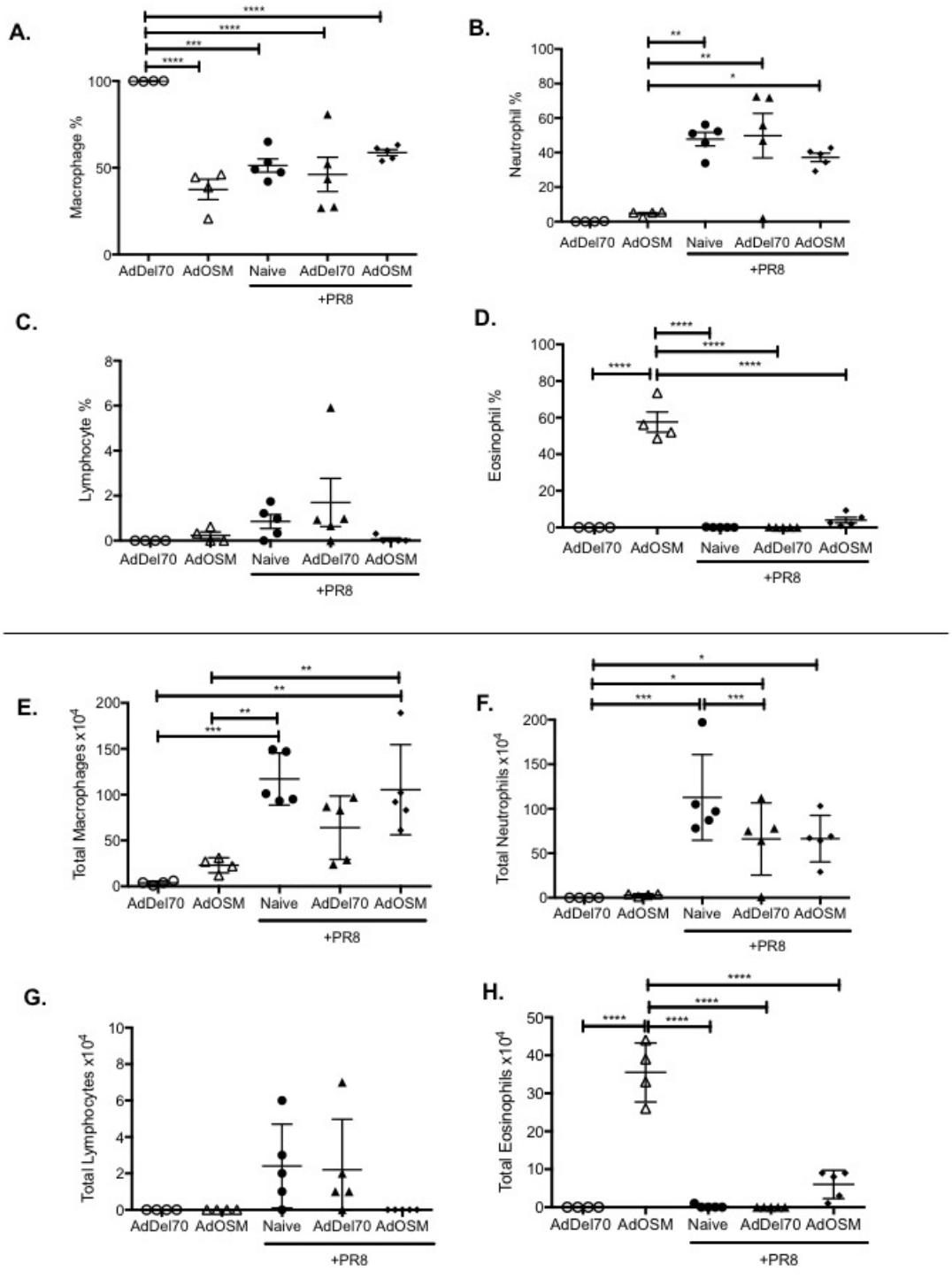
A.
Macrophage %
B.
Neutrophil %
C.
Lymphocyte %
D.
Eosinophil %
E.
Total Macrophages x10^4
F.
Total Neutrophils x10^4
G.
Total Lymphocytes x10^4
H.
Total Eosinophils x10^4
AdDel70
AdOSM
Naive
AdDel70
AdOSM
+PR8

Supplementary Figure 3. Immunopathology of lung tissue after co-infection (2 days). Wild-type C57Bl/6 mice pre-treated with AdDel70 or AdOSM ($5x10^7$ PFU/mouse for 7 days) and then infected with Influenza A (PR8) virus for 2 days.

Supplementary Figure 3

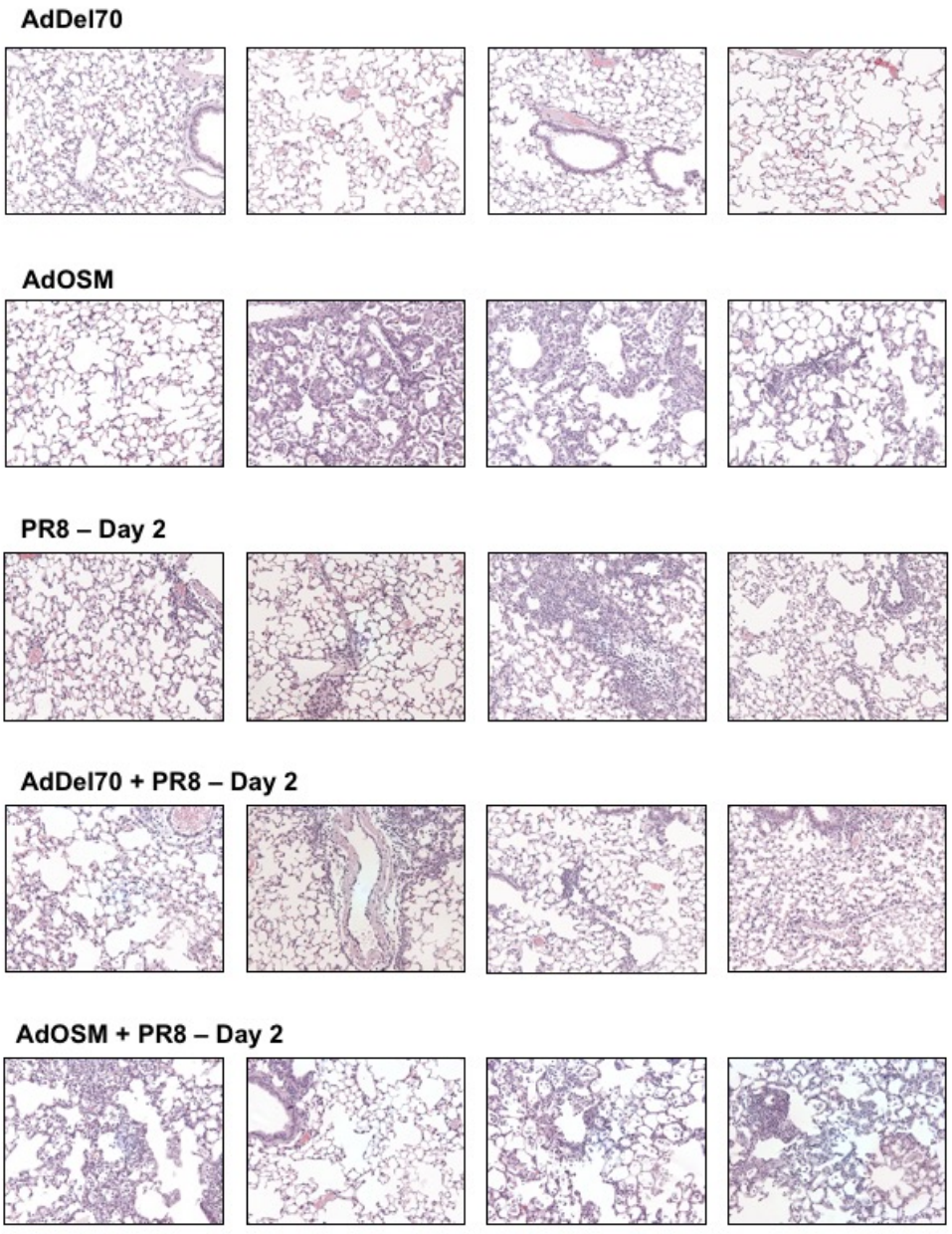

Supplementary Figure 4. Immunopathology of lung tissue after co-infection (5 days). Wild-type C57Bl/6 mice pre-treated with AdDel70 or AdOSM ($5x10^7$ PFU/mouse for 7 days) and then infected with Influenza A (PR8) virus for 5 days.

Supplementary Figure 4

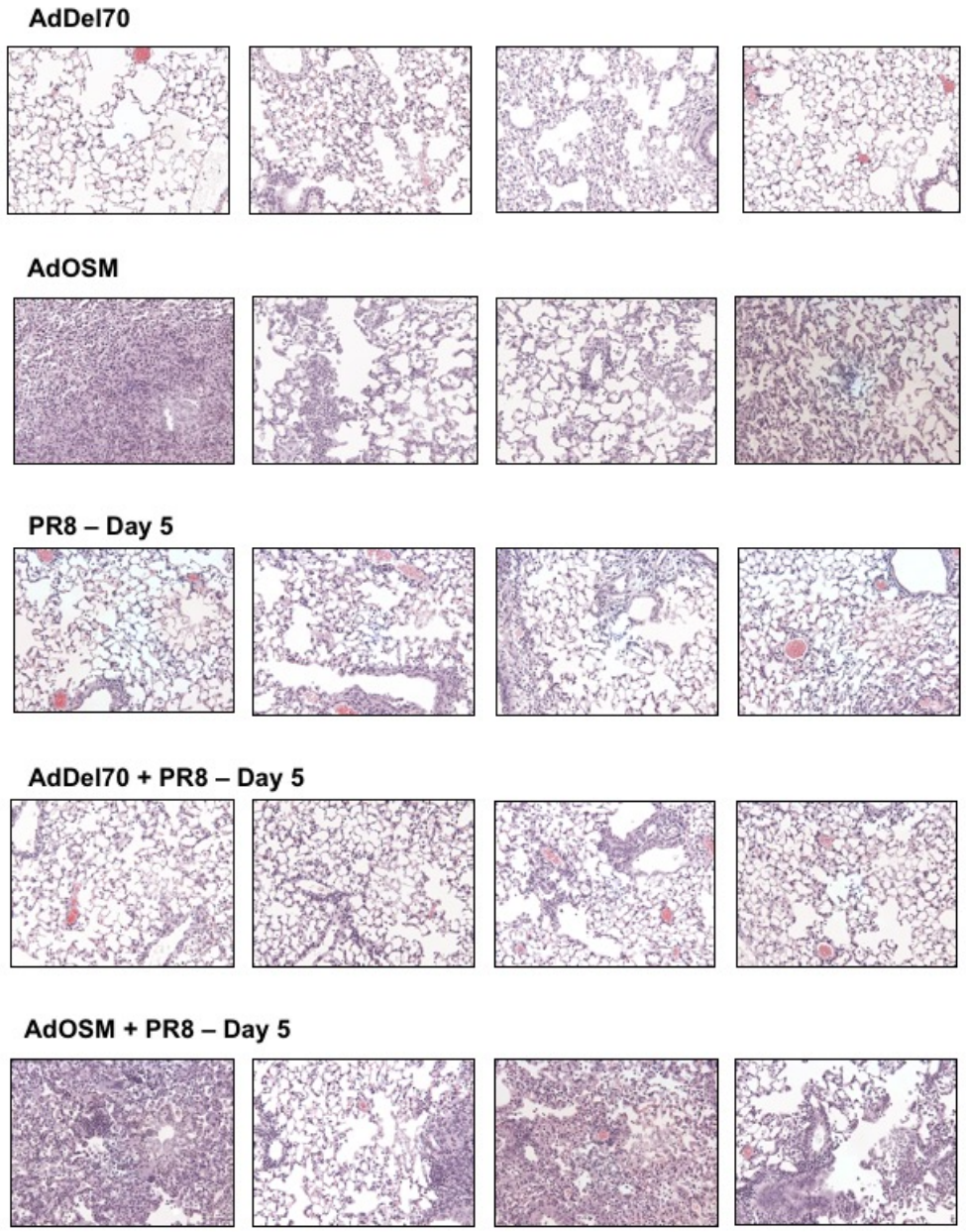

CHAPTER 5

- DISCUSSION -

5.1 Summary of Results

5.1.1 Results - Part 1

This thesis aimed to further characterize the OSM regulation of IL-33 and arginase-1 expression *in vitro* and *in vivo*. Data has shown that OSM-induced expression of the full-length IL-33 protein (approximately 35kDa) in mouse alveolar type 2 cells and in total mouse lung extracts. In human lung cells *in vitro*, OSM induced IL-33 protein expression within the A549 human type 2 alveolar epithelial cells, but not in human lung fibroblasts. IL-33 detection was verified using two anti-human IL-33 antibodies by Western blot, which depicted a signal corresponding to IL-33 at approximately 31kDa (corresponding to the full-length protein) similar to results observed within the mouse system.

In further experiments, differential functions of IL-6 and OSM on Arg1 and IL-33 regulation *in vivo* were identified. Results indicated that transient overexpression of IL-6 did not induce pulmonary IL-33 and Arg-1 expression nor Arg-1^{+} cell accumulation, in contrast to OSM overexpression in mouse systems (**Figure 8**). However, elevated Arg-1 expression as well as Arg-1^{+} cell accumulation by OSM in whole lung tissue was abrogated in IL-$6^{-/-}$ mice, suggesting IL-6- signaling is required for such OSM-mediated effects. Interestingly, IL-33 protein up-regulation was maintained within IL-$6^{-/-}$ mice treated with AdOSM, indicating separate mechanisms of IL-33 and Arg-1 protein regulation *in vivo* (**Figure 9**). Additionally, analysis of the cytokine milieu revealed that overexpression of OSM versus IL-6 produced distinct inflammatory microenvironment within the lung.

Specifically, IL-6 led to increase of several Th1-associated cytokines and chemokines, while OSM induced primarily Th2 cytokines, such as IL-5, IL-13 and IL-4 (**Supplementary Figure 1**). Arg1 abrogation in IL6$^{-/-}$ animals was consistent with analysis of BMDMs demonstrating that IL-6, in combination with IL-4/IL-13, directly stimulated Arg-1 activity *in vitro*, while OSM (nor LIF) did not (**Supplementary Figure 2**). Interestingly, analysis of IL-33$^{-/-}$ animals also demonstrated complete attenuation of Arg1 protein signal by Western blot in whole lung homogenates of mice administered AdOSM (**Figure 11A**). These results indicate that IL-33 plays an important role in mediating Arg1 expressing macrophage-like cell accumulation in the context of OSM-induced lung inflammation.

5.1.2 Results - Part 2

Chapter 3 focused on investigating the role of OSM and IL-33 in the context of an Influenza A virus infection. Contrary to the original hypothesis, findings revealed that mouse lung epithelial cells infected with the PR8 Influenza A virus strain *in vitro* showed decreased IL-33 release following infection (**Figure 13A and 13B**). However prior stimulation of cell *in vitro* with OSM led to increased IL-33 release within cell culture supernatants compared to unstimulated infected cells. These results suggest a role for OSM in potentiating release of IL-33 from virally-infected cells, however it is important to note that the levels of IL-33 detected were at or below the LOD of the ELISA. The supernatants were also assayed by Western blot in order to determine if this method of detection for IL-33 would produce similar results. Interestingly, the Western blot showed a stronger signal for full-length IL-33 within the same supernatants, which was unexpected based on the

ELISA results. These results suggest that future assessment of IL-33 release in cell culture supernatants, and perhaps BALF samples, may be more easily determined by Western blot.

In vivo analysis demonstrated that IL-33 and OSM protein was elevated in a time-dependent manner within the BALF of mice intranasally infected with Influenza A virus, with maximal detection at Day 2 post-infection. At a low dose of the PR8 virus, increased IL-33 was detected at Day 7 post-infection, which was attenuated in $OSMR^{-/-}$ animals, suggesting a role for OSM in mediating IL-33 regulation following a respiratory virus infection. Additionally, basal levels of IL-33 protein within whole lung homogenates was attenuated in naïve $OSMR^{-/-}$ mice relative to naïve wild-type mice. Upon infection, wild-type mice showed increased IL-33 protein within lung tissue at earlier time-points (Day 2 at high dose of virus), however this signal was attenuated by Day 7 relative to basal levels. Initial increase in IL-33 protein following infection was not observed in $OSMR^{-/-}$ mice, however decreased IL-33 signal compared to naïve mice was observed by Day 7 post-infection. These results were consistent with the alternative method of detection using IL-33 ELISA and OSM levels within the lung tissue homogenates, which also demonstrated a correlative trend in reduced IL-33 expression at Day 7. Analysis of histology within the lung tissue revealed slightly more inflammation in wild-type mice infected with Influenza compared to $OSMR^{-/-}$ animals. This qualitative observation was consistent with significantly less immune cell infiltration within the BALF of $OSMR^{-/-}$ mice infected with virus.

Overall, the findings from these experiments suggest that mice deficient in the OSM-receptor signalling subunit were somewhat compromised in the inflammatory

response to an Influenza A virus infection *in vivo*. Reduced immune cell infiltration into the BALF of infected animals suggests that OSM may play an important role in chemotaxis of cells into the lung for viral clearance and maintaining homeostasis. These experiments reveal that IL-33 was elevated within the BALF of influenza infected animals, however IL-33 regulation by OSM in the context of this respiratory infection was not clearly identified.

Lastly, the effect of OSM priming of the lung microenvironment prior to an Influenza A virus (PR8) infection. Results demonstrated that a PR8 infection for 2 days following AdOSM administration (until Day 7) did not alter IL-33 or Arg1 levels within the lung tissue as observed by Western blot. However, at day-5 post-influenza infection, levels of OSM-induced IL-33 and Arg-1 expression were significantly attenuated relative to AdOSM alone. This decrease in lung tissue IL-33 and Arg-1 was also associated with significantly decreased BALF eosinophil infiltration.

Overall, these results indicate that a subsequent influenza A virus infection led to the development of an immune response disrupting OSM-induced Th2-type inflammation within the lung microenvironment.

5.2 Arginase-1 and M2 Macrophages

Lung alveolar and interstitial macrophages assume a variety of cellular functions, including phagocytosis, antigen presentation and production of cytokines or chemokines during inflammatory processes[71]. Functional plasticity of macrophages into M1/M2 subtypes, based on localized signals, enables these cells to participate in multiple stages of injury or wound repair, from removal of pathogens to promoting cellular proliferation.

Murine M1/M2 macrophages can be identified by a unique set of markers. iNOS and CD40 are commonly used to identify M1 macrophages, whereas CD206, FIZZ-1 or Arg-1 are used to identify M2 macrophages[25], [72], [82], [83]. *In vivo* macrophages are highly plastic and could simultaneously adopt a range of M1/M2 markers depending on the local cytokine milieu. In this study, the marker Arg-1 was assessed as an indicator of M2 macrophage activation and accumulation in our model. Primarily expressed in the liver, Arg-1 is an enzyme that converts L-arginine into L-ornithine and urea in the urea cycle. However, extrahepatic Arg-1 expression in the lung has been associated with tissue repair processes through synthesis of L-ornithine, which is a precursor to polyamines and L-proline molecules involved in cell proliferation and collagen synthesis[72]. Therefore, increased Arg-1^{+} macrophages in AdOSM-exposed lungs may play a role in promoting cellular hyperplasia or tissue repair/fibrosis. Although levels of Arg-1 protein expression detected using Western blot and immunohistochemistry were significantly up-regulated in AdOSM-treated mice, we observed variability between samples as previously demonstrated in other models of inflammation[80]. This may be due to presence of other Arg-1-expressing cell types within the lung, such as innate lymphoid group 2 cells or fibroblasts[78]. In our system, we primarily observed Arg-1 localized to cells resembling macrophage morphology and thus pursued understanding alternative activation of macrophages.

Recently, the M1/M2 paradigm has evolved to include M2 macrophage subtypes, M2a, M2b and M2c, all of which have been associated with wound healing and immunosuppressive processes[82], [84]. M2a cells are known as the canonical IL-4/IL-13

stimulated alternatively activated macrophages, which promote cellular hyperplasia and secrete various growth factors. These cells can be identified by the markers Arg-1, FIZZ1, Ym1 and CD206[82], [85]. M2b and M2c macrophages appear to be mainly involved in inflammatory resolution, including extracellular matrix deposition, tissue stabilization and angiogenesis. M2b or M2c can be identified by other markers unique from M2a macrophages, such as CD86 or CD163[82]. Therefore, we speculate that OSM-induced AAM accumulation is comprised of primarily M2a macrophages due to robust increase in the M2a marker Arg-1, however studies exploring the modulation of other M2 macrophage subtypes would be required to determine if OSM may also modulate these cells.

Similar to previous publications, we have demonstrated here that IL-4/IL-13 signaling is sufficient to induce M2 macrophage polarization *in vitro* using BMDMs[84]–[87]. This finding was consistent with results *in vivo,* where OSM-induced Arg-1 expression was attenuated in STAT6$^{-/-}$ mice, the canonical signaling pathway activated by IL-4/IL-13 (data not shown). Since OSM was unable to induce Arg-1 activity *in vitro*, we speculate that the OSM-induced Th2 cytokine milieu produced *in vivo* sensitizes cells present in mouse lungs to IL-6-mediated effects. Work with collaborators have established that IL-6 potentiates Arg-1 in BMDMs. IL-6 overexpression alone *in vivo* (in the absence of a Th2 cytokine milieu) was not sufficient to induce pulmonary Arg-1 expression or M2 macrophage accumulation in mouse lungs. Additionally, since IL-6 has a clearly prominent effect on BMDMs compared to alveolar macrophages, we speculate that the decrease in Arg-1^{+} macrophage accumulation in IL-6$^{-/-}$ mice may also be due to a lack of newly recruited

macrophages to the lung, consistent with a decreased alveolar macrophage population in the BALF of AdOSM-treated IL-$6^{-/-}$ mice (data not shown).

5.3 Effect of GP130 Cytokines on Arg1 Macrophage Expression

Both OSM and IL-6 are gp130 family cytokines produced from activated lymphocytes and macrophages in the presence of inflammation and can regulate similar functions in certain cells, such as STAT3 activation or acute-phase protein synthesis[88]–[90]. However, OSM and IL-6 also exude distinct functions, which we have further delineated within our model. Albeit high levels of OSM and IL-6 within the system, OSM showed ability to up-regulate Th2 specific cytokines, whereas IL-6 led to elevation of some cytokines and chemokines associated with Th1-skewed inflammation. Cytokine specific receptor chains, OSMR and IL-6Rα, are differentially expressed among different cell-types, leading to overlapping and distinct roles in inflammatory processes. For instance, OSMR is highly expressed on stromal cells and can enable signaling and induction of chemokines that participate in inflammatory responses[91]. With collaborators, it was observed that IL-6Rα mRNA is expressed by BMDMs and alveolar macrophages, whereas OSMR mRNA levels were undetectable (experiment conducted by Ehab Ayaub in K. Ask's group). Thus, the absence of Arg-1 induction by OSM on BMDMs or alveolar macrophages indicates an indirect effect of OSM on macrophage polarization *in vivo* due to the lack of receptor expression on these cells. The indirect effect of OSM likely includes IL-4 up-regulation and the recruitment of monocytes from the bone marrow that are able to differentiate into M2 cells due to signals within the local lung microenvironment, such as

IL-4/IL-13 and IL-6. The results showing a lack of significant induction of Arg-1 activity by M2 stimuli, OSM, or IL-6 in cultures of naïve alveolar macrophages suggests the resident alveolar cells contribute little (if any) to the Arg-1^+ cell accumulation in the lung due to AdOSM.

5.4 Effect of IL-33 on Arg-1 Activity and Expression

Several researchers have studied the effect of IL-33 on the polarization of bone-marrow derived macrophages, as well as alveolar macrophages. We have shown here an association between IL-33 and the M2 macrophage marker, Arg-1, in the context of OSM-induced lung inflammation, as well as a requirement for IL-33 signalling in the expression of Arg-1 protein by OSM *in vivo*. Although this provides strong evidence for a connection between IL-33 and the alternative activation of macrophages, further experimentation is needed to assess whether IL-33 is able to directly induce Arg-1 in macrophages *in vitro* or if there is an indirect effect of IL-33 on macrophage polarization in this system. Yang et al., have previously demonstrated that stimulation of BMDMs with IL-33 (20ng/mL) for 72 hours led to significant increases in Arg-1 mRNA levels, as well as IL-13 mRNA and protein production[76]. They suggest that IL-33 can potentiate the polarization of macrophages through induction of IL-13 and subsequent autocrine stimulation. Li et al., later demonstrated that IL-33 was able to potentiate IL-13-induced Arg-1 mRNA levels within BMDMs *in vitro*, in combination with the pharmacological agent bleomycin[68].

A preliminary experiment within the laboratory demonstrated that IL-33 alone induced Arg-1 activity within BMDM after 24 hours of stimulation, as well as increased

OSM production within the cell-culture supernatants, as assessed by ELISA. However, further experiments did not produce similar results and therefore this experiment must be optimized and repeated in order to generate results within the laboratory about the ability of IL-33 to directly polarize BMDMs *in vitro*.

5.5 Oxidation and Reduction of IL-33

Recently, it has been discovered that IL-33 has separate biological activity when present in distinct conformational forms. Specifically, Cohen et al., demonstrated that IL-33 can be oxidized at free cysteine locations within the molecule to produce the addition of two disulphide bonds, preventing the molecule from binding to its receptor, ST2. Within this study, they have shown that *Alternaria*-induced IL-33 is oxidized in a time-dependent manner and unable to induce NFkB activation in HUVEC cells[42]. Therefore, they have concluded that this form of IL-33 is inactive and prevents any biological effect within the system. Researchers suggest that the conversion of reduced IL-33 to oxidized IL-33 based on a 'molecular clock' and acts as a unique method of self-regulation within the *Alternaria*-infection system[42]. Interestingly, they have also demonstrated that the commercially available IL-33 ELISA Duoset Kits from R&D Systems (human and mouse) preferentially binds to the oxidized IL-33 form, while reduced IL-33 was only detected using their in-house ELISA specific for the reduced form. These findings indicate that the use of the R&D IL-33 ELISA may lead to difficulty in interpreting results and in terms of active IL-33, complicates observations made using the ELISA. Therefore, in order to address this limitation, further experimentation is needed to assess the precise form of OSM-induced

IL-33. For instance, overexpression of OSM within the lung microenvironment may lead to a inflammatory milieu that generates the reduced form of IL-33 within the BALF. This reduced form then may not be detected using the ELISA, however is detected by Western. Additionally, AdOSM-treated whole lung tissue samples that are specifically reduced using RIPA buffer show increased IL-33 detection within the ELISA, suggesting a differential effect using different buffers. Therefore, experiments analyzing the BALF using reduced and non-reduced gels for Western blot would help to address this concern.

Overall, this would suggest that perhaps OSM may also participate in regulating IL-33 using this method in order to prevent exacerbated activation of IL-33 responsive cells. However, further experimentation is required in order to assess the possibility of this phenomenon.

5.6 Influenza A induces Apoptosis and Necrosis

Several studies have indicated that gp130 cytokines, such as IL-6 and IL-11, are elevated in the presence of a respiratory virus infection, including influenza [54], [92]–[95]. Oshansky et al., recently demonstrated a correlative increase in plasma IL-6 levels and hospitalization rates for age-matched children infected with influenza[92]. Within this study, researchers also adjusted for viral load, suggesting that IL-6 was up-regulated independent of viral dynamics[92]. Similar to IL-6, Oh et al., showed increased IL-11 in the nasopharyngeal aspirates of children with influenza infection[94]. Although these studies investigate some of the gp130 cytokines, the regulation of OSM in the context of an influenza virus infection remains unknown.

Influenza A virus is a significant pathogen which causes acute respiratory infection with high rates of morbidity and mortality. The pathogen enters the upper and lower respiratory tract and is internalized into epithelial cells within the lung via endocytosis. Upon replication, several newly formed virus particles are then released from the cell via budding or cellular rupture. The uncontrolled cellular death is also known as necrosis and leads to the release of endogenous molecules or alarmins, which can initiate and activate a subsequent immune response. Simultaneously, other infected cells have intracellular pattern-recognition receptors (PRRs) which recognize viral RNA or other pathogen associated molecular patterns (PAMPs) in order to promote downstream anti-viral immune responses, including induction of pro-inflammatory cytokines (as reviewed in [96].

The anti-viral response to influenza involves innate and adaptive immune mechanisms. The initial response consists of the release of alarmins and cytokines from virally-infected epithelial, endothelial as well as activation of innate immunity through PRRs. These events then lead to the secondary response, which includes release of type II interferons, such as IFNγ, and activation of cellular and humoral immunity. In particular, naïve T-lymphocytes are differentiated when presented with influenza-antigen and target virally-infected cells. Antigen-specific cytotoxic T-cells (CTLs) can mediate infected-cell apoptosis through various mechanism, such as perforin/granzyme-mediated lysis, Fas/FasL-mediated apoptosis or TRAIL/TRAIL-DR-mediated apoptosis[97]. In order to prevent widespread infection, the primary and secondary immune response are required for effective protection against influenza. Overall, this suggests that this pathogen can mediate both uncontrolled cell lysis as well as programmed cell death or apoptosis. Within this

thesis, it is hypothesized that IL-33 is primarily released from virally-infected cells through virus-mediated cellular necrosis. However, further experimentation is needed in order to address this aspect of the overall hypothesis. For instance, cells infected with influenza virus *in vitro* can be assayed for IL-33 as well as lactate dehydrogenase (LDH) within culture supernatants. This intracellular enzyme is released within the extracellular milieu when the plasma membrane of a cell is damaged and therefore it is commonly used as a marker of cellular necrosis. Although this assay can identify cytolysis *in vitro*, analysis of *in vivo* samples for Influenza-associated apoptosis vs. necrosis would not be as easily determined. Therefore, a limitation within this thesis is identifying the precise source of IL-33 from either necrotic or apoptotic cells within the lung.

As previously mentioned, IL-33 released from necrotic cells is thought to be released in its full-length form, which can bind to the ST2 receptor and activate cellular effects[98]. However, IL-33 released from cells undergoing apoptosis is cleaved by caspase 1, 3 or 7, which renders the protein biologically inactive[37], [38]. Therefore, future experiments investigating the release of IL-33 from necrotic versus apoptotic cells, at least *in vitro* would, further our understanding of OSM-induced IL-33 function. The results of the co-infection experiments *in vivo* (**Figure 23-28**) indicated a reduced level of IL-33 (and eosinophils) in PR8 infection of OSM-primed mice. Possible explanations for this may involve interferon mediated regulation.

5.7 Type I Interferon Regulation of IL-33 in a Respiratory Virus Infection

Type I interferons play an integral part of the innate immune response against an

influenza A virus infection. They are primarily produced from macrophages, pneumocytes, inflammatory monocytes or dendritic cells, however have also been shown to be up-regulated within several stromal cell-types, including fibroblasts[96], [99]. As part of the first line of defense, they induce a "anti-viral state" within the local microenvironment[100]. The type I interferons, IFNα and IFNβ, signal through the IFNAR heterodimeric receptor composed of IFNAR1 and IFNAR2. Activation of this receptor-complex initiates the signalling pathway JAK/STAT, which then leads to the induction of Interferon-stimulated genes (ISGs). ISG products molecules within the cell are potent in directly inhibiting viral replication and contribute to an anti-viral defense[100]. Upon analysis using *Ifnar*$^{-/-}$ mice, researchers have shown that several ISGs were attenuated following *in vivo* infection with H3N2 influenza virus compared to wild-type mice[101]. Additionally, *Ifnar*$^{-/-}$ epithelial cells infected with H1N1 virus showed reduced ability to up-regulate anti-viral genes and enhanced viral protein production, suggesting IFNAR-signalling within epithelial cells also plays an important role in inhibiting local viral replication[102]. It has also been shown that type I interferons can boost memory CD8+ T-cell activation and cytotoxic ability through induction of granzyme B[103]. Overall, type I interferons initiate important innate immune mechanisms, such as inhibition of viral replication or induction of anti-viral responses in order to protect the host from disease.

Type 1 interferons have also been shown to regulate IL-33 expression within lung systems following a virus infection. Firstly, levels of IL-33 protein are significantly elevated within the serum of patients infected with influenza A H1N1, suggesting a potential role for this alarmin in regulating disease pathology[54]. Upon influenza infection

in vivo, Jorg Fritz et al., demonstrated robust up-regulation of IL-33 and type 2 immune responses in *Ifnar*$^{-/-}$ mice infected with influenza A[104]. This increased IL-33 protein within the lung led to exacerbated lung inflammation and fibrosis, as assessed by Masson's Trichrome and BALF eosinophil infiltration[104]. Another study investigating human rhinovirus (HRV) infection of human bronchial epithelial cells showed up-regulation of the interferon-regulatory factor 7 (IRF7), which led to increased anti-viral responses. Interestingly, knock-down of IRF7 using siRNA in HRV-infected cells led to increased IL-33 expression, suggesting that type I interferons may play a role in down-regulating IL-33 expression in human lung cells[105]. In contrast, in a study conducted by Jackson et al., researchers demonstrated HRV induction of IL-33 in bronchial epithelial cells, which led to up-regulation of type-2 cytokines from cultured T-cells and ILC2s[106]. These results suggest that Type I interferon signalling may down-regulate IL-33 expression within the lung following a respiratory virus infection and to prevent exacerbated disease pathology. In terms of OSM, Hermanns et al., has recently demonstrated that OSM induces interferon-regulatory factor-1, 7 and 9 within human dermal and lung fibroblasts[107]. This is the first report to demonstrate direct regulation of IRFs by OSM. Within this thesis, type I interferon regulation of IL-33 or OSM regulation of type-1 interferons has not been assessed. Further experiments understanding OSM and type I interferon signalling will be necessary in order to determine if IL-33 down-regulation observed within these experiments is due to this innate immune mechanism.

5.8 Type-II Interferon Regulation of IL-33 in a Respiratory Virus Infection

In addition to type I interferon signalling, type II interferons, such as IFNγ, play a significant role in mediating an anti-viral response to respiratory virus infections. IFNγ is produced by and released from primarily T-cells and natural killer (NK) cells and signals through the IFNGR1/IFNGR2 complex to activate the JAK-STAT1 pathway[108]. Induction of this pathway leads to increased ISG production and subsequent interference with viral replication. Some studies investigating IFNγ during a influenza virus infection show no role for this cytokine in mediating viral clearance, while others suggest it is a key element for survival[109], [110]. In a study conducted by Weiss et al., researchers demonstrated that exogenous treatment with IFNγ protected mice from a PR8 virus infection through NK cell activation and proliferation[111].

Other studies have previously reported regulation of IL-33 by IFNγ. For instance, Shan et al., demonstrated that IFNγ stimulation of human esophageal epithelial cells up-regulated nuclear IL-33 expression, which mediated production of other inflammatory cytokines and chemokines, such as IL-6, IL-8 and MCP-1[112]. Additionally, Meephansan et al., showed IFNγ-dependent up-regulation of full-length IL-33 within human keratinocytes[46]. They also demonstrated that IFNγ and TNF-α induced synergistic effects on mature IL-33 (20kDa) induction[46]. Future experiments investigating type II interferon regulation of IL-33 and OSM-induced IL-33, could further clarify cytokine networks associated with lung inflammation. Furthermore, initial experiments in human type II alveolar epithelial cells (A549) demonstrated increased IL-33 (Figure 5). Whether type I or II interferons may also modulate TNF-α induction of IL-33 would also require further

experimentation.

Together, these observations suggest that type I and type II interferons have opposing effects on IL-33 regulation in the context of lung inflammation. *In vivo*, both mechanisms may have a role in regulation of IL-33, which are critical for host defense. For instance, type I interferon may down-regulate IL-33 early in the innate immune response to prevent exacerbated IL-33-mediated pathology and type II interferons may restore IL-33 levels to maintain homeostasis. Additionally, differential signalling pathways induced by type I and II interferons may also contribute to their distinct regulation of IL-33 protein.

Overall goals of this research program includes investigation of IL-33-dependent effects on extracellular matrix deposition and lung fibrosis. Since IL-33 has been shown to potentiate bleomycin-induced lung fibrosis, it was hypothesized that release of IL-33 from virally-infected cells would lead to increased ECM deposition within the lung, due to increased M2 macrophage accumulation or ILC2 activation. Jorg Fritz et al., showed that exacerbated lung fibrosis following an influenza infection in *Ifnar*$^{-/-}$ animals was dependent on increased IL-33 expression and ILC2 activation[104]. Additionally, Li et al., demonstrated that IL-33-dependent ILC2 activation and alternatively activated macrophage induction within the lung enhanced the fibrotic outcome[68]. Ongoing approaches to test this include analysis of ECM accumulation (PSR staining and quantification) in wild-type and IL-33$^{-/-}$ animals, as well as assessment of ECM in the co-infection experiments (Figures 23 to 28). Such results are not in the scope of this thesis but will contribute to characterizing the OSM-IL-33 axis in fibrosis mechanisms.

CHAPTER 6

- CONCLUSIONS -

Idiopathic pulmonary fibrosis (IPF) is an interstitial lung disease (ILD) of unknown cause characterized by scar tissue formation and extracellular matrix deposition. Patients diagnosed with IPF have a poor prognosis with a lack of effective treatments. Acute exacerbations in IPF (AE-IPF) involve rapid decline in lung function and is associated with a 70% mortality rate in patients with biopsy-confirmed IPF. High fatality rates for AE-IPF demonstrate a strong need to investigate underlying mechanisms for development of new therapeutic interventions. Current paradigms suggest that sustained epithelial cell damage may lead to the recruitment of immune cells and release of soluble mediators, such as the alarmin IL-33, and may contribute to disease pathogenesis. Although the precise cause of AE-IPF is unknown, it is postulated that bacterial and viral infections can initiate a cascade of inflammatory events, potentiate epithelial cell necrosis and activate specific cellular networks contributing to accelerated disease progression. Various pro-inflammatory cytokines, including OSM and IL-33, are elevated in the bronchoalveolar lavage fluid in response to such infections as well as in diagnosed IPF patients, and therefore may contribute to pathologic exacerbations.

Overexpression of Oncostatin M (OSM) induces ECM deposition and Arg1+ macrophage accumulation in mouse models. Elevated levels of OSM also leads to robust induction of interleukin-33 (IL-33), an IL1 family cytokine or alarmin, by OSM both *in vivo* and *in vitro* mouse lung systems. Other studies have shown that enhanced pulmonary IL-33 expression can lead to exacerbated bleomycin-induced lung fibrosis or augmented

Th2-type lung diseases, such as allergic asthma. It has been shown to have a direct effect on bone-marrow derived macrophage polarization through increased Arg1 mRNA expression *in vitro*. Therefore, it was postulated that IL-33 released from necrotic lung cells following a respiratory virus infection may contribute to increased macrophage polarization and subsequent exacerbations in IPF or other chronic lung conditions.

In conclusion, the findings presented in this thesis demonstrate that OSM induced robust up-regulation of pulmonary IL-33 and Arg1 mRNA and protein expression *in vivo*, in comparison to the gp130 cytokine, IL-6. OSM-induced IL-33 protein detected both *in vivo* and *in vitro* was in its full-length (35kDa) form, as determined by Western blot. IL-6 was required for OSM-induced arginase-1 expression *in vivo*, but not IL-33 expression, suggesting alternative mechanisms of induction. Interestingly, OSM-induced Arg1 expression was dependent upon IL-33 and IL-6, as demonstrated within IL-$33^{-/-}$ and IL-$6^{-/-}$ animals, respectively. Together, these findings implicate a role for both IL-33 and IL-6 in mediating OSM-induced M2 macrophage accumulation within the lung.

Regulation of IL-33 and Arginase-1 by OSM was also assessed in the context of a respiratory influenza A virus infection. Mice infected with the PR8 influenza A virus strain showed a time-dependent increase in OSM and IL-33 expression within the BALF. Lung tissue IL-33 expression was up-regulated 4-days post-influenza infection, however was significantly reduced below basal levels 7-days post-PR8 infection. Co-infection with AdOSM until day 7 and subsequent influenza A virus for 5 days *in vivo* led to decreased IL-33 and Arg1 expression, as well as BALF eosinophil infiltration within the lung. Collectively, these results suggest OSM is a key driver in mediating Th2-associated

pathology, as well as IL-33 and Arg1 expression. Contrary to the hypothesis, influenza A virus infection attenuated OSM-induced Th2-associated responses, such as induction of IL-33, Arg1 and eosinophil accumulation *in vivo*.

Further exploration into the OSM-IL-33 pathway will provide insight into novel innate immune mechanisms associated with chronic lung disease and exacerbations in lung disease due to respiratory virus infection.

CHAPTER 7

- REFERENCES -

[1] G. Sgalla, A. Biffi, and L. Richeldi, "Idiopathic pulmonary fibrosis: Diagnosis, epidemiology and natural history," *Respirol. Carlton Vic*, Nov. 2015.

[2] W. D. Travis *et al.*, "An Official American Thoracic Society/European Respiratory Society Statement: Update of the International Multidisciplinary Classification of the Idiopathic Interstitial Pneumonias," *Am. J. Respir. Crit. Care Med.*, vol. 188, no. 6, pp. 733–748, Sep. 2013.

[3] A. L. Olson, J. J. Swigris, D. C. Lezotte, J. M. Norris, C. G. Wilson, and K. K. Brown, "Mortality from Pulmonary Fibrosis Increased in the United States from 1992 to 2003," *Am. J. Respir. Crit. Care Med.*, vol. 176, no. 3, pp. 277–284, Aug. 2007.

[4] H. R. Collard *et al.*, "Health Care Utilization and Costs of Idiopathic Pulmonary Fibrosis in U.S. Medicare Beneficiaries Aged 65 Years and Older," *Ann. Am. Thorac. Soc.*, vol. 12, no. 7, pp. 981–987, Apr. 2015.

[5] A. T. Borchers, C. Chang, C. L. Keen, and M. E. Gershwin, "Idiopathic Pulmonary Fibrosis—an Epidemiological and Pathological Review," *Clin. Rev. Allergy Immunol.*, vol. 40, no. 2, pp. 117–134, Sep. 2010.

[6] S. C. Wootton *et al.*, "Viral Infection in Acute Exacerbation of Idiopathic Pulmonary Fibrosis," *Am. J. Respir. Crit. Care Med.*, vol. 183, no. 12, pp. 1698–1702, Jun. 2011.

[7] J. W. Song, S.-B. Hong, C.-M. Lim, Y. Koh, and D. S. Kim, "Acute exacerbation of idiopathic pulmonary fibrosis: incidence, risk factors and outcome," *Eur. Respir. J.*, vol. 37, no. 2, pp. 356–363, Feb. 2011.

[8] K. A. Johannson *et al.*, "Acute exacerbation of idiopathic pulmonary fibrosis associated with air pollution exposure," *Eur. Respir. J.*, vol. 43, no. 4, pp. 1124–1131, Apr. 2014.

[9] J. S. Lee *et al.*, "Bronchoalveolar lavage pepsin in acute exacerbation of idiopathic pulmonary fibrosis," *Eur. Respir. J.*, vol. 39, no. 2, pp. 352–358, Feb. 2012.

[10] Y. Kondoh *et al.*, "Acute exacerbation of interstitial pneumonia following surgical lung biopsy," *Respir. Med.*, vol. 100, no. 10, pp. 1753–1759, Oct. 2006.

[11] B. B. Moore and T. A. Moore, "Viruses in Idiopathic Pulmonary Fibrosis. Etiology and Exacerbation," *Ann. Am. Thorac. Soc.*, vol. 12, no. Supplement 2, pp. S186–S192, Nov. 2015.

[12] J. Hu and X. Liu, "Crucial role of PA in virus life cycle and host adaptation of influenza A virus," *Med. Microbiol. Immunol. (Berl.)*, vol. 204, no. 2, pp. 137–149, Apr. 2015.

[13] C. D. Richards, "The enigmatic cytokine oncostatin m and roles in disease," *ISRN Inflamm.*, vol. 2013, p. 512103, 2013.

[14] D. Heymann and A. V. Rousselle, "gp130 Cytokine family and bone cells," *Cytokine*, vol. 12, no. 10, pp. 1455–1468, Oct. 2000.

[15] M. Peters, A. M. Müller, and S. Rose-John, “Interleukin-6 and soluble interleukin-6 receptor: direct stimulation of gp130 and hematopoiesis,” *Blood*, vol. 92, no. 10, pp. 3495–3504, Nov. 1998.
[16] M. Tomida, “Structural and functional studies on the leukemia inhibitory factor receptor (LIF-R): gene and soluble form of LIF-R, and cytoplasmic domain of LIF-R required for differentiation and growth arrest of myeloid leukemic cells,” *Leuk. Lymphoma*, vol. 37, no. 5–6, pp. 517–525, May 2000.
[17] Y. P. Moodley *et al.*, “Inverse Effects of Interleukin-6 on Apoptosis of Fibroblasts from Pulmonary Fibrosis and Normal Lungs,” *Am. J. Respir. Cell Mol. Biol.*, vol. 29, no. 4, pp. 490–498, Oct. 2003.
[18] H. Takizawa *et al.*, “Increased IL-6 and IL-8 in bronchoalveolar lavage fluids (BALF) from patients with sarcoidosis: correlation with the clinical parameters,” *Clin. Exp. Immunol.*, vol. 107, no. 1, pp. 175–181, Jan. 1997.
[19] T. Kobayashi *et al.*, “Bidirectional role of IL-6 signal in pathogenesis of lung fibrosis,” *Respir. Res.*, vol. 16, no. 1, 2015.
[20] J. Mauer *et al.*, “Signaling by IL-6 promotes alternative activation of macrophages to limit endotoxemia and obesity-associated resistance to insulin,” *Nat. Immunol.*, vol. 15, no. 5, pp. 423–430, May 2014.
[21] J. M. Zarling, M. Shoyab, H. Marquardt, M. B. Hanson, M. N. Lioubin, and G. J. Todaro, “Oncostatin M: a growth regulator produced by differentiated histiocytic lymphoma cells.,” *Proc. Natl. Acad. Sci. U. S. A.*, vol. 83, no. 24, pp. 9739–9743, Dec. 1986.
[22] A. S. K. de Hooge *et al.*, “Adenoviral Transfer of Murine Oncostatin M Elicits Periosteal Bone Apposition in Knee Joints of Mice, Despite Synovial Inflammation and Up-Regulated Expression of Interleukin-6 and Receptor Activator of Nuclear Factor-κB Ligand,” *Am. J. Pathol.*, vol. 160, no. 5, pp. 1733–1743, May 2002.
[23] A. Mozaffarian *et al.*, “Mechanisms of Oncostatin M-Induced Pulmonary Inflammation and Fibrosis,” *J. Immunol.*, vol. 181, no. 10, pp. 7243–7253, Nov. 2008.
[24] S. Wong, F. M. Botelho, R. M. Rodrigues, and C. D. Richards, “Oncostatin M overexpression induces matrix deposition, STAT3 activation, and SMAD1 Dysregulation in lungs of fibrosis-resistant BALB/c mice,” *Lab. Invest.*, vol. 94, no. 9, pp. 1003–1016, Sep. 2014.
[25] S. Lauber *et al.*, “Novel function of Oncostatin M as a potent tumour-promoting agent in lung,” *Int. J. Cancer*, vol. 136, no. 4, pp. 831–843, Feb. 2015.
[26] D. Fairweather and D. Cihakova, “Alternatively activated macrophages in infection and autoimmunity,” *J. Autoimmun.*, vol. 33, no. 3–4, pp. 222–230, 2009.
[27] F. O. Martinez, L. Helming, and S. Gordon, “Alternative Activation of Macrophages: An Immunologic Functional Perspective,” *Annu. Rev. Immunol.*, vol. 27, no. 1, pp. 451–483, 2009.

[28] C. Bogdan, J. Paik, Y. Vodovotz, and C. Nathan, "Contrasting mechanisms for suppression of macrophage cytokine release by transforming growth factor-beta and interleukin-10.," *J. Biol. Chem.*, vol. 267, no. 32, pp. 23301–23308, Nov. 1992.
[29] K. Y. Nagahama *et al.*, "Oncostatin M Modulates Fibroblast Function via Signal Transducers and Activators of Transcription Proteins–3," *Am. J. Respir. Cell Mol. Biol.*, vol. 49, no. 4, pp. 582–591, May 2013.
[30] W. J. Leonard, "Role of Jak kinases and STATs in cytokine signal transduction," *Int. J. Hematol.*, vol. 73, no. 3, pp. 271–277, Apr. 2001.
[31] D. Knight, S. E. Mutsaers, and C. M. Prêle, "STAT3 in tissue fibrosis: Is there a role in the lung?," *Pulm. Pharmacol. Ther.*, vol. 24, no. 2, pp. 193–198, Apr. 2011.
[32] M. Pedroza *et al.*, "STAT-3 contributes to pulmonary fibrosis through epithelial injury and fibroblast-myofibroblast differentiation," *FASEB J. Off. Publ. Fed. Am. Soc. Exp. Biol.*, vol. 30, no. 1, pp. 129–140, Jan. 2016.
[33] J. J. Oppenheim and D. Yang, "Alarmins: chemotactic activators of immune responses," *Curr. Opin. Immunol.*, vol. 17, no. 4, pp. 359–365, Aug. 2005.
[34] E. S. Baekkevold *et al.*, "Molecular Characterization of NF-HEV, a Nuclear Factor Preferentially Expressed in Human High Endothelial Venules," *Am. J. Pathol.*, vol. 163, no. 1, pp. 69–79, Jul. 2003.
[35] J. Schmitz *et al.*, "IL-33, an interleukin-1-like cytokine that signals via the IL-1 receptor-related protein ST2 and induces T helper type 2-associated cytokines," *Immunity*, vol. 23, no. 5, pp. 479–490, Nov. 2005.
[36] S. Ali *et al.*, "The dual function cytokine IL-33 interacts with the transcription factor NF-κB to dampen NF-κB-stimulated gene transcription," *J. Immunol. Baltim. Md 1950*, vol. 187, no. 4, pp. 1609–1616, Aug. 2011.
[37] S. Ali, D. Q. Nguyen, W. Falk, and M. U. Martin, "Caspase 3 inactivates biologically active full length interleukin-33 as a classical cytokine but does not prohibit nuclear translocation," *Biochem. Biophys. Res. Commun.*, vol. 391, no. 3, pp. 1512–1516, Jan. 2010.
[38] A. U. Lüthi *et al.*, "Suppression of interleukin-33 bioactivity through proteolysis by apoptotic caspases," *Immunity*, vol. 31, no. 1, pp. 84–98, Jul. 2009.
[39] E. Lefrançais *et al.*, "IL-33 is processed into mature bioactive forms by neutrophil elastase and cathepsin G," *Proc. Natl. Acad. Sci. U. S. A.*, vol. 109, no. 5, pp. 1673–1678, Jan. 2012.
[40] M. Hayakawa, H. Hayakawa, Y. Matsuyama, H. Tamemoto, H. Okazaki, and S. Tominaga, "Mature interleukin-33 is produced by calpain-mediated cleavage *in vivo*," *Biochem. Biophys. Res. Commun.*, vol. 387, no. 1, pp. 218–222, Sep. 2009.
[41] J. Meephansan, H. Tsuda, M. Komine, S.-I. Tominaga, and M. Ohtsuki, "Regulation of IL-33 expression by IFN-γ and tumor necrosis factor-α in normal human epidermal keratinocytes," *J. Invest. Dermatol.*, vol. 132, no. 11, pp. 2593–2600, Nov. 2012.

[42] E. S. Cohen *et al.*, “Oxidation of the alarmin IL-33 regulates ST2-dependent inflammation,” *Nat. Commun.*, vol. 6, Sep. 2015.
[43] L. A. Borthwick, “The IL-1 cytokine family and its role in inflammation and fibrosis in the lung,” *Semin. Immunopathol.*, Mar. 2016.
[44] Q. Gao, Y. Li, and M. Li, “The potential role of IL-33/ST2 signaling in fibrotic diseases,” *J. Leukoc. Biol.*, vol. 98, no. 1, pp. 15–22, Jul. 2015.
[45] T. Mueller and A. S. Jaffe, “Soluble ST2--analytical considerations,” *Am. J. Cardiol.*, vol. 115, no. 7 Suppl, p. 8B–21B, Apr. 2015.
[46] J. Meephansan, H. Tsuda, M. Komine, S.-I. Tominaga, and M. Ohtsuki, “Regulation of IL-33 expression by IFN-γ and tumor necrosis factor-α in normal human epidermal keratinocytes,” *J. Invest. Dermatol.*, vol. 132, no. 11, pp. 2593–2600, Nov. 2012.
[47] A. Llop-Guevara *et al.*, “A GM-CSF/IL-33 pathway facilitates allergic airway responses to sub-threshold house dust mite exposure,” *PloS One*, vol. 9, no. 2, p. e88714, 2014.
[48] W.-H. Zhao and Z.-Q. Hu, “Up-regulation of IL-33 expression in various types of murine cells by IL-3 and IL-4,” *Cytokine*, vol. 58, no. 2, pp. 267–273, May 2012.
[49] J. Kearley *et al.*, “Cigarette smoke silences innate lymphoid cell function and facilitates an exacerbated type I interleukin-33-dependent response to infection,” *Immunity*, vol. 42, no. 3, pp. 566–579, Mar. 2015.
[50] D. E. Byers *et al.*, “Long-term IL-33-producing epithelial progenitor cells in chronic obstructive lung disease,” *J. Clin. Invest.*, vol. 123, no. 9, pp. 3967–3982, Sep. 2013.
[51] K. M. Robinson, K. Ramanan, M. E. Clay, K. J. McHugh, H. E. Rich, and J. F. Alcorn, “Novel protective mechanism for interleukin-33 at the mucosal barrier during influenza-associated bacterial superinfection,” *Mucosal Immunol.*, Apr. 2017.
[52] C. D. Richards *et al.*, “Regulation of IL-33 by Oncostatin M in Mouse Lung Epithelial Cells,” *Mediators Inflamm.*, vol. 2016, p. 9858374, 2016.
[53] M. Kurowska-Stolarska, A. Hueber, B. Stolarski, and I. B. McInnes, “Interleukin-33: a novel mediator with a role in distinct disease pathologies,” *J. Intern. Med.*, vol. 269, no. 1, pp. 29–35, Jan. 2011.
[54] J.-R. Bian, W. Nie, Y.-S. Zang, Z. Fang, Q.-Y. Xiu, and X.-X. Xu, “Clinical aspects and cytokine response in adults with seasonal influenza infection,” *Int. J. Clin. Exp. Med.*, vol. 7, no. 12, pp. 5593–5602, 2014.
[55] R. Le Goffic *et al.*, “Infection with Influenza Virus Induces IL-33 in Murine Lungs,” *Am. J. Respir. Cell Mol. Biol.*, vol. 45, no. 6, pp. 1125–1132, Dec. 2011.
[56] D. K. Chu *et al.*, “IL-33, but not thymic stromal lymphopoietin or IL-25, is central to mite and peanut allergic sensitization,” *J. Allergy Clin. Immunol.*, vol. 131, no. 1, pp. 187–200.e1–8, Jan. 2013.
[57] I. G. Luzina *et al.*, “Full-Length IL-33 Promotes Inflammation but not Th2 Response *In vivo* in an ST2-Independent Fashion,” *J. Immunol.*, vol. 189, no. 1, pp. 403–410, Jul. 2012.

[58] A. R. Teufelberger *et al.*, "The IL-33/ST2 axis is crucial in type 2 airway responses induced by the Staphylococcus aureus protease SplD," *J. Allergy Clin. Immunol.*, May 2017.
[59] Y. Jia *et al.*, "IL-13+ Type 2 Innate Lymphoid Cells Correlate with Asthma Control Status and Treatment Response," *Am. J. Respir. Cell Mol. Biol.*, vol. 55, no. 5, pp. 675–683, Jun. 2016.
[60] D.-M. Lai, Q. Shu, and J. Fan, "The origin and role of innate lymphoid cells in the lung," *Mil. Med. Res.*, vol. 3, p. 25, 2016.
[61] J.-E. Turner *et al.*, "IL-9-mediated survival of type 2 innate lymphoid cells promotes damage control in helminth-induced lung inflammation," *J. Exp. Med.*, vol. 210, no. 13, pp. 2951–2965, Dec. 2013.
[62] S. Saglani and C. M. Lloyd, "Eosinophils in the pathogenesis of paediatric severe asthma," *Curr. Opin. Allergy Clin. Immunol.*, vol. 14, no. 2, pp. 143–148, Apr. 2014.
[63] J. C. Nussbaum *et al.*, "Type 2 innate lymphoid cells control eosinophil homeostasis," *Nature*, vol. 502, no. 7470, pp. 245–248, Oct. 2013.
[64] A. B. Molofsky *et al.*, "Innate lymphoid type 2 cells sustain visceral adipose tissue eosinophils and alternatively activated macrophages," *J. Exp. Med.*, vol. 210, no. 3, pp. 535–549, Mar. 2013.
[65] J. L. Barlow *et al.*, "IL-33 is more potent than IL-25 in provoking IL-13-producing nuocytes (type 2 innate lymphoid cells) and airway contraction," *J. Allergy Clin. Immunol.*, vol. 132, no. 4, pp. 933–941, Oct. 2013.
[66] I. G. Luzina *et al.*, "FULL-LENGTH INTERLEUKIN-33 PROMOTES INFLAMMATION BUT NOT TH2 RESPONSE *IN VIVO* IN AN ST2-INDEPENDENT FASHION," *J. Immunol. Baltim. Md 1950*, vol. 189, no. 1, pp. 403–410, Jul. 2012.
[67] I. G. Luzina *et al.*, "Interleukin-33 potentiates bleomycin-induced lung injury," *Am. J. Respir. Cell Mol. Biol.*, vol. 49, no. 6, pp. 999–1008, Dec. 2013.
[68] D. Li *et al.*, "IL-33 promotes ST2-dependent lung fibrosis by the induction of alternatively activated macrophages and innate lymphoid cells in mice," *J. Allergy Clin. Immunol.*, vol. 134, no. 6, pp. 1422–1432.e11, Dec. 2014.
[69] Q. Gao, Y. Li, X. Pan, X. Yuan, X. Peng, and M. Li, "Lentivirus expressing soluble ST2 alleviates bleomycin-induced pulmonary fibrosis in mice," *Int. Immunopharmacol.*, vol. 30, pp. 188–193, Jan. 2016.
[70] Z. Jiang and L. Zhu, "Update on the role of alternatively activated macrophages in asthma," *J. Asthma Allergy*, vol. 9, pp. 101–107, Jun. 2016.
[71] U. Juhas, M. Ryba-Stanisławowska, P. Szargiej, and J. Myśliwska, "Different pathways of macrophage activation and polarization," *Postepy Hig. Med. Doswiadczalnej Online*, vol. 69, pp. 496–502, Apr. 2015.
[72] H. Maarsingh, T. Pera, and H. Meurs, "Arginase and pulmonary diseases," *Naunyn. Schmiedebergs Arch. Pharmacol.*, vol. 378, no. 2, pp. 171–184, Aug. 2008.
[73] A. Ostriker, H. N. Horita, J. Poczobutt, M. C. M. Weiser-Evans, and R. A. Nemenoff, "Vascular smooth muscle cell-derived transforming growth factor-β promotes

maturation of activated, neointima lesion-like macrophages," *Arterioscler. Thromb. Vasc. Biol.*, vol. 34, no. 4, pp. 877–886, Apr. 2014.
[74] P. J. Carneiro *et al.*, "Bosutinib Therapy Ameliorates Lung Inflammation and Fibrosis in Experimental Silicosis," *Front. Physiol.*, vol. 8, p. 159, 2017.
[75] M. Cai *et al.*, "CCL18 in serum, BAL fluid and alveolar macrophage culture supernatant in interstitial lung diseases," *Respir. Med.*, vol. 107, no. 9, pp. 1444–1452, Sep. 2013.
[76] Z. Yang *et al.*, "Macrophages as IL-25/IL-33-Responsive Cells Play an Important Role in the Induction of Type 2 Immunity," *PLoS ONE*, vol. 8, no. 3, Mar. 2013.
[77] L. Tu *et al.*, "IL-33-induced alternatively activated macrophage attenuates the development of TNBS-induced colitis," *Oncotarget*, vol. 8, no. 17, pp. 27704–27714, Apr. 2017.
[78] J. K. Bando, J. C. Nussbaum, H.-E. Liang, and R. M. Locksley, "Type 2 innate lymphoid cells constitutively express arginase-I in the naïve and inflamed lung," *J. Leukoc. Biol.*, vol. 94, no. 5, pp. 877–884, Nov. 2013.
[79] D. Piehler *et al.*, "The IL-33 receptor (ST2) regulates early IL-13 production in fungus-induced allergic airway inflammation," *Mucosal Immunol.*, vol. 9, no. 4, pp. 937–949, Jul. 2016.
[80] J. M. Bratt, L. M. Franzi, A. L. Linderholm, E. M. O'Roark, N. J. Kenyon, and J. A. Last, "Arginase Inhibition in Airways from Normal and Nitric Oxide Synthase 2-Knockout Mice Exposed to Ovalbumin," *Toxicol. Appl. Pharmacol.*, vol. 242, no. 1, pp. 1–8, Jan. 2010.
[81] S. B. Weisser, K. W. McLarren, E. Kuroda, and L. M. Sly, "Generation and characterization of murine alternatively activated macrophages," *Methods Mol. Biol. Clifton NJ*, vol. 946, pp. 225–239, 2013.
[82] J. C. Gensel and B. Zhang, "Macrophage activation and its role in repair and pathology after spinal cord injury," *Brain Res.*, vol. 1619, pp. 1–11, Sep. 2015.
[83] K. Kambara *et al.*, "*In vivo* Depletion of CD206+ M2 Macrophages Exaggerates Lung Injury in Endotoxemic Mice," *Am. J. Pathol.*, vol. 185, no. 1, pp. 162–171, Jan. 2015.
[84] C. J. Ferrante and S. J. Leibovich, "Regulation of Macrophage Polarization and Wound Healing," *Adv. Wound Care*, vol. 1, no. 1, pp. 10–16, Feb. 2012.
[85] M. R. Fernando, J. L. Reyes, J. Iannuzzi, G. Leung, and D. M. McKay, "The pro-inflammatory cytokine, interleukin-6, enhances the polarization of alternatively activated macrophages," *PloS One*, vol. 9, no. 4, p. e94188, 2014.
[86] F. O. Martinez, A. Sica, A. Mantovani, and M. Locati, "Macrophage activation and polarization," *Front. Biosci. J. Virtual Libr.*, vol. 13, pp. 453–461, Jan. 2008.
[87] Y. Zhang *et al.*, "Eosinophils Reduce Chronic Inflammation in Adipose Tissue by Secreting Th2 Cytokines and Promoting M2 Macrophages Polarization," *Int. J. Endocrinol.*, vol. 2015, p. 565760, 2015.
[88] T. Kishimoto, S. Akira, M. Narazaki, and T. Taga, "Interleukin-6 family of cytokines and gp130," *Blood*, vol. 86, no. 4, pp. 1243–1254, Aug. 1995.

[89] S. I. Grivennikov, F. R. Greten, and M. Karin, “Immunity, Inflammation, and Cancer,” *Cell*, vol. 140, no. 6, pp. 883–899, Mar. 2010.
[90] M. Tanaka and A. Miyajima, “Oncostatin M, a multifunctional cytokine,” *Rev. Physiol. Biochem. Pharmacol.*, vol. 149, pp. 39–52, 2003.
[91] H. M. Hermanns, “Oncostatin M and interleukin-31: Cytokines, receptors, signal transduction and physiology,” *Cytokine Growth Factor Rev.*, vol. 26, no. 5, pp. 545–558, Oct. 2015.
[92] C. M. Oshansky *et al.*, “Mucosal immune responses predict clinical outcomes during influenza infection independently of age and viral load,” *Am. J. Respir. Crit. Care Med.*, vol. 189, no. 4, pp. 449–462, Feb. 2014.
[93] L. Kaiser, R. S. Fritz, S. E. Straus, L. Gubareva, and F. G. Hayden, “Symptom pathogenesis during acute influenza: interleukin-6 and other cytokine responses,” *J. Med. Virol.*, vol. 64, no. 3, pp. 262–268, Jul. 2001.
[94] J.-W. Oh, H.-B. Lee, I.-K. Park, and J.-O. Kang, “Interleukin-6, interleukin-8, interleukin-11, and interferon-gamma levels in nasopharyngeal aspirates from wheezing children with respiratory syncytial virus or influenza A virus infection,” *Pediatr. Allergy Immunol. Off. Publ. Eur. Soc. Pediatr. Allergy Immunol.*, vol. 13, no. 5, pp. 350–356, Oct. 2002.
[95] J. Białek, M. Kowalska, T. Szydłowska, and A. Denys, “Cell phenomena in experimental viral-bacterial infections in mice. I. The release of leukocyte inhibiting factor (LIF) from mouse spleen leukocytes in the presence of specific antigens,” *Arch. Immunol. Ther. Exp. (Warsz.)*, vol. 35, no. 4, pp. 447–451, 1987.
[96] X. J. Guo and P. G. Thomas, “New fronts emerge in the influenza cytokine storm,” *Semin. Immunopathol.*, pp. 1–10, May 2017.
[97] S. Duan and P. G. Thomas, “Balancing Immune Protection and Immune Pathology by CD8+ T-Cell Responses to Influenza Infection,” *Front. Immunol.*, vol. 7, 2016.
[98] V. Mehraj, R. Ponte, and J.-P. Routy, “The Dynamic Role of the IL-33/ST2 Axis in Chronic Viral-infections: Alarming and Adjuvanting the Immune Response,” *EBioMedicine*, vol. 9, pp. 37–44, Jul. 2016.
[99] F. Li and H. Karlsson, “Antiviral Effect of IDO in Mouse Fibroblast Cells During Influenza Virus Infection,” *Viral Immunol.*, Apr. 2017.
[100] F. McNab, K. Mayer-Barber, A. Sher, A. Wack, and A. O’Garra, “Type I interferons in infectious disease,” *Nat. Rev. Immunol.*, vol. 15, no. 2, pp. 87–103, Feb. 2015.
[101] S. Davidson, S. Crotta, T. M. McCabe, and A. Wack, “Pathogenic potential of interferon αβ in acute influenza infection,” *Nat. Commun.*, May 2014.
[102] C. M. Rosenberger *et al.*, “Characterization of innate responses to influenza virus infection in a novel lung type I epithelial cell model,” *J. Gen. Virol.*, vol. 95, no. Pt 2, pp. 350–362, Feb. 2014.
[103] J. E. Kohlmeier, T. Cookenham, A. D. Roberts, S. C. Miller, and D. L. Woodland, “Type I interferons regulate cytolytic activity of memory CD8(+) T cells in the lung

airways during respiratory virus challenge," *Immunity*, vol. 33, no. 1, pp. 96–105, Jul. 2010.

[104] C. U. Duerr *et al.*, "Type I interferon restricts type 2 immunopathology through the regulation of group 2 innate lymphoid cells," *Nat. Immunol.*, vol. 17, no. 1, pp. 65–75, Jan. 2016.

[105] A. Bosco, S. Wiehler, and D. Proud, "Interferon regulatory factor 7 regulates airway epithelial cell responses to human rhinovirus infection," *BMC Genomics*, vol. 17, p. 76, Jan. 2016.

[106] D. J. Jackson *et al.*, "IL-33-dependent type 2 inflammation during rhinovirus-induced asthma exacerbations *in vivo*," *Am. J. Respir. Crit. Care Med.*, vol. 190, no. 12, pp. 1373–1382, Dec. 2014.

[107] S. Hergovits, C. Mais, C. Haan, A. P. Costa-Pereira, and H. M. Hermanns, "Oncostatin M induces RIG-I and MDA5 expression and enhances the double-stranded RNA response in fibroblasts," *J. Cell. Mol. Med.*, May 2017.

[108] L. C. Platanias, "Mechanisms of type-I- and type-II-interferon-mediated signalling," *Nat. Rev. Immunol.*, vol. 5, no. 5, pp. 375–386, May 2005.

[109] S. J. Turner, E. Olivas, A. Gutierrez, G. Diaz, and P. C. Doherty, "Disregulated Influenza A Virus-Specific CD8+ T Cell Homeostasis in the Absence of IFN-γ Signaling," *J. Immunol.*, vol. 178, no. 12, pp. 7616–7622, Jun. 2007.

[110] M. B. Graham, D. K. Dalton, D. Giltinan, V. L. Braciale, T. A. Stewart, and T. J. Braciale, "Response to influenza infection in mice with a targeted disruption in the interferon gamma gene.," *J. Exp. Med.*, vol. 178, no. 5, pp. 1725–1732, Nov. 1993.

[111] I. D. Weiss *et al.*, "IFN-γ Treatment at Early Stages of Influenza Virus Infection Protects Mice from Death in a NK Cell-Dependent Manner," *J. Interferon Cytokine Res.*, vol. 30, no. 6, pp. 439–449, Mar. 2010.

[112] J. Shan, T. Oshima, L. Wu, H. Fukui, J. Watari, and H. Miwa, "Interferon γ-Induced Nuclear Interleukin-33 Potentiates the Release of Esophageal Epithelial Derived Cytokines," *PLoS ONE*, vol. 11, no. 3, Mar. 2016.